Master's Theses   Master's Theses and Graduate Research

2002

Electrochemical potential study of metals and alloys in a simulated BWR

Rahbar Sadeque Suva
San Jose State University

Follow this and additional works at: https://scholarworks.sjsu.edu/etd_theses

INFORMATION TO USERS

NOTE TO USERS

This reproduction is the best copy available.

UMI

ELECTROCHEMICAL POTENTIAL STUDY OF METALS AND ALLOYS IN A SIMULATED BWR

A Thesis

Presented to

The Faculty of the Department of Chemical and Materials Engineering

San Jose State University

In partial fulfillment

Of the Requirements for the Degree

Master of Science

By

Rahbar Sadeque Suva

May 2002

UMI Number: 1408817

UMI®
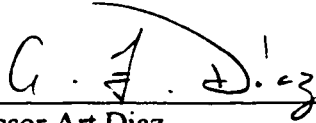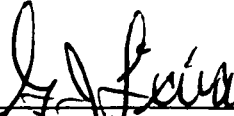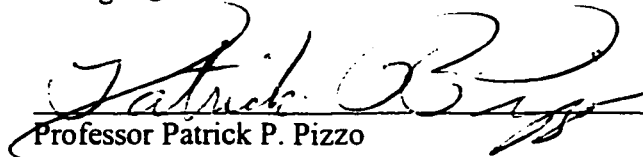
APPROVED FOR THE DEPARTMENT OF CHEMICAL
AND MATERIALS ENGINEERING

_____
Professor Art Diaz
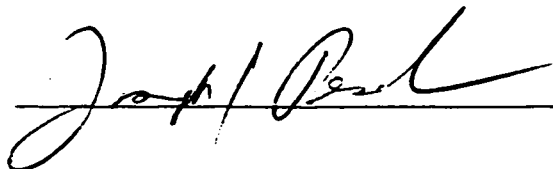
_____
George Licina

_____
Professor Patrick P. Pizzo

APPROVED FOR THE UNIVERSITY

_____

Electrochemical Potential Study of Metals and Alloys in a Simlated BWR

by Rahbar Sadeque Suva

Selected internal components of Boiling Water Nuclear Reactors (BWRs) are damaged by the Intergranular Stress Corrosion Cracking (IGSCC). The development of a sacrificial anode provides the solution to this problem. The standard electrochemical potentials for different metal specimens were studied by both the open circuit measurement and potentiodynamic scan techniques in pressurized water at 50 ppb, 200 ppb and 8000 ppb dissolved oxygen content and 250°F, 350°F and 550°F temperature. The two approaches show that the electrochemical potentials for these sacrificial anode materials depend strongly on both dissolved O_2 and temperature. The corrosion potentials of the different metal specimens were also determined against stainless steel. Magnesium and Zirconium were found to be the best candidate for use in the BWR. This development requires selecting the metal specimens based on their expected open circuit potential in a BWR environment.

ACKNOWLEDGEMENTS

TABLE OF CONTENT

viii

LIST OF TABLES

LIST OF FIGURES

1. Introduction

The development of a means to protecting selected internal components of Boiling Water Nuclear Reactors (BWRs) in nuclear power plants from damage by Intergranular Stress Corrosion Cracking (IGSCC) has become of interest in recent years. IGSCC of Stainless Steel piping has cost BWR owners hundreds of millions of dollars in downtime and inspections. Only a very small amount of material is attacked in IGSCC, (i.e. the interaction of the corrosive environment and stress to produce cracks along grain boundaries of austinitic stainless steel (SS - 316).

Chemical injection methods such as Hydrogen Water Chemistry (HWC) have been shown to be an effective mitigation method for pipe cracking. However, hydrogen injection causes higher operating dose of ^{16}N. In core areas, hydrogen injection rates must be high due to their proximity to the sites of the generation of oxidizing species and the distance from oxygen recombination sites. This increases the radiation level during operation (due to ^{16}N) and is a disadvantage. This increase in radiation limits the access to many areas for routine maintenance. Thus, while HWC works for piping, it is not being helpful for reducing IGSCC in some of the in-vessel core components. So, the focus is to reduce the IGSCC in core components such as core spray nozzles, core spray pipe brackets, core support plate, core shroud etc.

The use of a sacrificial anode could provide an economical and reliable alternative to prevent environmentally assisted cracking in high temperature, high-pressure water systems. The objective of this investigation is to measure the ECPs and E_{corr} values of

1
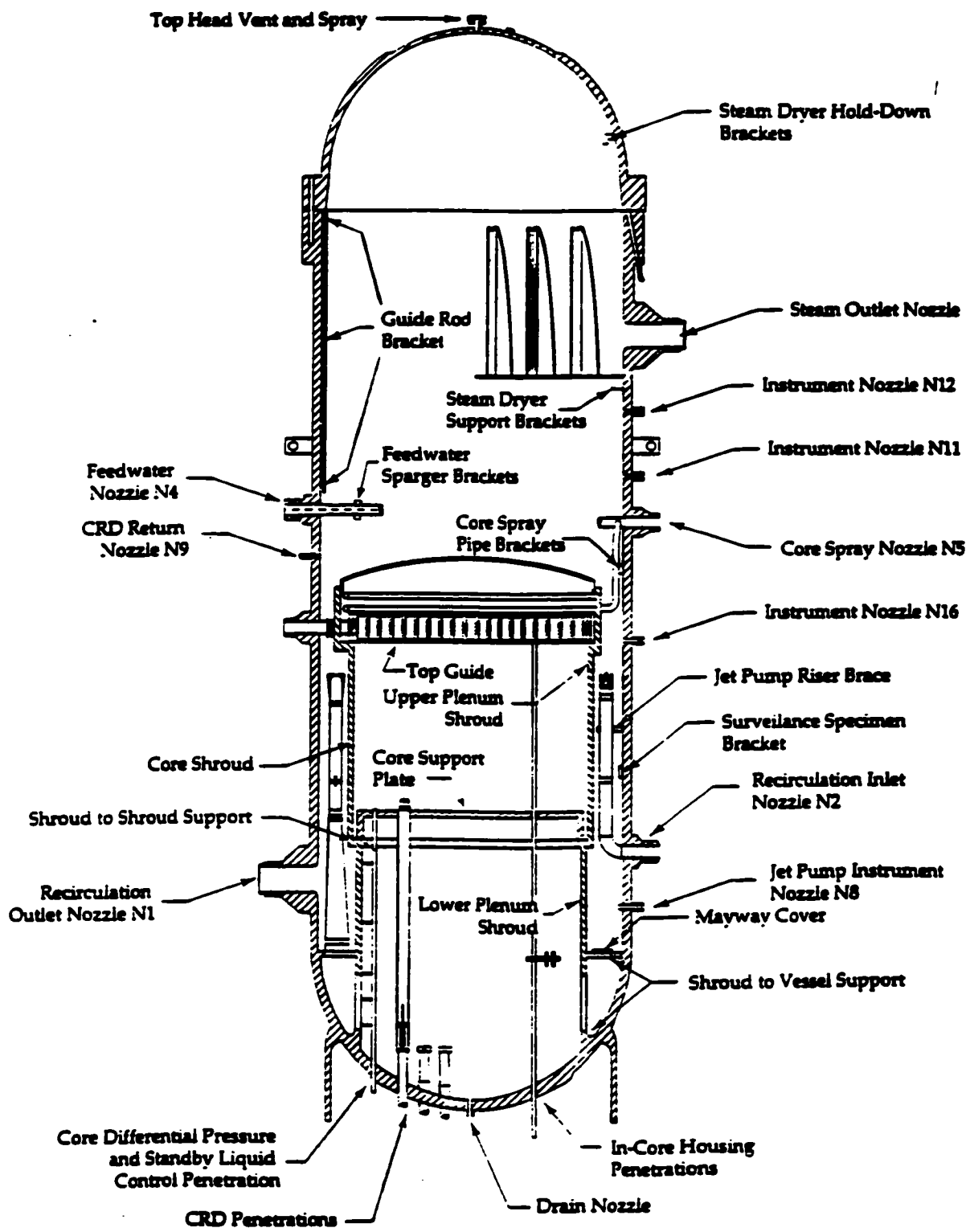
Figure 1. In-vessel Components Identified as IGSCC Concerns [1].

candidate sacrificial anode materials at different dissolved O_2 contents and temperatures, of 1000 psi pressurized water and to select the best candidate metal for mitigation of IGSCC. ECP or electrochemical potential is the relative tendency for metals to oxidize to ions in aqueous solution is to compare their half-cell oxidation or reduction potentials (voltages) relative to a standard reference electrode such as the hydrogen, hydrogen-ion, half-cell potential. E_{corr} is the electrochemical potential of the coupled materials.

This project is sponsored by Structural Integrity Associates San Jose, CA and is funded by EPRI, Palo Alto, CA

1.1 Background

1.1.1 Intergranular Stress Corrosion Cracking (IGSCC)

IGSCC is one form of environmentally assisted cracking of particular concern to BWR owners. IGSCC of recirculating piping systems has been the major form of degradation in BWRs and produced a significant loss of plant availability in the 1970s and 1980s.[1]

IGSCC occurs on the microscopic level and can propagate at the rate of 10^{-9} m/s or more. Cracks produced by IGSCC jeopardize the structural integrity of the piping or components leading to concerns with the safe operation of the plant. These concerns lead to increased costs for inspection, for analyses to demonstrate that the plant can continue to be operated safely, mitigation measures and repairs. [1]

A number of BWR reactor vessel internal components have also been recognized as being susceptible to IGSCC. These in-vessel components include control rod drive stub tubes, shroud and shroud-to-vessel welds, jet pump riser braces, a variety of nozzles and penetrations, and the top guide (Figure 1). Access to these components for inspection and repair is limited. This difficulty with access dramatically increases the costs associated with inspections for stress corrosion cracking. Further, the costs associated with the repair of these internal components are very high [1].

So, the sacrificial anode can be used to protect the internal components of BWR without inspection and repair of those components. Thus the use of sacrificial anode reduces the inspection and repair cost of the BWR.

1.2 Electrochemical Potential

Every metal has a tendency to corrode in a particular environment. One method for comparing the relative tendency for metals to oxidize to ions in aqueous solution is to compare their half-cell oxidation or reduction potentials (voltages) relative to a standard reference electrode such as the hydrogen, hydrogen-ion, half-cell potential. This potential is called the Electrochemical Potential (ECP). The Electrochemical Potential is defined by the equation:

$$\eta_k = \mu_k + z_k F \phi \qquad \text{Eq 1.1}$$

The property η_k is the electrochemical potential of component k, μ_k is the chemical potential of component k in the system, z_k is an integer (zero, positive or negative depending on the valance of the component), F is Faraday's constant and is equal to 96512 Coulombs/mole; and ϕ is the electrical potential.

1.3 Standard Hydrogen Electrode (SHE)

An experiment setup for the determination of half-cell standard electrode potentials is shown in Figure 2. For this determination two beakers of aqueous solutions are used which are separated by a salt bridge so that mechanical mixing of the solutions is prevented. The metal whose standard potential is to be determined is immersed in one beaker containing 1 M solution of H^+ ions at 25°C. The platinum electrode is immersed in the other beaker containing a 1 M solution at 1 atmosphere of H^+ ions into which hydrogen gas is bubbled. A wire in series with a switch and a voltmeter connects the two electrodes. When the switch is closed, the voltage between the half-cells is measured. The potential due to the hydrogen half-cell reaction $H_2 \rightarrow 2H^+ + 2e^-$ is arbitrarily assigned zero voltage. Thus, the voltage of any other element is measured directly against the hydrogen standard half-cell electrode. The standard electrode potentials were shown in Table 1.

5

Table 1. Standard Electrode Potentials of selected elements at 25°C (77°F).

Oxidation (corrosion) reaction	Electrode Potential, E^{θ} (volts vs. Standard hydrogen electrode)
$Fe^{2+} \rightarrow Fe^{3+} + e^{-}$	+0.771
$4(OH)^{-} \rightarrow O_2 + 2H_2O + 4e^{-}$	+0.401
$Fe \rightarrow Fe^{2+} + 2e^{-}$	-0.44
$Cr \rightarrow Cr^{3+} + 3e^{-}$	-0.744
$Zn \rightarrow Zn^{3+} + 2e^{-}$	-0.763
$Al \rightarrow Al^{3+} + 3e^{-}$	-1.662
$Mg \rightarrow Mg^{2+} + 2e^{-}$	-2.363
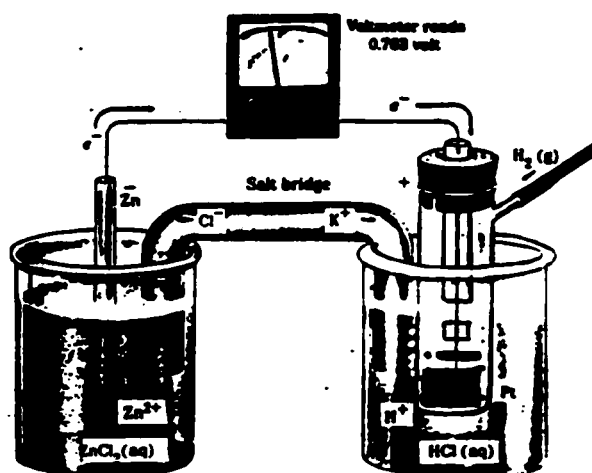
Figure 2. Experimental setup for the determination of the standard emf of zinc.[2]

1.4 IGSCC in BWR

The sensitized grain boundaries in austenitic stainless steel are susceptible to IGSCC in the oxidizing environment of the BWR. The oxidizing nature of the BWR environment results from radiolysis of the reactor coolant (water) as it passes through the reactor core. Typical ECP is +100 to +150 mV $_{SHE}$ due primarily to the presence of dissolved oxygen and other oxidizing species. The rate of IGSCC propagation has been shown to be negligible when the ECP of the stainless steel is less than -230mV$_{SHE}$ as seen in Figure 3. Concentrations of dissolved oxygen in BWR environments can be reduced by recombination with hydrogen in the water. When this occurs, the electrochemical potential (ECP) is brought below -230mV$_{SHE}$, and the formation and propagation of IGSCC cracks is effectively mitigated. One downfall of this technique is that it has never been proven completely for reactor internals. A second limitation is the much higher operating radioactivity associated with ^{16}N. In hydrogen water chemistry (HWC), the radioactivity levels on the turbine deck and other internal reactor areas increase dramatically due to the presence of ^{16}N concentrations. The ^{16}N increases as the hydrogen content to the feed water increases. Since much higher concentrations of hydrogen are required to mitigate IGSCC in vessel internals than in piping areas, protection of internals by HWC could raise operating doses of ^{16}N to unacceptable levels.

The basis of employing a sacrificial anode in the reactor pressure vessel to alter the ECP provides another tool to protect internal components from IGSCC. The sacrificial anode works by shifting the electrical potential of the protected part to below

7

-230 mV$_{SHE}$, thereby reducing the susceptibility to IGSCC. The anode material employed then becomes the point of corrosive dissolution, and is thus "sacrificed" in preference to the system. A sacrificial anode that can effectively mitigate IGSCC in a BWR without hydrogen injection will provide protection without increasing operating dose of ^{16}N. A comprehensive model for sacrificial anode protection needs to consider the potentials of all the different species present in the environment and the interactions that they will have with the candidate anode. This will next be discussed.
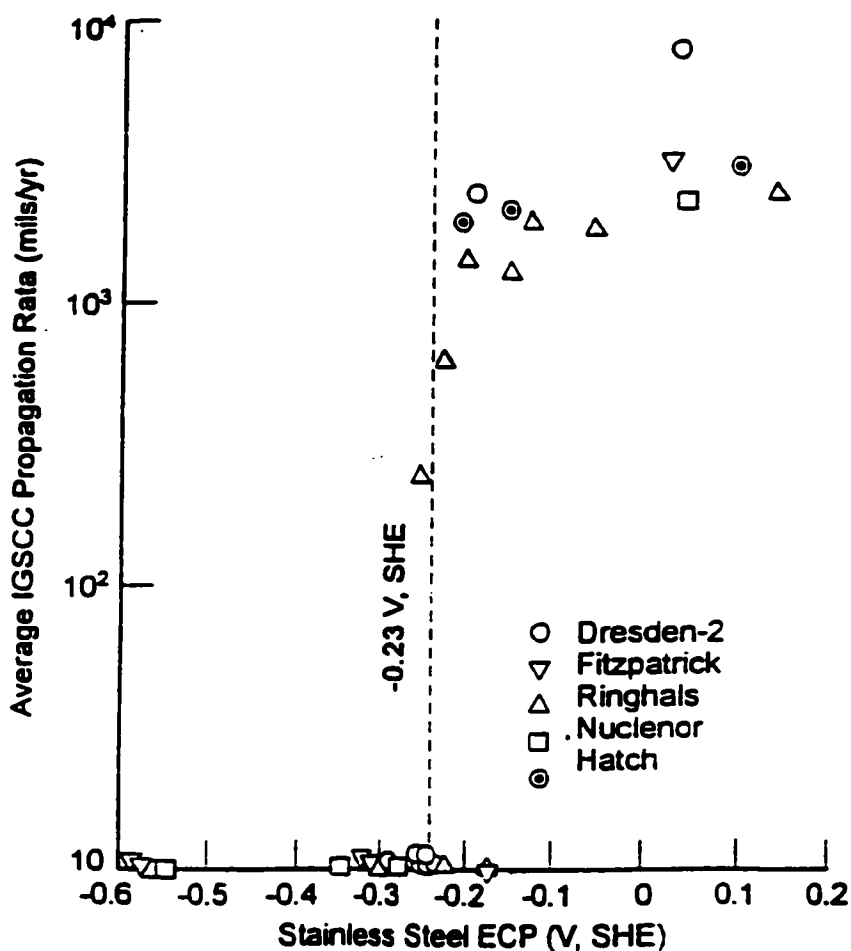
Figure 3. Crack Propagation vs. ECP of Stainless Steel in BWRs [3].

1.5 Mixed Potential Model (MPM)

The mixed potential theory is based on two simple hypotheses:

1. Any electrochemical reaction can be divided into two or more partial oxidation and reduction reactions.

2. There can be no net accumulation of electrical charge during an electrochemical reaction.

The first hypothesis is quite obvious, and it can be experimentally demonstrated that electrochemical reactions are composed of two or more partial oxidation or reduction reactions. The second hypothesis is merely a restatement of the law of conservation of charge. That is, a metal immersed in an electrolyte cannot spontaneously accumulate electrical charge. During the corrosion of an electrically isolated metal sample, the total rate of oxidation must equal the total rate of reduction.

The mixed potential theory constitutes the basis of modern electro-kinetics theory. The utilization of the mixed-potential theory can be best demonstrated by considering mixed electrodes. A mixed electrode is an electrode or metal sample, which is in contact with two or more oxidation-reduction systems. The corrosion behavior of iron in water is shown in Figure 4. Under these conditions the water corrodes the iron and the electrochemical reactions occurring can be represented as shown in Figure 4. If we consider an iron electrode in equilibrium with its ions, it would be represented by a reversible potential corresponding to the iron-iron ion electrode reaction (E_{Fe}), and a corresponding exchanging density, i^{Fe} . (reference Figure 4)

9

Likewise, if we consider the oxygen-hydroxyl-electrode reaction occurring on an iron surface under equilibrium conditions, then this particular equilibrium state would be represented by the reversible potential of the hydroxyl ion electrode (E_{OH}) and the corresponding exchange current density for this reaction on an iron surface, i^{OH}. (See Figure 4).

However, if a piece of iron is immersed in water containing some iron ions and dissolved oxygen, the electrode will not remain at either of these two reversible potentials but will seek an intermediate potential. Iron, since it is metallic, is an excellent
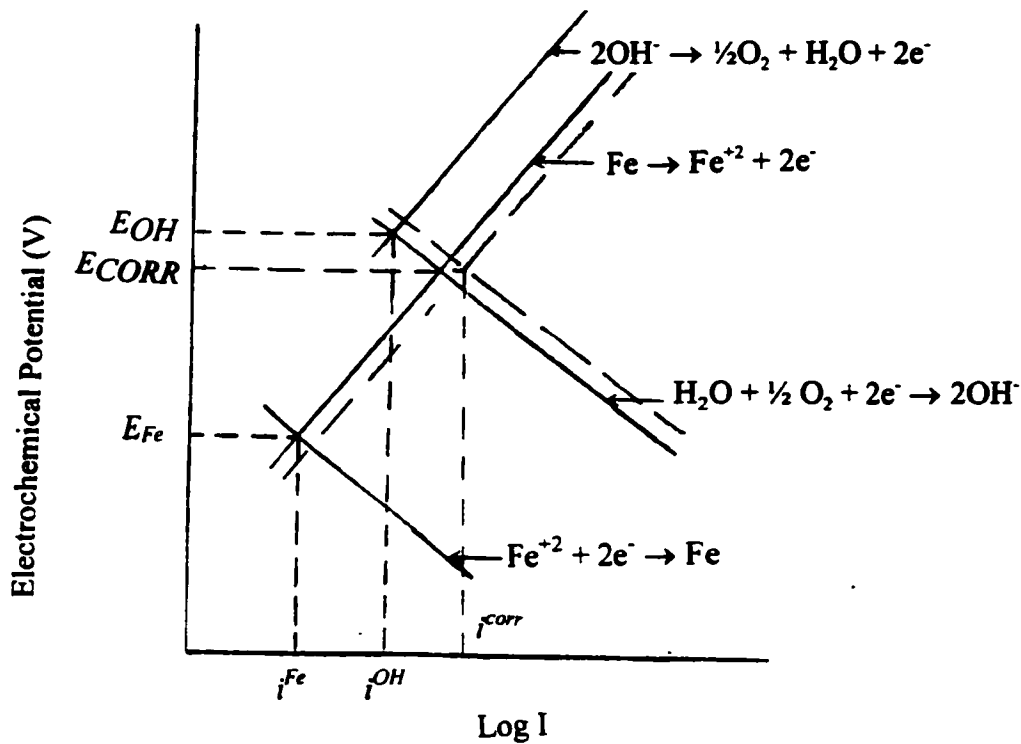
Figure 4. Electro-kinetic behavior of iron in the oxygenated water solution.

conductor, and its entire surface must be at a constant potential. This potential is achieved

when the second hypothesis of the mixed potential theory is satisfied; that is, the total rate

of oxidation must equal the total rate of reduction. Examination of Figure 4. Illustrates

this principle graphically. The total rate of oxidation is determined by summing the

individual oxidation currents corresponding to hydroxyl ion oxidation and iron oxidation

at constant potential. In a similar fashion, the total rate of reduction is determined by

summing the total reduction currents corresponding to hydroxyl ion reduction and iron

reduction at constant potential. A horizontal line is drawn at E_{corr} since the metal is in

equipotential.

The only point of intersection is represented by a "mixed" or corrosion potential

E_{corr} and corrosion current density i^{CORR} At this point; the rate of iron dissolution is equal

to the rate of oxygen consumption expressed in terms of current density. For every iron

ion which is released, two electrons are used in the reduction of oxygen to hydroxyl ion.

The current corresponding to this point is usually called corrosion current density i_{corr},

since it represents the rate of iron dissolution. This is shown along the current density axis

on the logarithmic plot of Figure 4.

The effect of the hydrogen water chemistry is shown in Figure 5. In HWC,

hydrogen is supplied to reduce the oxygen content of the water. As the oxygen content of

the solution is reduced, the reversible potential for the reduction of oxygen is shifted from

the original E_0 to E_0'. As shown in Figure 5, this also serves to lower the E_{corr} value to

E_{corr}'.

An entirely different effect is shown in Figure 6. A sacrificial anode is immersed in the iron electrode and the oxygen-hydroxyl ion electrode. This system is schematically illustrated in Figure 6. Note that potentials are indicated for the three redox systems, iron-iron ion, oxygen-hydroxyl ion, and sacrificial anode-sacrificial anode ions. The basic principles of the mixed - potential theory also apply to this system. At steady state, the total rate of oxidation is determined by summing the individual oxidation currents corresponding to sacrificial anode oxidation, hydroxyl ion oxidation and iron
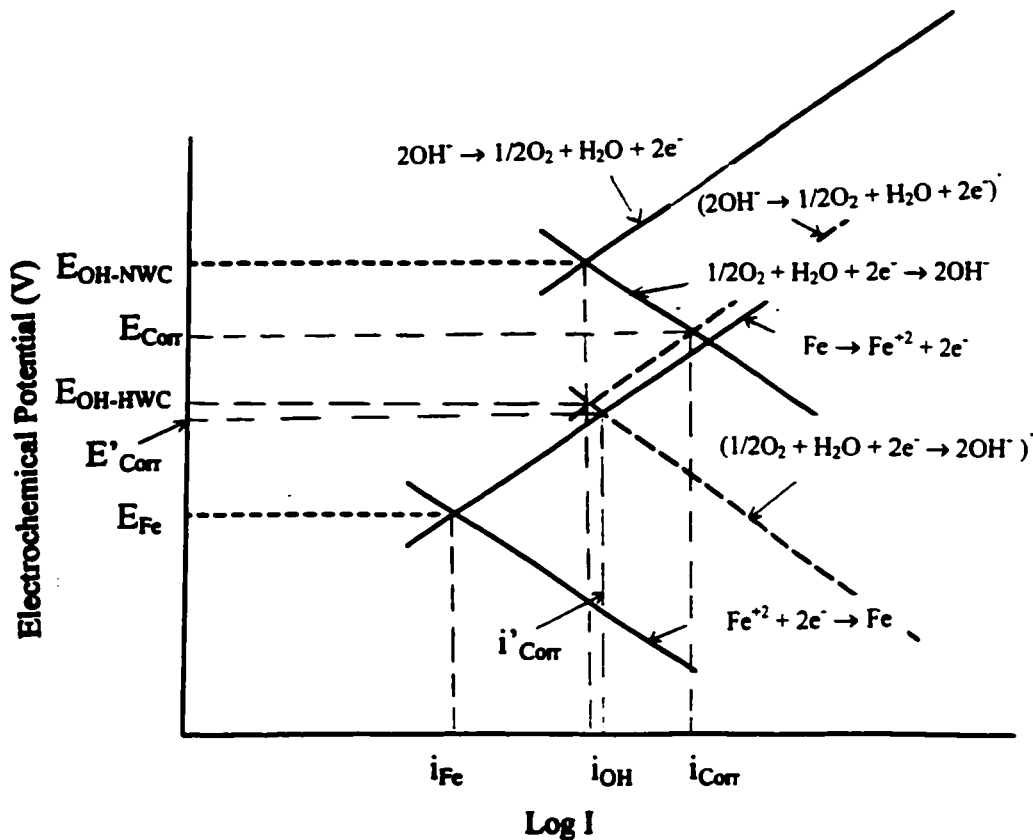
Figure 5. Electro-kinetic behavior of iron in a lower than the 200 dissolved oxygen water solution.

12

oxidation at constant potential. This is shown by the dashed lines in Figure 6. In a similar fashion, the total rate of reduction is determined by summing the total reduction at constant potential. A horizontal line is drawn at E_{corr} since the metal is equipotential. As a result, the addition of the sacrificial anode shifts the corrosion potential to E_{corr}' and decreases the corrosion from the iron i_{corr}' to i_{O2}. Based on this principle, this study investigated whether the E_{corr} value could reduced to or below the critical E_{corr} (-230 mV_{SHE}) value when the SS-304 was connected to the sacrificial anodes.
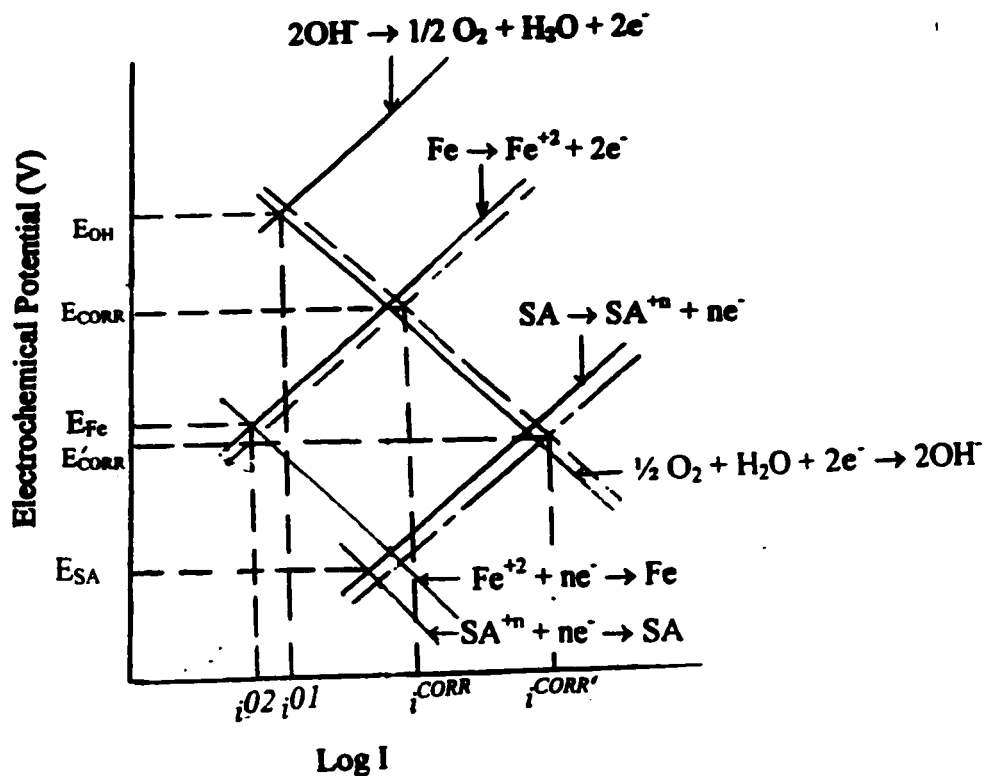
Figure 6. Electro-kinetic behavior of iron in the presence of sacrificial anode.

13

2. Literature Review

2.1 D. D. Macdonald's Research

D.D.Macdonald et.al. reported the following: [2]

(1) The corrosion potentials of SS-304 in simulated BWR environments become more positive with time and eventually approach an equilibrium value, provided that the composition of the aqueous environment is invariant.

(2) The pH of the water increases slightly (by approximately 0.1 to 0.2 units from neutral) over a typical 10-day experiment, presumably due to consumption of protons by corrosion of the metallic flow loop.

(3) Little difference exists between the corrosion potentials of type 304 stainless steel and Alloy 182, thus indicating that the kinetics of corrosion and the reduction of oxygen and hydrogen peroxide and the oxidation of hydrogen are similar.

(4) At intermediate oxygen concentrations (10-500 ppb), the corrosion potentials of type SS-304 is sensitive to the flow velocity as predicted by the mixed potential model (MPM). The MPM predicts that at low to moderate oxygen concentrations (1 to 100 ppb), it is possible to increase the potential of the steel to above the crucial value for IGSCC simply by changing the flow velocity of the fluid.

(5) Hydrogen peroxide is more effective in displacing the ECP of 304 SS in the positive direction than oxygen for equivalent concentrations and flow rates. However, the increase is not as large as expected from theory. The discrepancy is attributed to the thermal decomposition of H_2O_2 in the experiments, particularly at high peroxide concentrations.

The electrochemical potentials of SS-304 were reported as a function of dissolved oxygen content. So, we aim to compare our values with the values reported by Macdonald, et al.

2.2 C.C. Lin's Research

C.C. Lin et. al. [3] in their paper came to the following three points:

(1) Preliminary stainless steel ECP models for O_2/H_2 and H_2O_2/H_2 were developed. A simple method to estimate the combined ECP in a mixture of O_2, H_2O_2 and H_2 was presented.

(2) The calculated results agreed fairly well with actual plant in-core ECP measurements.

(3) The ECP model should be improved with an expanded database and a theoretical formulation. Overall accuracy of ECP prediction could be improved with improved radiolysis model calculations.

Similar to the report by Macdonald, the electrochemical potentials of SS-304 were reported as a function of dissolved oxygen content at 550°F. Our values can be compared with lin's result.

2.3 Kim's Research

Kim [4] reported that Pt and Pd alloying additions to engineering materials improved the catalytic efficiency of hydrogen and oxygen recombination in high

temperature with relatively small amounts of hydrogen. Low ECP values (below the critical value of -230 mV$_{SHE}$ for IGSCC protection) were achieved even at relatively high oxygen and hydrogen-peroxide levels. This study gives the idea of the critical value of the electrochemical potential below which we can protect the IGSCC in BWR.

2.4 Detailed MPM Modeling

The development of a Mixed Potential Model (MPM) requires the values of certain constants to fit the model to a particular corrosion system. Such a model was developed by D.D. Macdonald [4]. The MPM is based on the basic principal of charge neutrality. Thus conservation of electric charge demands that the summation of the currents generated by any redox couples be equivalent to the total corrosion current.

$$\sum_{j=1}^{n} i_{O/R,j}(E) + i_{corr} = 0$$

Eq 2.1

where $i_{R/O,j}$ is the partial current density generated by the jth redox couple in the system and i_{corr} is the corrosion current density on the substrate [6]. The current density for any redox couple

$$R \Leftrightarrow O + ne$$

Eq 2.2

may be expressed in terms of a general Butler-Volmer equation as:

$$i_{O/R} = \frac{e^{(E-E_{O/R}^{\circ})/b_a} - e^{-(E-E_{O/R}^{\circ})/b_c}}{\dfrac{1}{i_{o,O/R}} + \dfrac{1}{i_{l,f}}e^{(E-E_{O/R}^{\circ})} - \dfrac{1}{i_{l,r}}e^{-(E-E_{O/R}^{\circ})/b_c}}$$

Eq 2.3

16

where $i_{0,O/R}$ is the exchange current density of the oxidation/reduction couple and $i_{l,f}$ and $i_{l,r}$ are the mass-transfer limited currents for the forward and reverse directions of reaction in Eq. 2.2 respectively, $E_{c/R}^e$ is the equilibrium electrode potential for this reaction as computed from the Nernst equation

$$E_{O/R}^e = E_{O/R}^o - \frac{2.303RT}{nF} \log\left(\frac{a_R}{a_O}\right)$$

Eq 2.4

where a_R and a_O are the thermodynamic activities of reductants and oxidants, respectively. $E_{c/R}^e$ is the equilibrium electrode potential, $E_{o/R}^o$ is the standard electrode potential and b_a and b_c are the anodic and cathodic Tafel constants [6]. Limiting currents can be calculated using

$$i_{l,O/R} = \frac{\pm 0.016nFDC_{O/R}^b \ Re^{0.86} \ Sc^{0.33}}{d}$$

Eq 2.5

where the sign depends upon the direction of the reaction (+ for forward), $C_{O/R}^b$ is the bulk concentration of O or R, as appropriate, Re is the Reynolds number (Re=Vd/v) of the electrolyte (cooling water), Sc is the Schmidt number (Sc=v/D), d is the channel diameter, V is the flow velocity, v is the kinematics viscosity, F is the Faraday constant, and D is the diffusivity of the reacting species [6]. Equation 2.5 was derived from the hydrodynamic correlation for turbulent flow through a pipe [6]. The channel diameter can be taken as the physical diameter of the pipe or as the hydrodynamic diameter calculated from hydrodynamic correlations when known.

The redox reactions of interest in this study are oxidation of the hydrogen

$$H_2 \Leftrightarrow 2\,H^+ + 2e^-$$ Eq 2.6

and the reduction of oxygen and hydrogen peroxide

$$O_2 + 4H^+ + 4e^- \Leftrightarrow 2\,H_2O$$ Eq 2.7

$$H_2O_2 + 2\,H^+ + 2e^- \Leftrightarrow 2\,H_2O$$ Eq 2.8

The Equilibrium potentials are calculated from the Nernst equation

$$i_{corr} = \frac{e^{(E-E_0)/b_{f}.s} - e^{-(E-E_0)/b_{r}.s}}{\dfrac{1}{i_p^o} + x}$$ Eq 2.9

$$x = \frac{e^{(E-E_0)/b_r.s}}{i_p^o e^{[0.523(E-E_0)^5]}}$$ Eq 2.10

The values for the various parameters are given in Table 2. Equation 2.9 These values were developed empirically and provide a reasonable representation of existing data [6].

Because of uncertainty in the kinetic parameters for the oxidation of hydrogen and the reduction of oxygen and hydrogen peroxide, Macdonald chose to regard the exchange current densities for these reactions as adjustable parameters so that the model species are known simultaneously. This is done by multiplying the exchange current densities for the oxidation of hydrogen and the reduction of oxygen and hydrogen peroxide by the scaling factors, SF(H$_2$), SF(O$_2$), SF(H$_2$O$_2$) respectively. These scaling factors can initially be taken from systems, where possible, that contain only a single eletroactive species. This

taken from systems, where possible, that contain only a single eletroactive species. This

can subsequently be adjusted to fine-tune the model to a system containing multiple

Table 2. Values for parameters in the Mixed Potential Model [6].

Parameter	Value
$E_{H_2}^0$ (V vs SHE)	0
$E_{O_2}^0$ (V vs SHE)	$1.518489-0.001121T + 6.024 \times 10^{-7}T^2 -3.2733 \times 10^{-10}T^3$
$E_{H_2O_2}^0$ (V vs SHE)	$1.978968-7.23 \times 10^{-4}T-9.888 \times 10^{-6}T^2+3.6793\times10^{-10}T^3-1.37202\times10^{-13}T^4$
PK_{H_2}	$-1321/T+10.703-0.010468T$
PK_{O_2}	$-1202/T+9.622-0.009049T$
ρ (g/cm2)	$-4.1359-5.1788 \times 10^{-2}T-1.0911 \times 10^{-4}T^2+3.0193\times10^{-7}T^3-1.7809\times10^{-16}T^4$
ln [v(cm²/s)	$-6.140834-1103.164/T-457155.3/T^2$
ln[D_{H_2} (cm²/s)]	$-5.700267-296.7439/T-288379.2/T^2$
D_{O_2} (cm²/s)	$8.03\times10^{-3} \exp (-3490/RT)$
$D_{H_2O_2}$ (cm²/s)	D_{O_2}
$i_{H_2}^0$ (A/cm²)	$0.0114841xC_{H_2}^{0.5}$ x exp(-14244/RT)
$i_{O_2}^0$ (A/cm²)	$0.0114841xC_{H_2}^{0.48633}$ x exp(-14244/RT)
$i_{H_2O_2}^0$ (A/cm²)	$i_{O_2}^0$
b_{1,H_2} (V)	0.065
b_{1,O_2} (V)	0.071
b_{1,H_2O_2} (V)	b_{1,O_2}
$b_{1,ss}$ (V)	0.06
E_0 (V vs SHE)	$0.1211-15286 \times 10^{-3}T$
i_p^0 (A/cm²)	$2.6 \times 10^{-3}\exp(-4416/T)$

electroactive species [6]. This approach provides the opportunity to employ these

relationships in various pressure vessels, both BWRs and laboratory autoclaves, by

modifying this exchange current density scaling factor so that the equations accurately

predict the behavior of alloys in a specific vessel. This is one of the primary goals of the

characterization of an autoclave for BWR/ECP studies.

The Eq 2.9 shows that the Reynolds Number is related to the limiting currents. Since, the flow rate is related to the Reynolds Number, the flow rate is also related to the corrosion current and the electrochemical potential.

3. Experimental

The use of applied potentials may provide a reasonable alternative to use of HWC and the Pt/Pd method to reduce and maintain the ECP of BWR internal components to less than -230mV (SHE), which is the level considered essential for complete protection against IGSCC. That is, electrons will be "injected" directly into the structure to decrease the ECP rather than relying upon hydrogen to recombine with oxygen in order to decrease the ECP. By polarizing the components themselves, rather than relying upon the introduction of hydrogen to recombine with the oxygen generated in the core, problems associated with ^{16}N could be eliminated. Further, components near the top of the vessel which cannot be effectively protected by hydrogen injection, can be polarized to potentials that are below the critical potential for protection. This is essentially the same approach that is used to cathodically protect buried piping, condenser water boxes, and numerous other components which are exposed to aggressive environments.

3.1 Environment Facility

Because of the difficulty in accessing the inner workings of a BWR and the inherent dangers of such, the fabrication of a small controlled environment that accurately depicts a BWR environment is highly desirable. Laboratory autoclaves, when properly constructed, have been shown to accurately simulate the environment found in light water reactors[6]. Several studies have been published in the last several years using both recirculating and single pass systems. The recirculating system has the primary overall

21

advantage of being a closed system, thus making the control of the water chemistry for extended run periods less cumbersome. A recirculating autoclave system has been chosen as the environment for this study and its design and fabrication have become an integral part of the project (Figure 7).
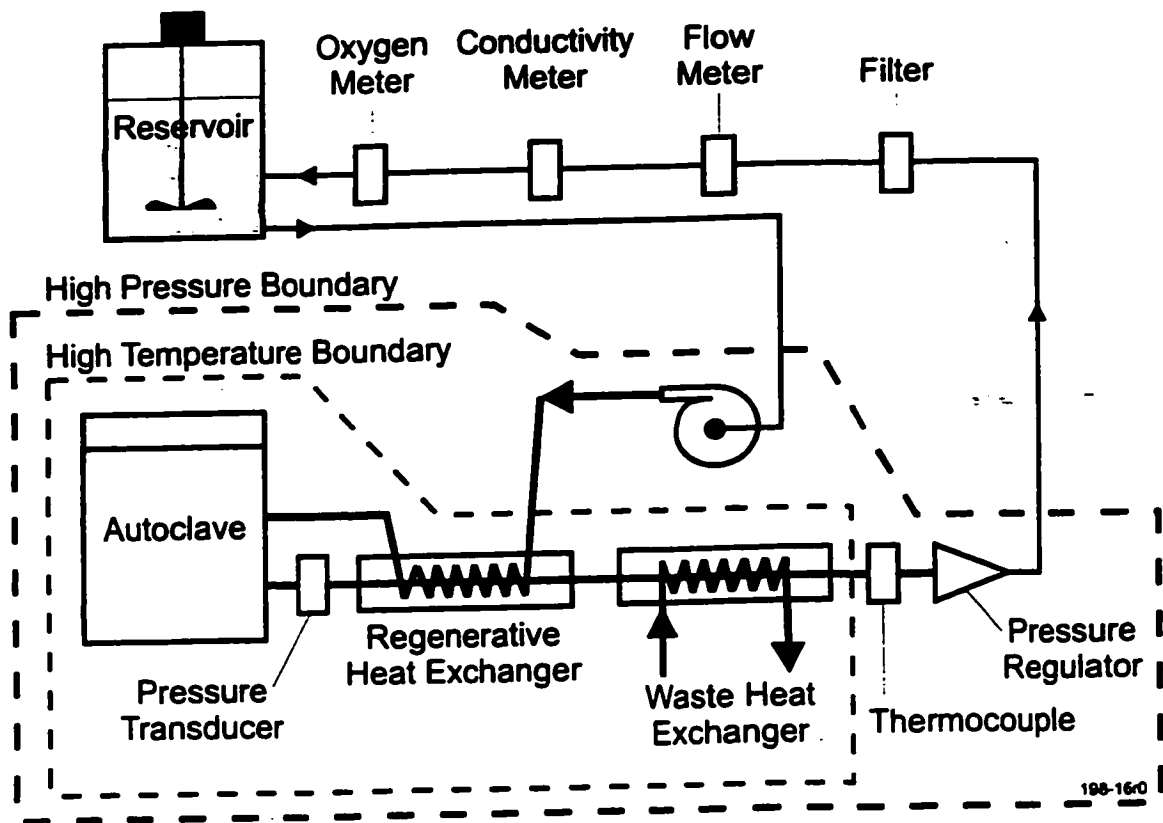

Figure 7. Schematic drawing of laboratory autoclave system.

3.1.1 Pressure Vessel

The autoclave was designed by Autoclave Engineers in Erie, Pennsylvania, and has the specifications listed in Table 3.

Table 3. Autoclave Design Specifications.

Property	Specification
Internal Volume	1 liter
Design / Operating Pressure	5000psig
Operating Temperature	550°F
Material	Inconel Alloy 600
Head #1	Solid Inconel Alloy 600
Head #2	Same as #1 fitted with a load rod and cage for CERT tests (1000lb max. loads)
Flow Rate	30GPH
Inlet / Outlet Size	¼" (for ¼" SS tubing)

3.1.2 High Pressure Loop

The high-pressure loop begins at the system pump. The pump is a Milton Roy model Milroyal B simplex unit with a SS-316 head and PTFE/Elastomer bond diaphragm. The unit is capable of delivering 36.5 GPH at 1000psig. The pressure loop also contains two heat exchangers. The regenerative heat exchanger utilizes the pressure vessel outlet stream to heat the inlet stream prior to its final heating in the autoclave. The waste heat exchanger transfers the remaining heat to a closed cooling system, bringing the fluid to ambient temperature before entering the low-pressure loop. Both heat exchangers were constructed of SS-316 fittings and tubing. The system is shown schematically in Figure 7.

The high-pressure portion of the loop terminates at the pressure regulator. The back pressure regulator used in this system is a diaphragm type regulator with nitrogen gas pressure on one side of the diaphragm and the test environment on the other. This allows for maximum control over the pressure of the system. The pressure is regulated by the application of a pressurized gas on the outside of the diaphragm equal to the pressure desired in the system. This type of back pressure regulator gives superior control over system pressure to that of spring type regulators. This control capability permits the operator to increase or decrease the system pressure with temperature allowing for higher flow rates from the pump and faster cool down times. The operation of this device at high pressures is overridden by a rupture disc at the autoclave. If the system is allowed to attain too high pressures, the diaphragm will burst venting the water to a drain, and allowing the system to equilibrate with the surroundings. This ensures maximum safety of the environment around the system.

The autoclave is fabricated from Inconel 600. The high-pressure loop piping is entirely constructed of SS-316 and is designed to carry nominal operating loads of 5,000psig. All calculation packages used to justify pressure and thermal load carrying capability and thermal stability (heat exchanger efficiency) were reviewed by qualified personnel prior to fabrication.

3.1.3 Low Pressure Loop

The low-pressure loop is constructed of the same materials as the high-pressure loop but contains devices that cannot operate at either the high temperatures or high

pressures. The control of the chemistry and flow of the loop is originated from the low-pressure loop. As can be seen in Figure 7, the low pressure loop contains devices for monitoring water flow, oxygen concentration and water conductivity. The polyethylene reservoir/mixing station is the point of mixing and introducing the chemicals that will simulate the BWR environment. These additives include, oxygen gas, hydrogen peroxide, aqueous ferric ions and hydrogen gas. The low-pressure loop is operated at less than 100°F and 30 psig.

3.1.4 Reference Electrode

The silver/silver chloride half-cell was the first solid reference electrode used in anodic protection systems [12]. It is also used in laboratory investigations and in marine applications of cathodic protection. Silver/silver chloride electrodes are based on the reaction in equation 4.1.

Ives and Janz [5] report that the electrodes can be formed by electrolytic, thermal or precipitation methods[6]. These electrodes have also been formed using melt-casting techniques. Electrodes used in anodic protection systems have been formed by one or more variations of the melt casting techniques in which molten silver chloride is poured around silver metal or the metal is dipped in the melt.

$$AgCl + e^- \rightarrow Ag + Cl^-$$
<div align="right">Eq 4.1</div>

There are difficulties in manufacturing the melt-cast electrodes. If the casting is made at a temperature much above the melting point, the electrode develops a high internal impedance. This impedance is so high that measurement of the potential of Ag-

AgCl reference electrode requires an electrometer or other high-input voltmeter. Melt-cast electrodes of this type are rugged and stable and can be easily mounted for entry into a vessel. Silver/silver chloride electrode half-cells have been used in storage vessels containing sulfuric acid at concentrations up to 100%.[9]

3.2 Candidate Materials and Considerations

Candidate anode materials were selected based upon their expected open circuit potential in a BWR environment. Successful candidates met the following minimum criteria:

1) Must shift the ECP of SS-304 to a value less than -230mV$_{SHE}$.

2) Must have a reasonable expected life in a BWR environment. This includes consideration of corrosion rate, structural integrity, resistance to neutron and hydrogen embrittlement, and vibrational fatigue.

3) Must not produce undesirable corrosion products that would create problems in the core of the reactor (i.e., harmful isotope generation), deposit on existing parts, or compromise the clarity of the water in the system.

A limited galvanic series in typical BWR environments will be defined for the candidate anode materials:

(A) Carbon steel

(B) Iron

(C) Gray Cast Iron.

(D) Aluminum

(E) Zirconium,

(F) Zircalloy.

(G) Magnesium

(H) Zinc

3.3 Laboratory Demonstrations

The ECPs of the candidate sacrificial anode materials were measured in high purity water between the 250°F to 550°F, 50-8000 ppb dissolved O_2 and at 1000 psi pressure in the laboratory. Their effectiveness in reducing the potential of stainless steel specimens and thus their ability to mitigate IGSCC, was evaluated.

Task 1. Simulated BWR Conditions

Table 4. The tests temperatures and dissolved oxygen contents.

Temperature (°F)	Dissolved Oxygen Content (ppb)
250	50 (typical HWC)
350	200 (typical BWR normal level)
550	8000 (equilibrium with air; useful for accelerated IGSCC testing)

Task 2. Coupled Potentials.

The electrochemical effectiveness of candidate anodes was tested in typical and accelerated (e.g., high oxygen) BWR environments. The key question asked was, "Can the

27

potential of sensitized stainless steel in oxygenated water be brought to <-230 mV by coupling to a more active metal"? Environmental factors such as temperature and dissolved oxygen content were evaluated. This was done by measuring the open circuit potential between the Ag-AgCl reference electrode and the coupled SS-304 and the candidate sacrificial anode materials. The distance between each electrode was 1.5 inch and the shape of the candidate materials was long cylindrical shape.

3.4 Experimental Preparation

The first subsection discusses the design of the specimens, the specimen holder and the design of the Ag-AgCl reference electrode. The experimental measurements and calculations section outlines the measurement using a saturated calomel reference electrode and a Ag-AgCl reference electrode. The last section discusses potentiostatic and potentiodynamic scanning procedures.

3.4.1 Design of specimens and specimen holder

The diagram of the metal test specimen is shown in Figure 8. The specimens prepared were Iron, Gray Cast Iron, Magnesium, 1018 Carbon Steel, Zinc, Zirconium, Aluminum, Zr-Alloy, Steel-316 and Steel-304. All the specimens were tapped (56 threads per inch) so that they could be attached to the specimen holder.

A diagram of the specimen holder with the specimen is shown in Figure 9. The specimen holder was made of cylindrical steel rod with the external thread 3/32" size at both ends of the rod. In order to prevent the internal corrosion of the unthreaded portion of the specimen holder, the holder was protected by plastic (transparent) shrink tube.

Threads at both ends were unwrapped. One end of the threaded rod held the specimen and the other end held the gland. The gland is shown in Figure 11. This gland sealed the sample holder through the ceramic insulator gland and the whole assembly was housed in the autoclave. The diagram of the autoclave flange with the indication of electrodes is shown in Figure 10.
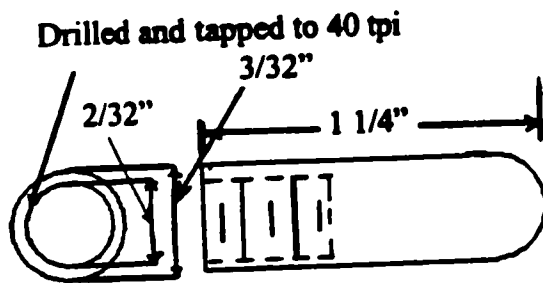
Figure 8. Design of Specimen.
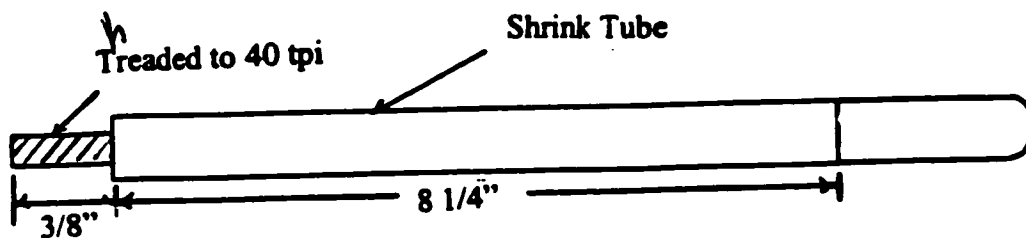
Figure 9. Design of the specimen holder.

3.4.2 Design of Ag-AgCl reference electrode

The Ag-AgCl reference electrode was designed by NWT Manufacturing Corporation (Santa Clara, CA). This electrode is designed to withstand a working pressure of 4000 psig and a maximum working temperature of 330°C (626°F) provided that the Teflon seal temperature was kept ≤45°C. A diagram of this electrode is shown in

Figure 12. The electrode demonstrated long term reliability at pressures ranging from 900

psig to 1350 psig and dozens of thermal cycles. The source impedance of the reference
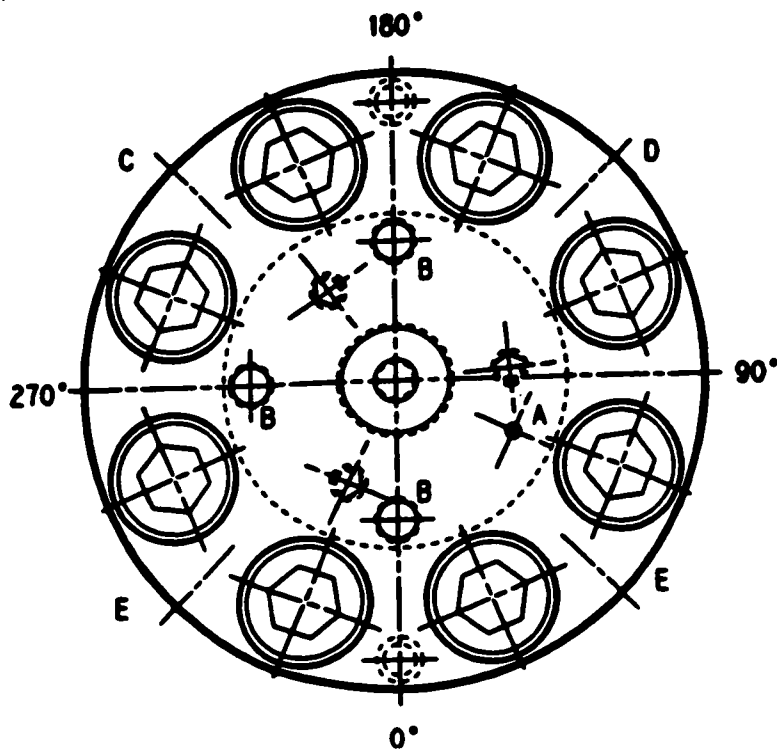
Opening	Purpose
A	Thermowell
B	Opening for sample holder
C	Safety head
D	Vent/Gauge
E	Supply water
F	Position for Ag-AgCl reference electrode

Figure 10. Design of the autoclave head. [11]
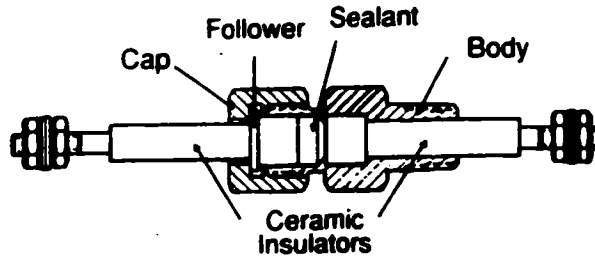
Figure 11. Design of the sealing. [9]

electrode is approximately one mega-ohm resistance. The materials used in the construction of the electrode are the following:

1. Electrode housing with integral cooler, ASME Specification SA-479, Grade 304.

2. Conax fitting, ASTM Specification SA-479, Grade 304.

3. Teflon, virgin TFE.

The electrochemical potential (ECP) measuring circuit was designed as follows. A high impedance voltmeter with a nominal 10^{11} ohms input impedance was used. A coaxial cable connected the electrode output to the high impedance voltmeter. The standard electrical connection for the R201 electrode was a LEMO brand coaxial connector. The electrode was supplied complete with a cable-connectable mating component.
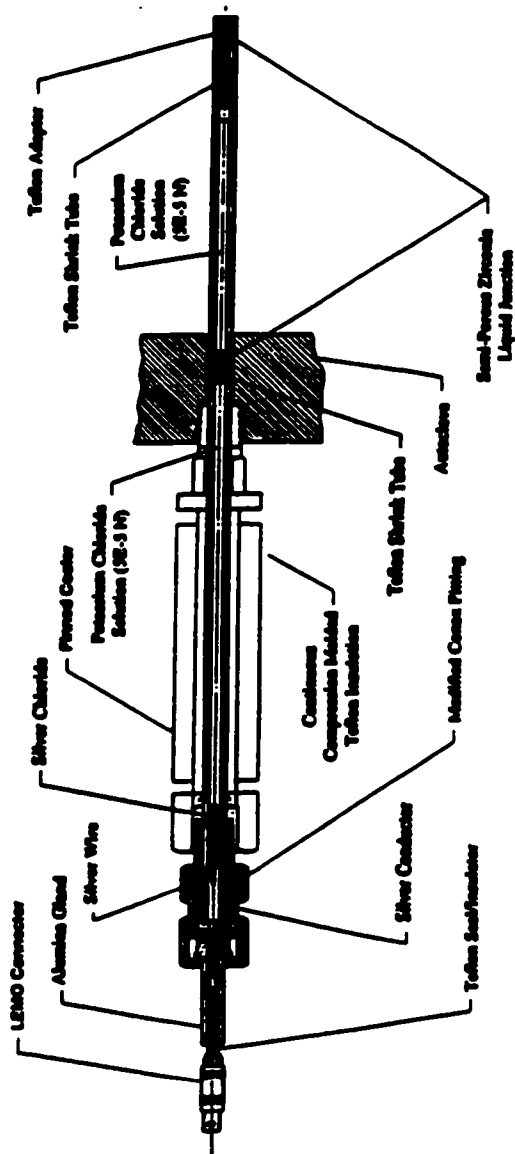
Figure 12. NWT R201, High temperature, High Pressure Ag-AgCl reference electrode.

The R201 Ag-AgCl reference electrode was filled with 5N potassium chloride and had long-term, drift-free reference electrode performance.

3.4.3 Specimen Preparation

Before each electrochemical potential study the specimen surfaces were cleaned with 600 grit paper. After that, the specimens were soaked in soapy water and then rinsed and dried.

3.5 Measurement and calculation of electrochemical potential (ECP)

3.5.1 Measurement of Electro-Chemical Potential (ECP) with respect to Saturated Calomel Electrode at ambient condition

The elctrochemical potential (ECP) values were measured with respect to the saturated calomel electrode (SCE). However, the ECPs were reported vs. the standard hydrogen electrode (SHE) potential for comparison. A diagram of the saturated calomel electrode is shown in Figure 13. This electrode consists of a platinum wire in contact with mercury and mercurous chloride solution. This is held within a thin glass tube by a porous plug, and the glass tube is contained inside a large glass tube, again with a porous tube at the end. The larger tube contains saturated potassium chloride solution. The porous plugs allow the passage of ions (and hence current) without causing significant cross contamination of the potassium chloride and the electrolyte of the test cell. [11]

In these measurements, the SCE reference electrode and the sample holder were held with clamps. Both the reference electrode and the metal sample were immersed in distilled water and connected to the Fluke multimeter, and the electrochemical potentials (ECP) were measured. The Fluke multimeter was used because the saturated calomel electrode

did not have high resistance electrode (one megohm resistance) like Ag-AgCl reference. This procedure was repeated with each of the test specimens: Iron, Gray Cast Iron, Magnesium, Carbon Steel1018, Cadmium, Zirconium, Zinc, Aluminum, Zr- alloy, Stainless Steel-316, Stainless Steel-304.
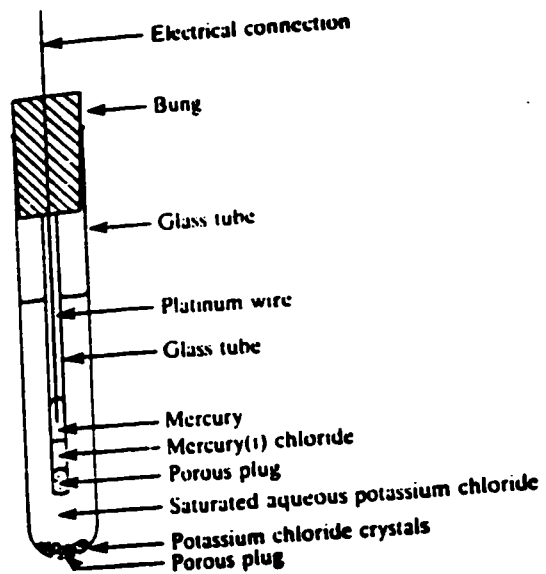
Figure 13. Saturated calomel reference electrode. [11]

3.5.2 Measurement of Electro-Chemical Potential (ECP) with respect to Ag-AgCl reference Electrode at different temperature, dissolved oxygen and 1000 psi pressure conditions

The electrochemical potential (ECP) of the specimen at high temperature and pressure was measured using the Ag-AgCl reference electrode which was designed for these conditions. First, the Ag-AgCl reference electrode and specimen holder plus the specimen were placed in the proper position in the autoclave as shown in Figure 13. The HP Model 342 high impedance voltmeter was connected to the reference electrode (positive) and the other end to the specimen (negative). Then the BWR loop was filled with water from the reservoir .

3.5.3 Setting up experimental conditions and ECP measurement

The dissolved oxygen content in the distilled water supplied to the BWR loop was initially more than 8000 ppb. Argon-gas was purged through the reservoir water in the BWR to reduce the oxygen content to less than 8000ppb. Since the argon is a noble gas, it does not react with other elements, and the oxygen from the reservoir water is mechanically removed to reduce the dissolved O_2 in the reservoir water. The content of the dissolved oxygen was measured by the dissolved oxygen probe which was attached to the low pressure side of the loop.

The pressure at the high pressure side of the loop was set at 1000 psi. Under these conditions the conductivity of the water was found to be 0.76 to $0.73\mu\Omega/cm^2$. High

impedance voltmeter readings were taken at this condition. The temperature was set at 250°F. The same procedure was repeated for samples at 350°F and 550°F.

The dissolved oxygen content was next reduced to 200ppb and 50ppb and the above steps were repeated. High impedance voltmeter readings were taken at 250°F, 350°F and 550°F.

This procedure was repeated for each of the specimens. It took ten minutes to get the equilibrium readings and then readings were taken every five minutes at each experimental condition and the average of the high impedance voltmeter was calculated.

3.6 Setting up the Potentiostat

A Princeton Applied Research (PARC), Model 173 potentiostat was used for the potentiodynamic scanning. The schematic for the experimental setup is shown in Figure 14. For general operations, two cables were used to connect the Model 173 to the cell. The cell cable was connected to the color clip leads (red, green, white), and the electrometer cable was connected to the Model 173 electrometer.
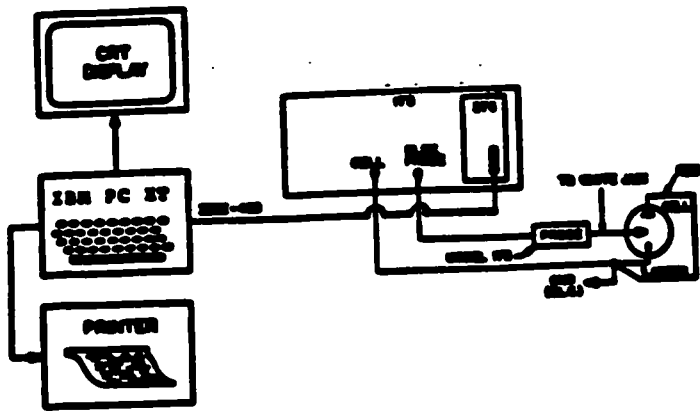
Figure 14. PARC Model - 173 Connections. [13]

4. Results and Discussion

There are three sections in this chapter. The first section presents the electrochemical potentials (ECPs) for different metals with respect to a saturated calomel electrode (SCE) at ambient conditions. The second section presents the electrochemical potentials (ECPs) for different metals with respect to a Ag/AgCl reference electrode at high temperature with controlled amounts of dissolved oxygen. That is, both series of measurements are the open circuit potential (OCP). The third section presents ECP measured from the potentiodynamic scans and determines the effect of dissolved oxygen and temperature. The analysis of the potentiodynamic scans are included.

4.1 Electrochemical Potentials of different metals with respect to saturated calomel electrode at room temperature and atmospheric pressure

The ECP values of the eleven metals and alloys were measured against a saturated calomel electrode in water using a Fluke multimeter. The ECP values are listed "as-measured" with respect to standard calomel electrode (SCE) in Table 5. In ECP measurement, the distance between the saturated calomel electrode (SCE) and the specimen was kept constant because the values could change with the distance. For comparison with our results, the Galvanic Series (at 77°F and distilled water environment) of different metals against the saturated calomel electrode (SCE) is shown in Figure 15. The ECPs in Table 5 for Fe, Mg, Al, Zn and SS-304 were within the range

38

of the reported values in published ECPs. SS-316 was just outside the reported range. So, there is a good agreement between our measurements and the published ECPs [1].

Table 5. Electrochemical potentials (vs. SCE) for different metals measured in distilled and ambient conditions.

Materials	Measured ECP (V_{SCE})	Values from Figure 15. (V_{SCE})
Magnesium	-0.703	-0.6 to -1.3
Aluminum	-0.513	-0.45 to -0.55
Zinc	-0.304	-0.1 to -0.75
Grey Cast Iron	-0.154	
Carbon Steel 1018	-0.037	
Iron	-0.032	+0 to -0.5
Cadmium	+0.003	
Zirconium	+0.018	
Zirconium-alloy	+0.02	
Stainless Steel-316	+0.05	+0.07 to +0.09
Stainless Steel-304	+0.08	+0.07 to +0.09

[1] Values reported in Jones, et al [16], and shown in Figure 15, this report.
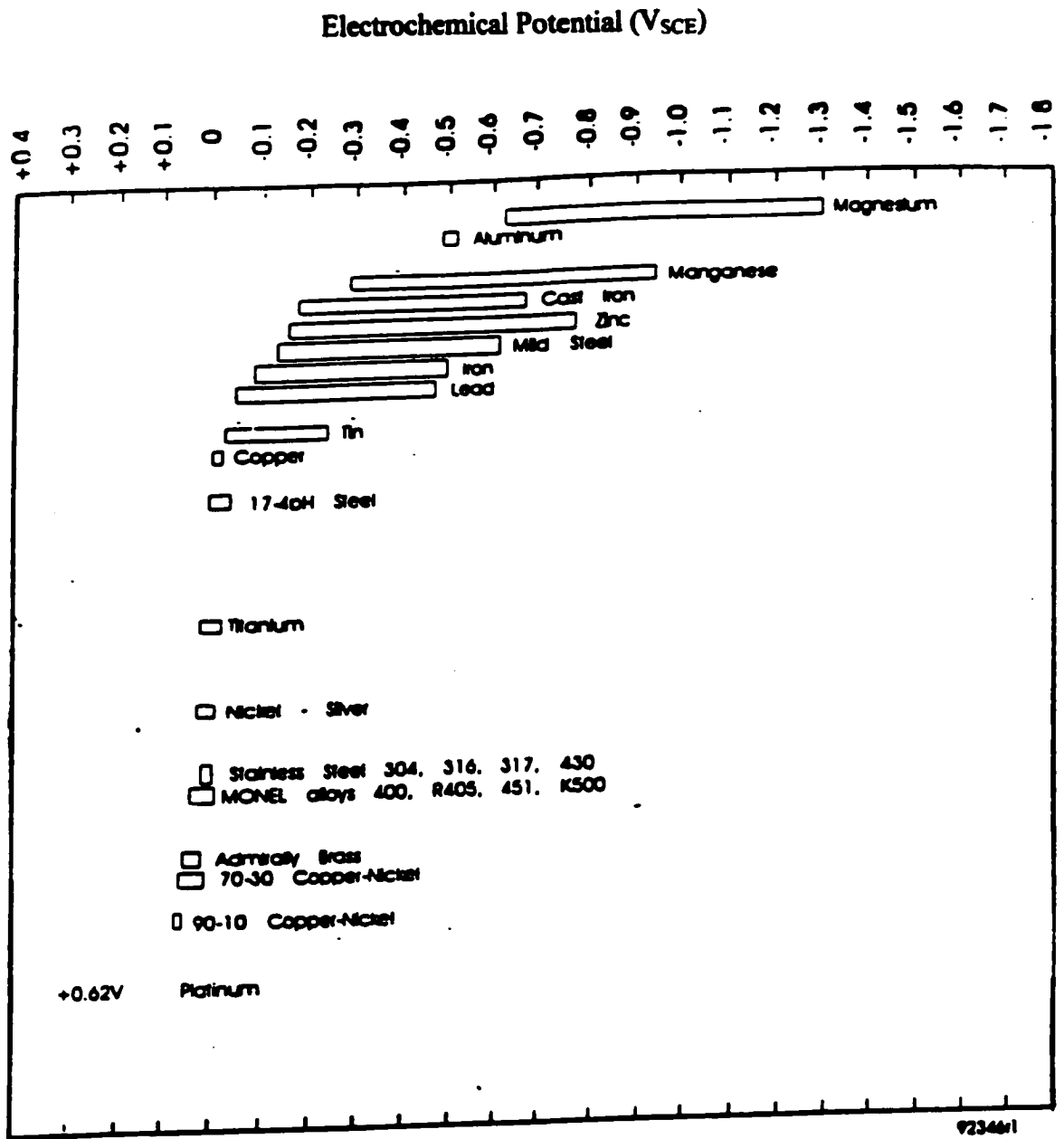
Figure 15. Galvanic series - Distilled Water at 25°C vs SCE. [16]

Table 6. Electrochemical Potential of various metals measured at different dissolved O_2 and temperatures obtained in a high impedence voltmeter (E_V) and, potentiodynamic scans (E_{PS}).

Metal Specimens	Temperature (°F)	ECP (V_{SHE}) vs. Standard Hydrogen Electrode *					
		Ev at 50 ppb	Eps at 50 ppb	Ev at 200 ppb	Eps at 200 ppb	Ev at 8000 ppb	Eps at 8000 ppb
SS-304	250	0.445	0.411	0.469	0.461	0.532	0.535
	350	0.323	0.315	0.367	0.331	0.514	0.445
	550	0.177	0.172	0.188	0.195	0.295	0.213
Zr	250	-0.036	0.063	0.282	0.162	0.136	0.212
	350	-0.156	-0.514	-0.135	-0.062	-0.216	0.124
	550	-0.697	-0.891	-0.627	-0.231	-0.598	0.121
Zr-alloy	250	0.074	-0.312	0.094	-0.272	0.152	0.445
	350	-0.253	-0.485	-0.221	-0.383	-0.186	0.091
	550	-1.047	-0.651	-1.002	-0.709	-0.617	-0.051
Mg	250	0.039	0.034	0.091	0.112	0.175	0.152
	350	-0.218	-0.185	-0.181	-0.162	0.026	-0.052
	550	-0.507	-0.505	-0.465	-0.455	-0.336	-0.182
Zn	250	-0.145	-0.115	-0.103	-0.091	-0.034	-0.065
	350	-0.608	-0.545	-0.455	-0.364	-0.255	-0.261
	550	-0.769	-0.832	-0.728	-0.631	-0.408	-0.495

* The ECPs are determined against the Ag-AgCl reference electrode then converted into standard hydrogen electrode potential.

4.2 Effect of dissolved oxygen content and temperature on the ECPs

__50 ppb O_2__ : In hydrogen water chemistry (HWC), the dissolved O_2 in water is decreased from 200 ppb to 50 ppb by injecting hydrogen into the BWR feedwater. So, the 50 ppb dissolved oxygen level is an important condition for measuring the ECPs of the different metals. The ECP values measured in water containing 50 ppb dissolved O_2 at 250°F, 350°F and 550°F are listed in Table 6 and plotted in Figure 16. In Table 6, the E_V is the electrochemical potential measured from the high impedence voltmeter and E_{PS} represents the electrochemical potential obtained from the voltammograms in the potentiodynamic study (Section 4.3). As can be seen, at 50 ppb dissolved O_2, the ECPs of SS-304, Zr, Zr-alloy, Mg and Zn become less noble as the temperature increases. The ECP of Zr-alloy is the most temperature sensitive.

The ECPs for all metals are approximately the same in high impedence voltmeter measurements and in potentiodynamic scans except for the Zr and Zr-alloy. In Zr and Zr-alloy, the oxide film forms in atmosphere or as soon as the specimen contacts the water. So, the voltmeter measured ECPs were actually the ECP of oxidized Zr in the 50 ppb oxygen water against the Ag-AgCl reference electrode. But in the potentiodynamic study, the voltage was varied from the cathodic to the anodic side of the ECP. When this happens, the oxide film of the Zr is reduced completely and we get the actual ECP for the metal. So, this oxide film makes the difference between the two measurements. This is a usual phenomenon in all conditions for Zr and Zr-alloy but for other metals this effect is negligible.
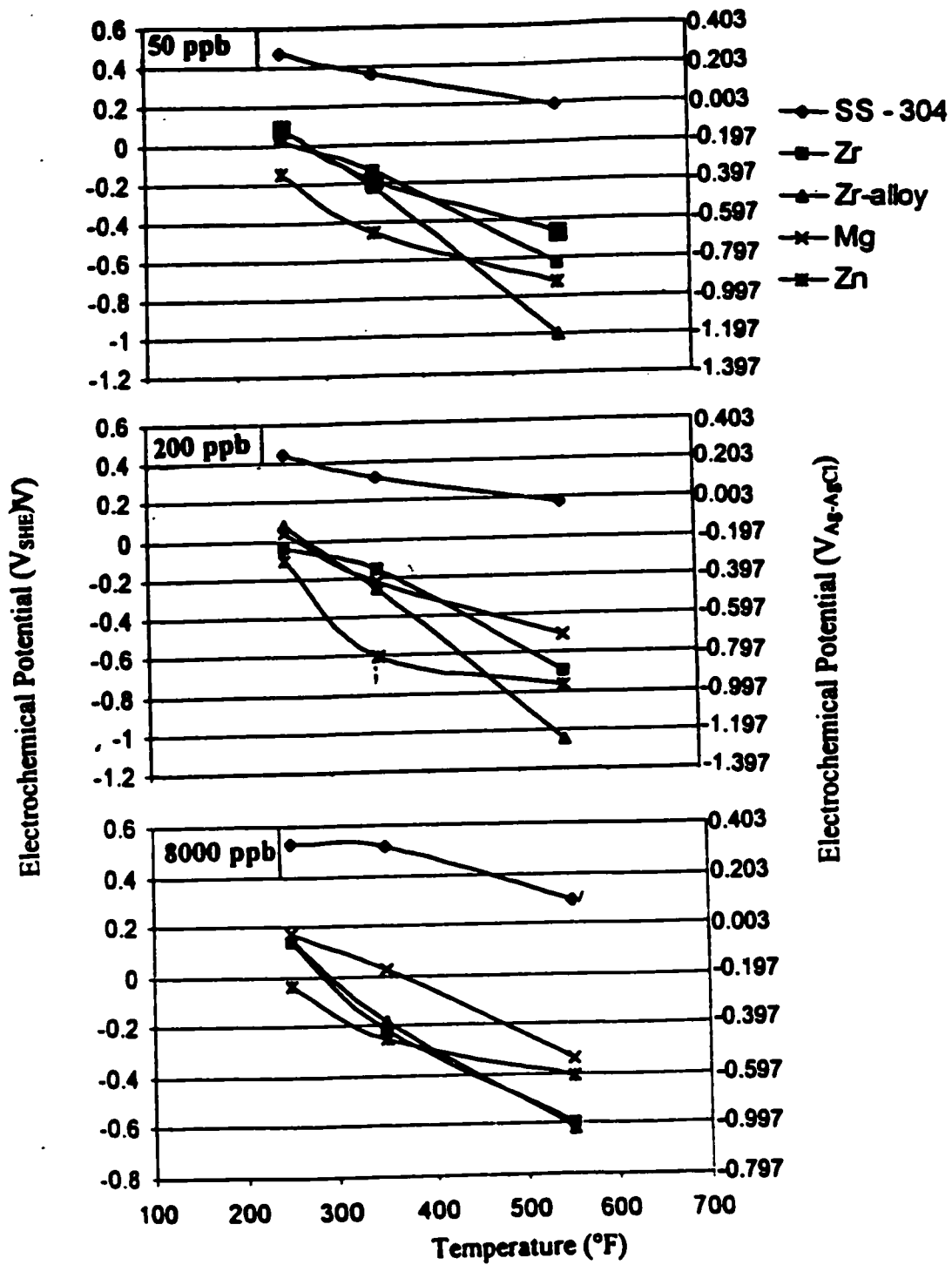
Figure 16. The voltmeter ECPs of SS-304, Zr, Mg, Zr-alloy, Zn at different temperatures

and dissolved O_2.

200 ppb O₂ : The ECPs at 200 ppb dissolved O_2 and 550°F are also very important because this is the condition during normal operation of the boiling water reactor (BWR). The ECP values are listed in Table 6. Again, the corrosion potential of all of the metals becomes more active as the temperature increases. This is observed in Figure 16. The slopes of the ECP vs. temperature plots for the different metals are less at 200 ppb O_2 than at 50 ppb dissolved O_2. The slopes are tabulated in Table 6. Zr-alloy and Mg are more sensitive to temperature than the other metals as was observed with the 50 ppb O_2 measurements. But with Zn the slope becomes more shallow above 350°F temperature. The ECP values for Zr, Zr-alloy, Mg and Zn are negative at the three temperatures while for SS-304 the values remain positive vs. the reference electrode. So, Zr, Zr-alloy, Mg and Zn remain active relative to SS-304. The ECPs of different metals in both measurements (voltmeter and potentiodynamic scans) are the same for all metals except in Zr-Zr-alloy. The reason is stated in the discussion for the 50 ppb dissolved oxygen measurements.

8000 ppb O₂ : The ECPs measured in water containing 8000 ppb dissolved O_2 at 250°F, 350°F, 550°F temperatures and 1000 psi pressure are listed in Table 6 and the plot is shown in Figure 16. The dissolved oxygen content in water at ambient is 8000 ppb. So, the 8000 ppb dissolved oxygen was chosen as a parameter for the experiments. 8000 ppb (= 8 ppm) has also been used as an aggressive test condition in many other tests. Three

Table 7. Slopes from the ECP - temperature plots.

Metal	Slope (V/°F) from Figures 16 and 18					
Specimens	S_V 50 ppb	S_{PS} 50 ppb	S_V 200 ppb	S_{PS} 200 ppb	S_V 8000 ppb	S_{PS} 8000 ppb
Mg	-0.00178	-0.00215	-0.00273	-0.0027	-0.00149	-0.002
Zn	N.L.	N.L.	N.L.	-0.0027	N.L.	-0.00195
SS-304	-0.00122	-0.00095	-0.00102	-0.0013	-0.000184	N.L.
Zr	-0.00159	N.L.	-0.00107	-0.0022	-0.00352	-0.0011
Zr-alloy	-0.00357	-0.00185	-0.00314	-0.0011	-0.00337	N.L.

generalities are evident from Figure 16. At high temperatures the ECPs of all the alloys (SS-304, Zr, Zr-alloy, Mg and Zn) are more active. The ECPs for Zn are not linear with temperature. Zr, Zr-alloy, Mg and Zn are more active than the stainless steel at all temperatures.

The effect of O_2 on the ECP at constant temperatures is seen in Figure 17. In every case, the electrochemical potentials of every metal become more noble as the dissolved O_2 increases. The ECPs change linearly as the dissolved O_2 increases except for Mg (at 550°F), Zn (at 550°F), Zr-alloy (at 550°F) and Zr (at 350°F).

For comparison, the values for SS-304 at the BWR operating conditions, and those reported by Macdonald [3] and Lin [2] are collected in Table 8. All the values from the three separate laboratories which are reported in Table 8 are relative to the standard hydrogen electrode (SHE) potential. Macdonald's ECP measurements were made using an external pressure balanced reference electrode (EPBRE) containing an Ag-AgCl electrode, and were measured at 0.3 μS/cm conductivity and at 0.12 cm/s flow rate.
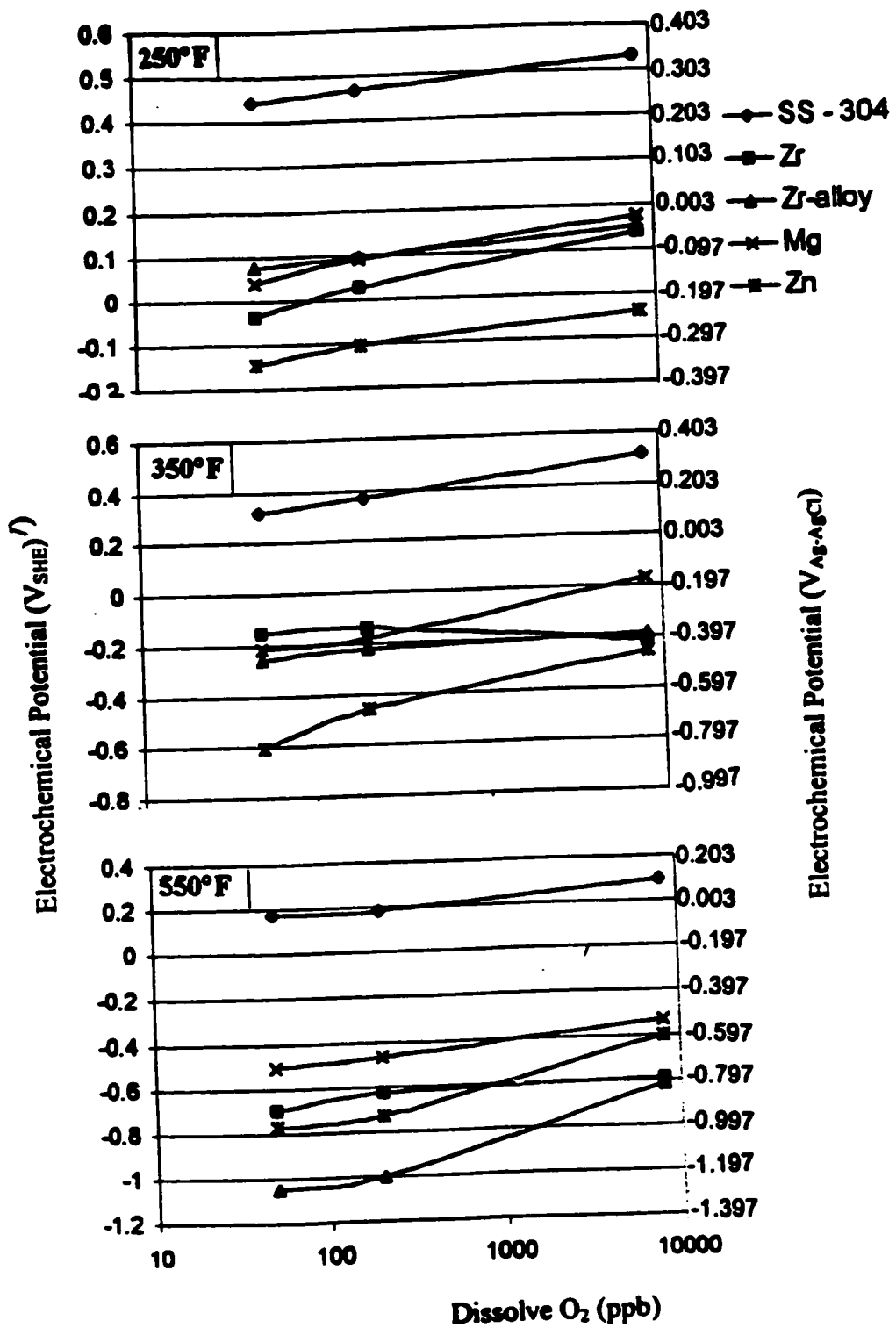
Figure 17. The ECPs at different dissolved O_2 and temperatures.

Macdonald's data indicates that SS-304 becomes more noble as the dissolved O_2 increases. In Lin's experiment, the measurements were made using a high temperature pH sensor / reference electrode with zirconia (ZrO_2) electrolyte and a copper-cuprous oxide ($Cu-Cu_2O$) internal juction used as a reference electrode. His values are more noble than those from Macdonald at lower dissolved O_2 and appear to become nearly constant at higher dissolved O_2. The ECPs from this study are more noble. This is because of the oxygen reduction kinetics. The water flow in this experiment is 200 cc/min. The values in this study were nearly constant at lower dissolved oxygen but increased at higher dissolved oxygen as shown in Figure 18.

Table 8. Comparison of SS-304 ECPs at 550°F from three studies.

Dissolved Oxygen Content (ppb)	Macdonald's ECP (V_{SHE}) [2] *	Lin's ECP (V_{SHE}) [3]	This study ECP (V_{SHE}) **
50	-0.6	-0.2	0.177
200	-0.3	0.19	0.295
8000	0	0.2	0.188

* Measured at 0.12 cm/s flow rate.

** Measured at 200 cc/min water flow.

4.3 Effect of temperature and dissolved oxygen content on Electrochemical Potentials determined from Potentiodynamic Scans.

The ECP of each metal was also determined from the potentiodynamic voltammogram produced by scanning between the ECP -100mV to ECP +100mV. The voltammograms are collected in Appendix B and are shown in Figures 20 to 64. In this
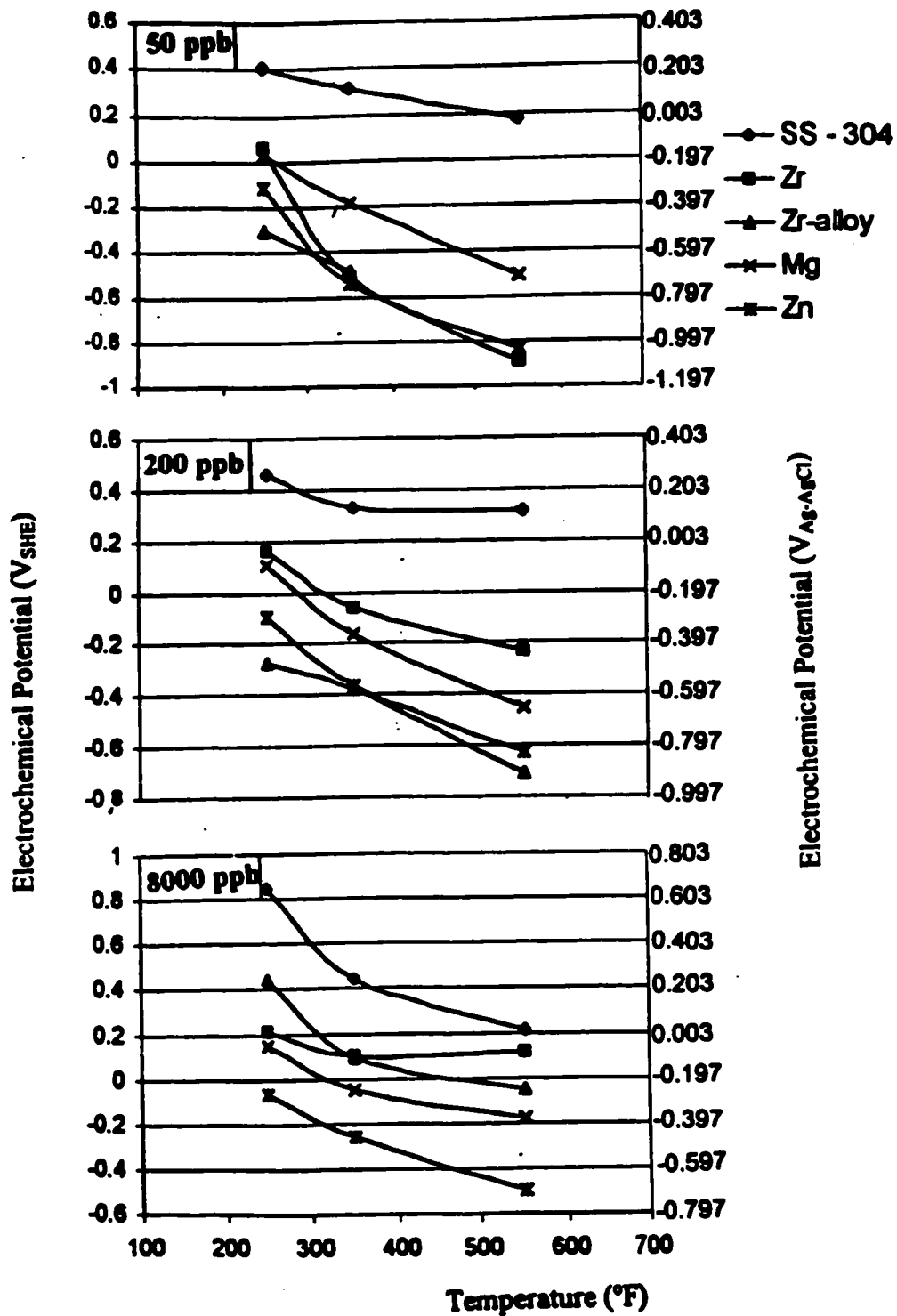
Figure 18. The voltammogram ECPs of SS-304, Zr, Mg, Zr-alloy, Zn at different dissolved O_2 and temperatures.

measurement, the cell had each of the metal specimens as the working electrode, Ag-AgCl as the reference electrode, and SS-304 as the counter electrode. The potentiodynamic voltammograms are divided into two distinct regions, the oxidation and reduction region. The chemical reactions of the metals in these regions are shown in Table 9.

50 ppb O_2 : The ECPs determined from the potentiodynamic voltammograms are listed in Table 6 in the columns labeled E_{ps}. The ECPs for SS-304, Zr, Zr-alloy, Mg and Zn are plotted in Figure 18 and reveal a shift to more active values as the temperature increases. The ECPs for Zr and Zn are very sensitive to temperature as was observed with the open circuit measurements. The ECPs for Zr-alloy, Mg and SS-304 are slightly less sensitive to the temperature. The ECPs for SS-304 are the most noble at every temperature.

200 ppb O_2 : The ECP values from the potentiodynamic scans measured in water containing 200 ppb dissolved O_2 at 250°F, 350°F and 550°F are tabulated in Table 6 and plotted in Figure 18. The trends are similar to those observed with the other dissolved O_2 contents. The slope of the different curves are more shallow at 200 ppb dissolved O_2 than at 50 ppb dissolved O_2. The ECPs for all alloys become more active as the temperature goes up. This trend is different from the open circuit measurements at 200 ppb O_2 and 50 ppb O_2. The ECPs for Zn and Mg cross, that is, they change places in a galvanic series. as the temperature goes up. SS-304 remains the most noble metal.

49

8000 ppb O_2 : The ECPs in water containing 8000 ppb dissolved oxygen are listed in Table 6 and the plot is shown in Figure 18. Again all the ECPs become more active as the temperature increases. Zn and Zr-alloy have the greatest temperature dependence.

4.4 Analysis of Potentiodynamic Scans at different Dissolved Oxygen content and temperature

E_{corr} is the resultant potential when two metals are connected at any experimental condition. The E_{corr} value is determined analytically by superimposing the voltammograms of the different metals at the same condition. The E_{corr} values are listed in Table 9. A comparison of the E_{corr} for a SS-304/metal couple at 50 ppb, 200 ppb and 8000 ppb O_2 shows that the E_{corr} becomes more active as the dissolved O_2 deceases at a constant temperature (Table 9). Also, at a constant dissolved O_2 the E_{corr} becomes more active as the temperature increases (Table 9). This behavior is common for all the metals. At BWR operating conditions, the E_{corr} values for Mg/SS-304 couples and Zr/SS-304 are -170 mV$_{SHE}$ and -180 mV$_{SHE}$ (approximately) respectively.

The potential of SS-304 becomes less noble when it is connected to the other metals because the ECPs of the other metals are less, i.e. they are more active than the SS-304. The previous research depicted in BWR operations that the ECP of SS-304 should be lower than -230 mV$_{SHE}$ in order to prevent intergranular stress corrosion cracking (IGSCC). [4] At 550°F and 200 ppb dissolved oxygen, the normal BWR operating conditions, from Tables 10 and 11 the E_{corr} for the SS-304 coupled to Mg and Zr are -207 mV$_{SHE}$ and -187 mV$_{SHE}$. None of our metals coupled to SS-304 gave E<-230 mV$_{SHE}$ but Mg and Zr came closest.

Table 9. Summary of the Potentiodynamic Scan Experiments.

Metal Specimens	Oxidation Reaction	Reduction Reaction	Dissolved Oxygen Content (ppb)	E_{corr} (V)			Potentiodynamic Scans (Figures)
				250°F	350°F	550°F	
SS-304	Fe → Fe⁺² + 2e⁻	H₂O + ½O₂ + 2e⁻ → 2OH⁻	50	--	--	--	20-28
			200	--	--	--	
			8000	--	--	-0.23	
Mg	Mg → Mg⁺² + 2e⁻	H₂O + ½O₂ + 2e⁻ → 2OH⁻	50	+0.05	-0.06*	-0.17	38-46
			200	+0.22	+0.06	-0.03	
			8000	+0.24	+0.15	-0.18	
Zn	Zn → Zn⁺² + 2e⁻	H₂O + ½O₂ + 2e⁻ → 2OH⁻	50	+0.06*	-0.04*	-0.18*	56-64
			200	+0.21	-0.01*	-0.02*	
			8000	+0.28	+0.19*	-0.17*	
Zr	Zr → Zr⁺⁴ + 4e⁻	H₂O + ½O₂ + 2e⁻ → 2OH⁻	50	--	-0.04	-0.17	47-55
			200	+0.06	-0.02	-0.15	
			8000	+0.61	0.48	0.28	
Zr-alloy	Zr → Zr⁺² + 4e⁻	H₂O + ½O₂ + 2e⁻ → 2OH⁻	50	+0.05	-0.03	-0.17	65-74
			200	+0.08	-0.01*	-0.25*	
			8000	+0.55	0.40	0.26	

* These are the approximate values.

Note : E_{corr} measured from the Figure to Figure in Apprendix B.

51

Table 10. E_{corr} against the standard hydrogen electrode for stainless steel coupled to Mg.

Temperature (°F)	E_{corr} (mV$_{SHE}$) at Dissolved [O_2]		
	50 ppb	200 ppb	8000ppb
250	230	194	201
350	-64	29	104
550	-269	-207	-57

Table 11. E_{corr} against the standard hydrogen electrode stainless steel coupled to Zr.

Temperature (°F)	E_{corr} (mV$_{SHE}$) at Dissolved [O_2]		
	50 ppb	200 ppb	8000ppb
250	97	109	622
350	-74	-49	374
550	-211	-187	177

5. Conclusion

The electrochemical potential (ECP), the open circuit potential of different candidate metals against a reference electrode, and E_{corr}, the coupled potential between the SS-304 and the candidate metals strongly depend on the dissolved O_2 content of water and the temperature. In addition, the ECP and E_{corr} become more active as the dissolved O_2 decreases and the temperature increases. At normal BWR operating conditions (200 ppb dissolved O_2 and 550°F), when Mg or Zr were coupled to SS-304, potentials of the couple were about -0.2 mV_{SHE}; not as good as desired but far better than the E_{corr} for SS-304 alone.

6. References

[1] Licina, G.J., "Electrode Methods for Mitigation of IGSCC in BW Reactor Pressure Vessel Internals", Structural Integrity Associates Project Proposal (SI-95-017P) 1995: 15-24.

[2] Smith, William F. Principles of Materials Science and Engineering. New York: McGraw Hill, Third Edition, 1995. 709-11.

[3] Macdonald, D. D. "Viability of Hydrogen Water Chemistry for Protection In vessel Components of the Boiling Water Reactors". Corrosion 48 (1992): 195-205.

[4] Macdonald, D. D. et.al. "Corrosion Potential Measurements on Type 304 SS and Alloy 182 in Simulated BWR Environments", Corrosion 49 (1993): 8-16.

[5] Lin, C.C. et. al., "Electrochemical Corrosion Potential Models for Boiling Water Reactor Applications," Corrosion 52 (1996): 618-25.

[6] Kim Y. J. et. al., "Corrosion Potential Behavior of Noble Metal-Modified Alloys in High Temperature Water," Corrosion 52 (1996): 738-43.

[7] Beuerman, Douglas, ed. Design of a Sacrificial Anode for Use in BWRs, San Jose: San Jose State University Materials Engineering Department, 1995.

[8] Macdonal, D. D. "Discussion on Electrochemical Potential Measurements under Simulated BWR Water Chemistry Conditions", Corrosion 49 (1993): 90-91.

[9] Trethewey and J. Chamberlin. Corrosion for Students of Science and Engineering. New York. Longman Scientific & Technical and J. Wiley, 1988. 70-71.

[10] Conax Incorporated. Manual for Conax Fittings. Pennsylvania: Philadelphia, 1995.

[11] NWT Manufacturing Corporation. <u>Technical Data NWT R201, Water-Cooled, High Temperature, High Pressure, External Reference Electrode</u>. California: San Jose, 1996: 3.

[12] Trethewey and J. Chamberlin. <u>Corrosion for Students of Science and Engineering</u>. New York. Longman Scientific & Technical and J. Wiley, 1988. 73.

[13] Autoclave Engineering. <u>Operating Manual of Autoclave</u>. Pennsylvania: Philadelphia, 1995.

[14] NWT Manufacturing Corporation. <u>Technical Data NWT R201, Water-Cooled, High Temperature, High Pressure, External Reference Electrode</u>. California: San Jose, 1996. 5.

[15] Prienceton Applied Research Corporation. <u>Model-173 Potentiostat / Galvanostat Instructional Manual</u>. New Jersey: Princeton, 1985.

[16] American Society of Metals. <u>Corrosion of Nickel Base Alloys Conferences Proceedings</u>. New York: New York, 1985.

Appendix A

Calculation of electrochemical potential(ECP) for Ag/AgCl

The observed voltmeter readings were not the actual E (SHE) voltage. The corrections were made by the following equations:

E(SHE) = E(Reading) + Correction

Temperature Correction = $0.402 - 1.003 \times 10^{-3} \Delta T + 1.745 \times 10^{-7} \Delta T^2 - 3.030 \times 10^{-9} \Delta T^3$

The correction voltage at 250°F is 0.31V and at 350°F is 0.24V and 550°F is 0.12V.

At 250°F the E(SHE) value was calculated by the equation,

$$E(SHE) = E(Reading) + 0.31 \qquad \text{A.1}$$

At 350°F the E(SHE) value was calculated by the equation,

$$E(SHE) = E(Reading) + 0.24 \qquad \text{A.2}$$

At 550°F the E(SHE) value was calculated by the equation,

$$E(SHE) = E(Reading) + 0.12 \qquad \text{A.3}$$

Correction = 0.402 - 1.003x10⁻³ ΔT
+1.745x10⁻⁷ ΔT² -3.030x10⁻⁹ ΔT³
At T>275C, Correction =0.120
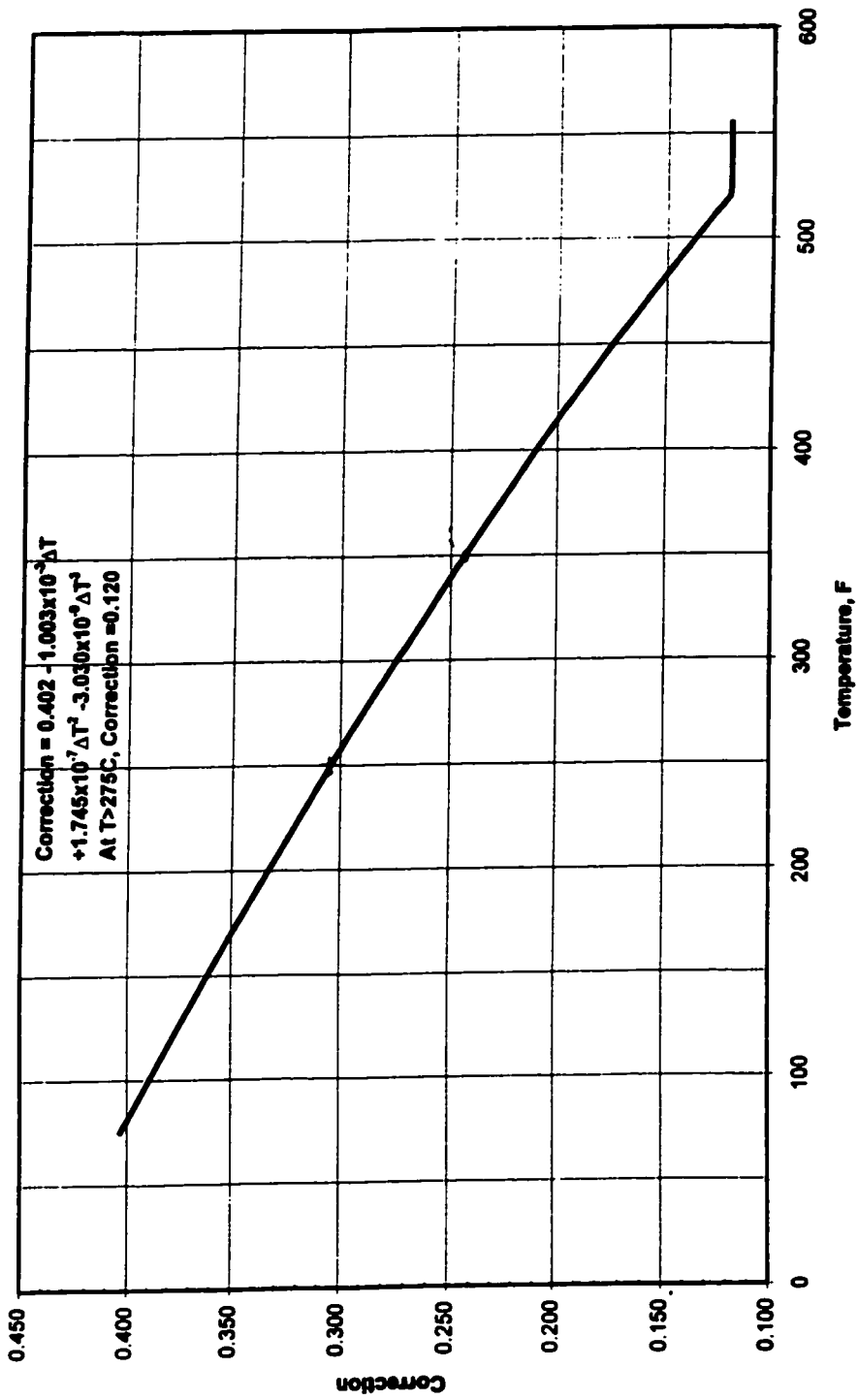
Figure 19. Correction curve for NWT Ag-AgCl reference electrode.

57

APPENDIX B

Voltammograms of different metals for the determination of electrochemical potentials (ECPs)

Electrochemical Potentials in voltammograms are denoted by E_{ps} from Figure 20 to 64.
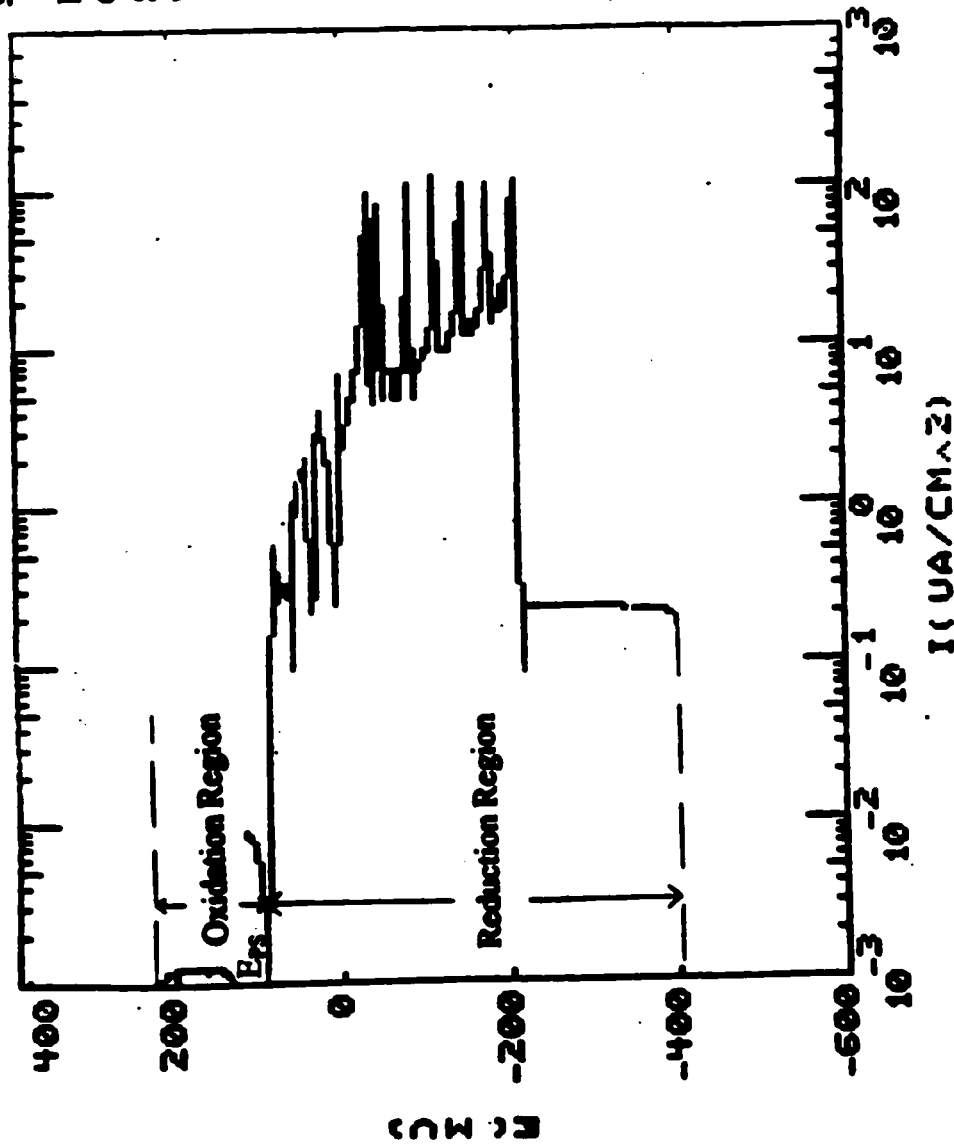
Figure 20. Potentiodynamic Scan of SS-304 at 50 ppb dissolve O_2 and 250°F.

Conditions:

Dissolve O_2 of water: 50 ppb
Conductivity of water: 0.76
Set up temperature: 250°F
Water temperature of water: 250°F
Furnace Temperature: 168°F
Pressure in high pressure loop: 1000 psi
Water Flow : 200 sccm
Nitrogen Pressure: 1000psi
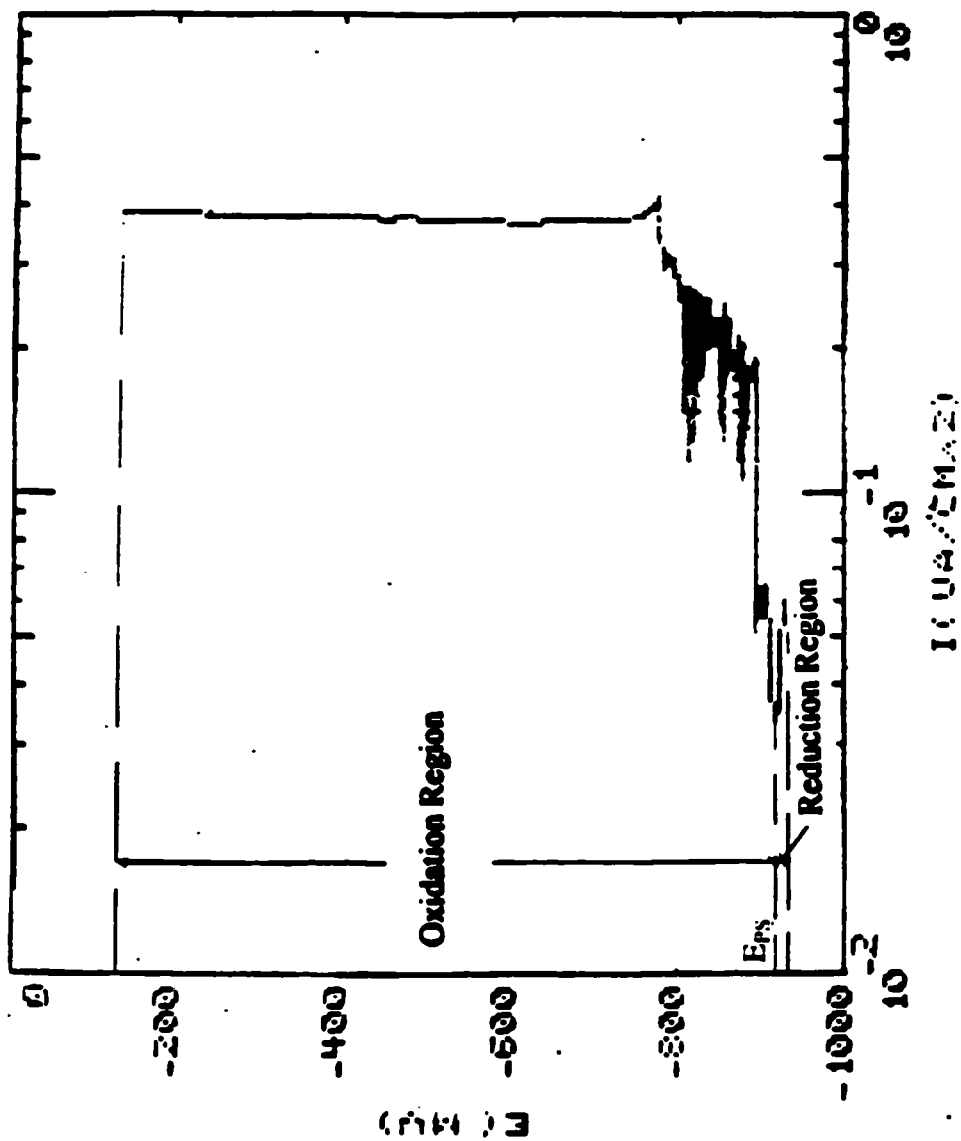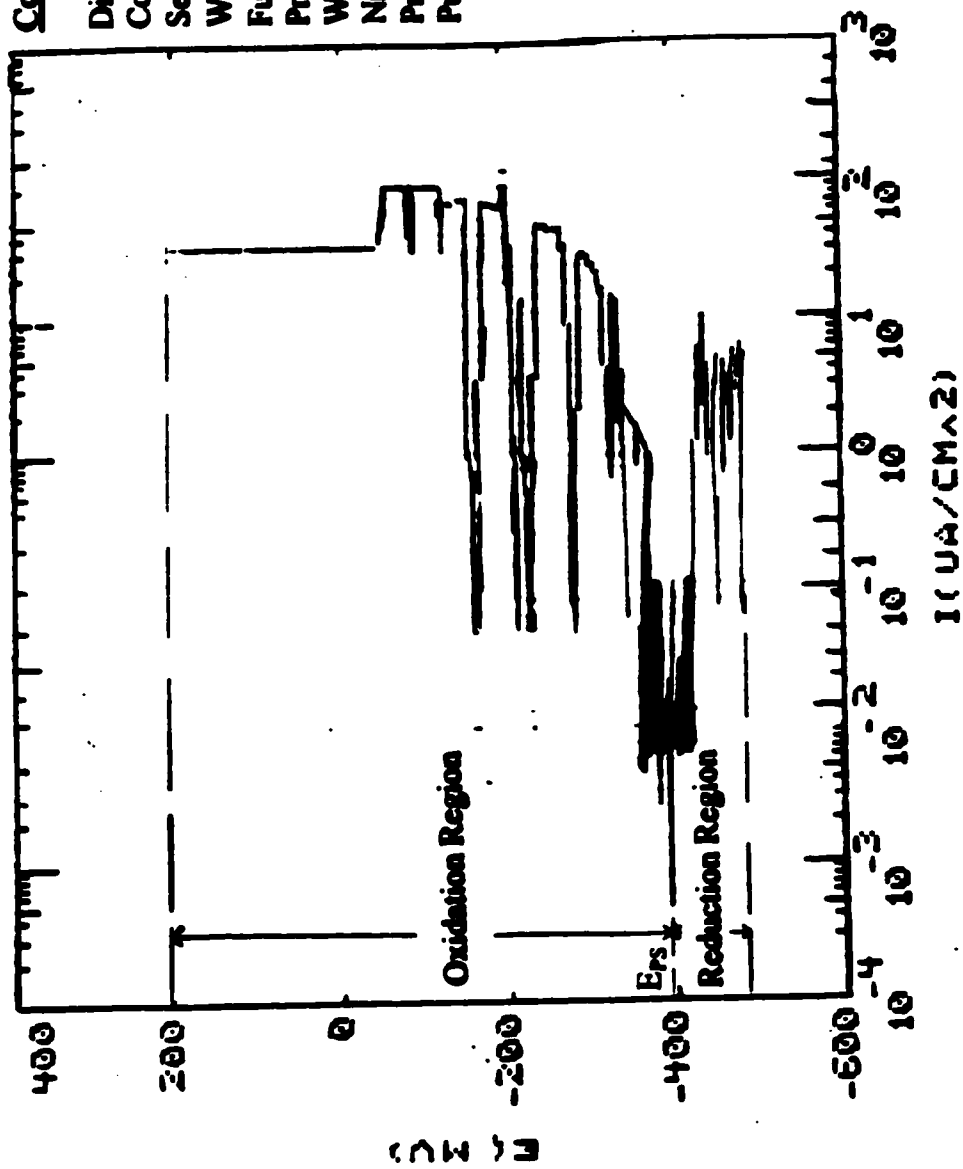Pressure in low pressure loop: 30 psi
Pump Stroke: 18%
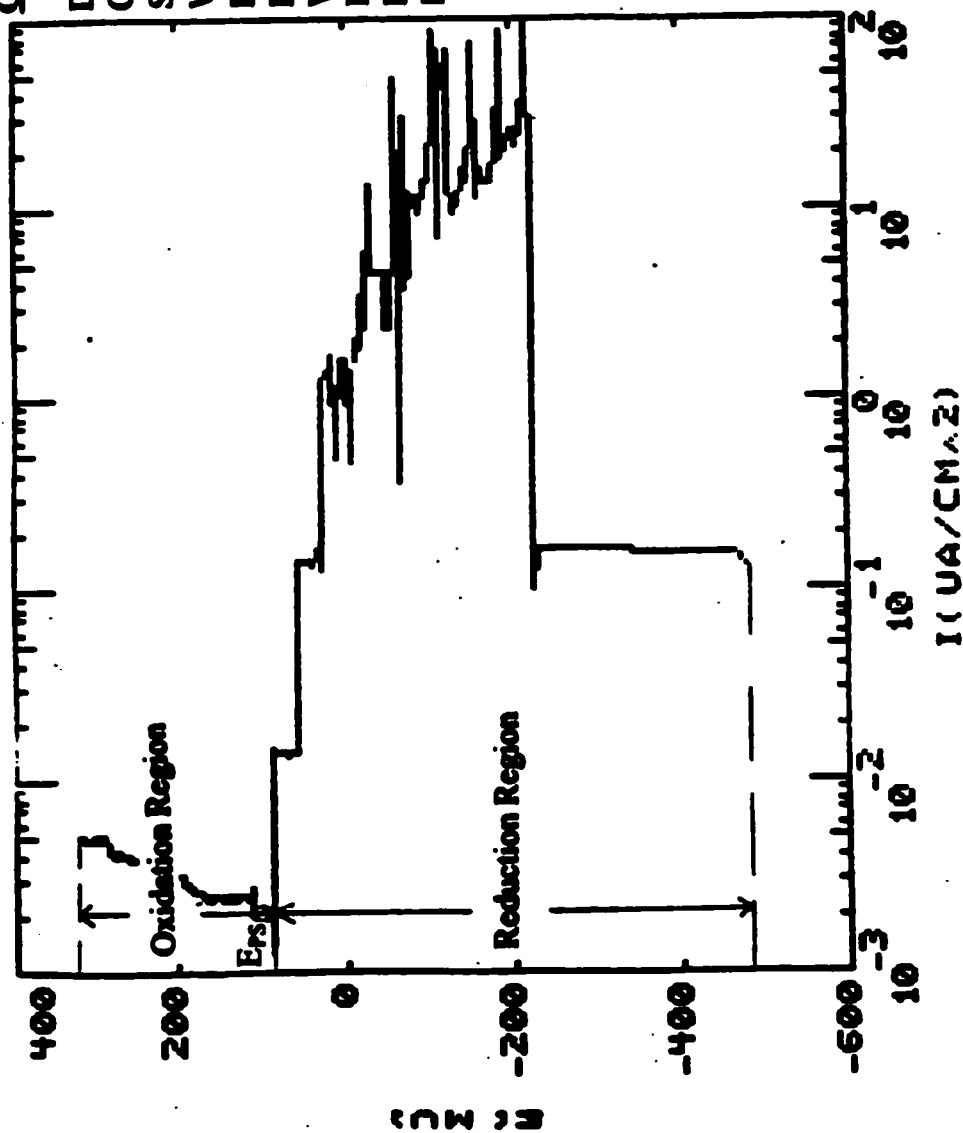
Figure 21. Potentiodynamic Scan of SS-304 at 50 ppb dissolve O_2 and 350°F.

Conditions:

Dissolve O_2 of water: 50 ppb
Conductivity of water: 0.76
Set up temperature: 350°F
Water temperature of water: 350°F
Furnace Temperature: 218°F
Pressure in high pressure loop: 1000 psi
Water Flow : 200 sccm
Nitrogen Pressure: 1000psi
Pressure in low pressure loop: 30 psi
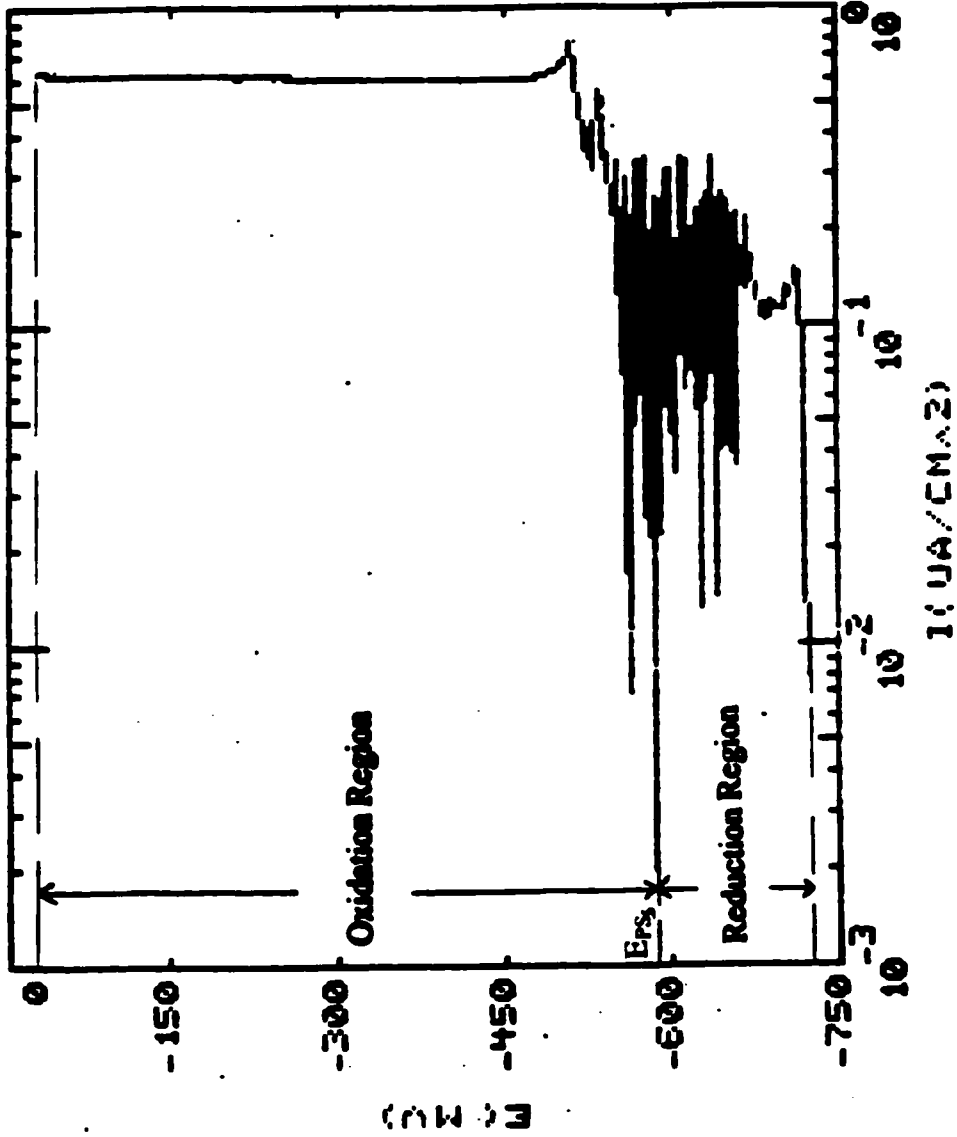Pump Stroke: 18%

60
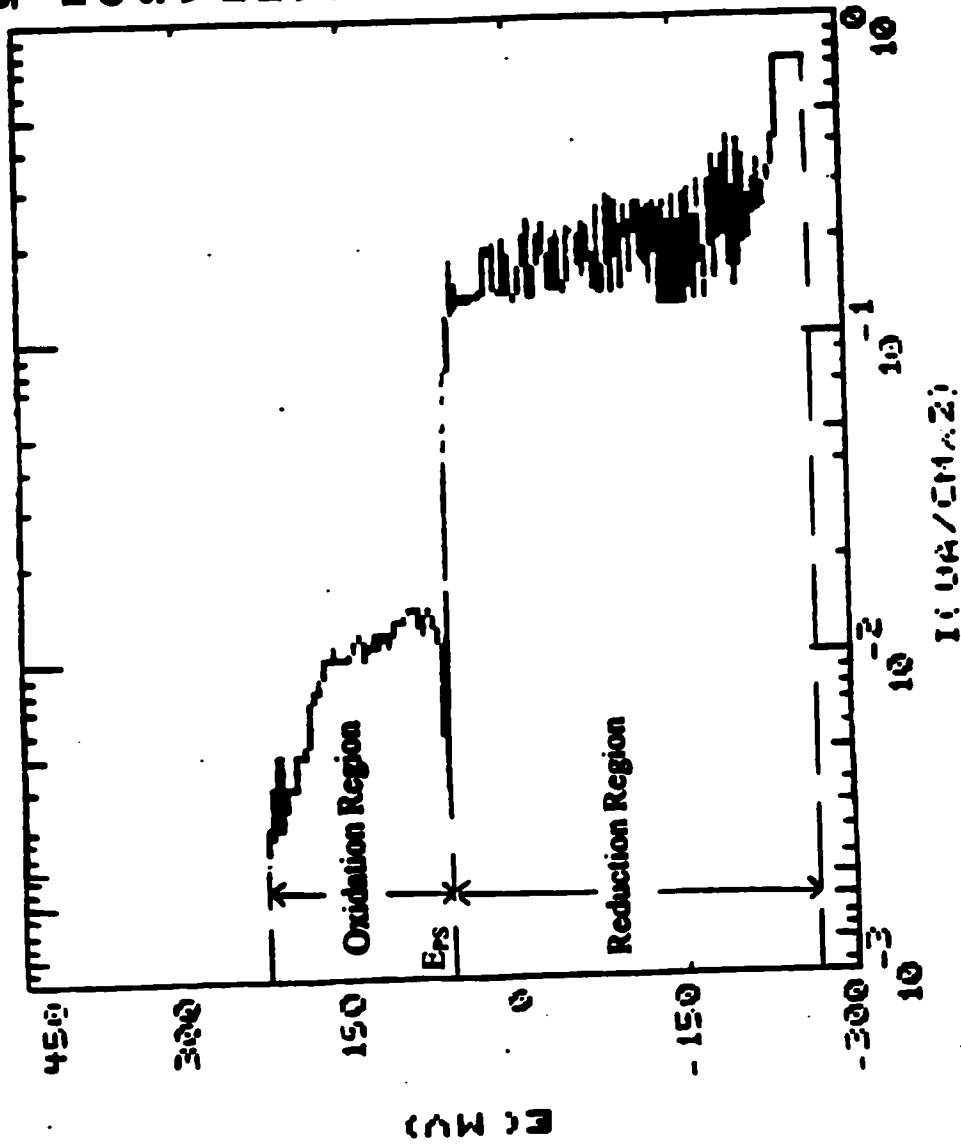
Figure 22. Potentiodynamic Scan of SS-304 at 50 ppb dissolve O_2 and 550°F.

61
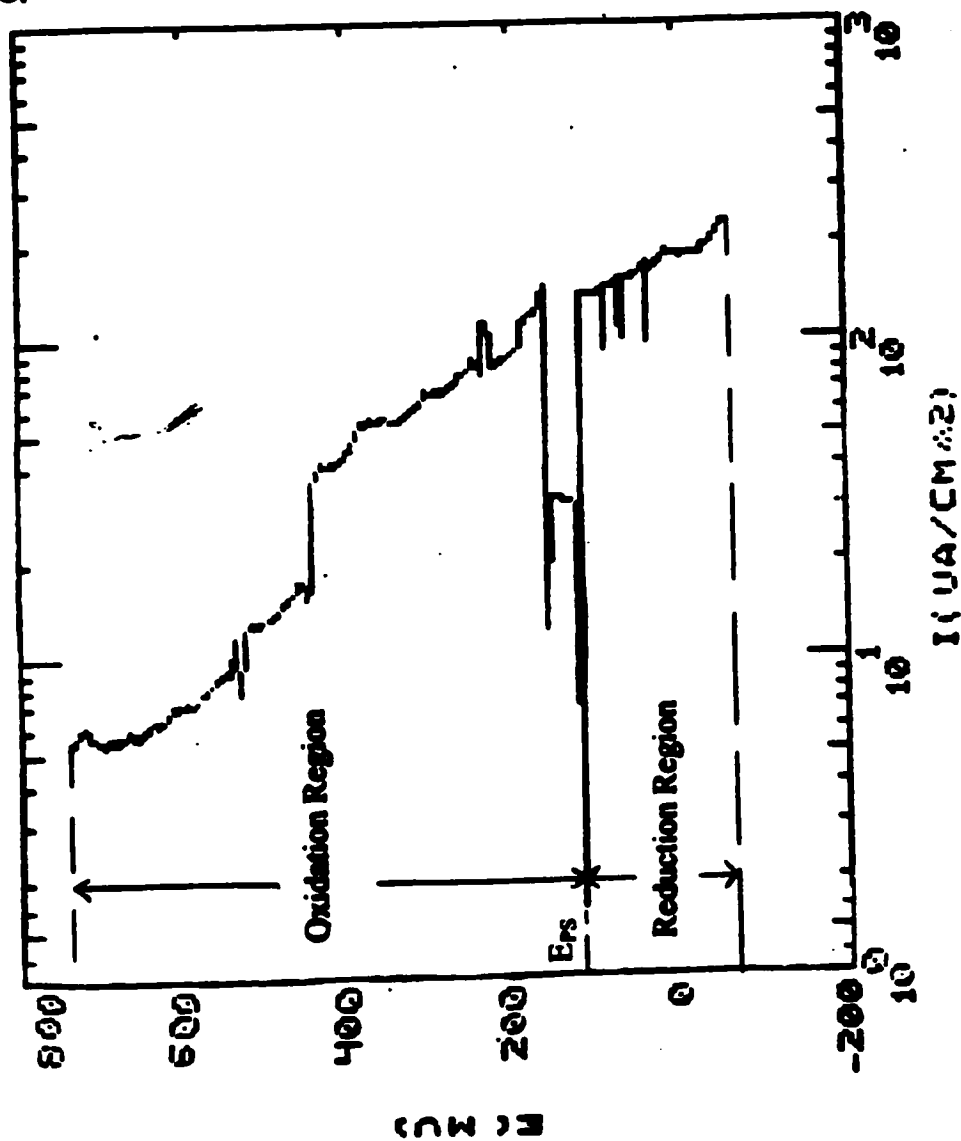
Figure 23. Potentiodynamic Scan of SS-304 at 200 ppb dissolve O_2 and 250°F.

Conditions:

Dissolve O_2 of water: 200 ppb
Conductivity of water: 0.76
Set up temperature: 350°F
Water temperature of water: 350°F
Furnace Temperature: 217°F
Pressure in high pressure loop: 1000 psi
Water Flow: 200 sccm
Nitrogen Pressure: 1000psi
Pressure in low pressure loop: 30 psi
Pump Stroke: 18%
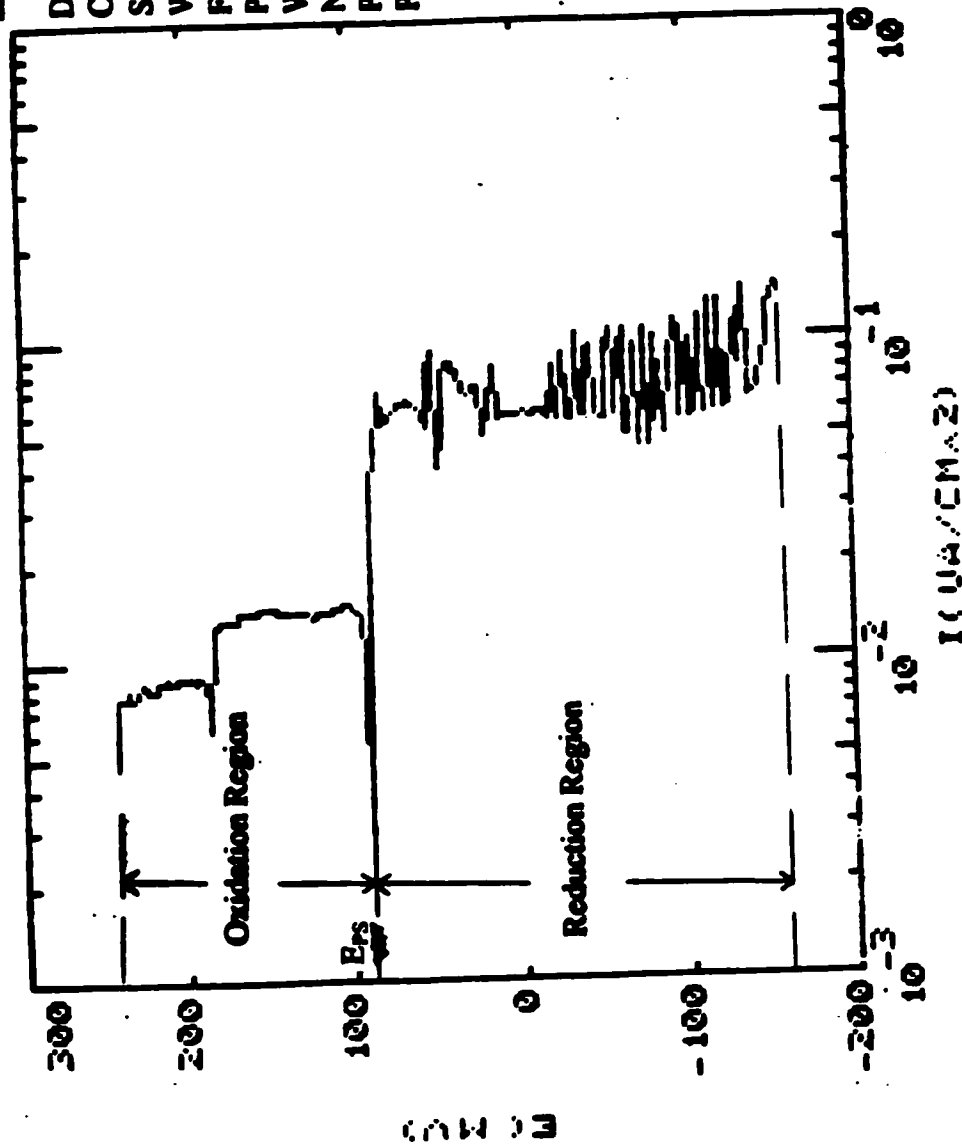
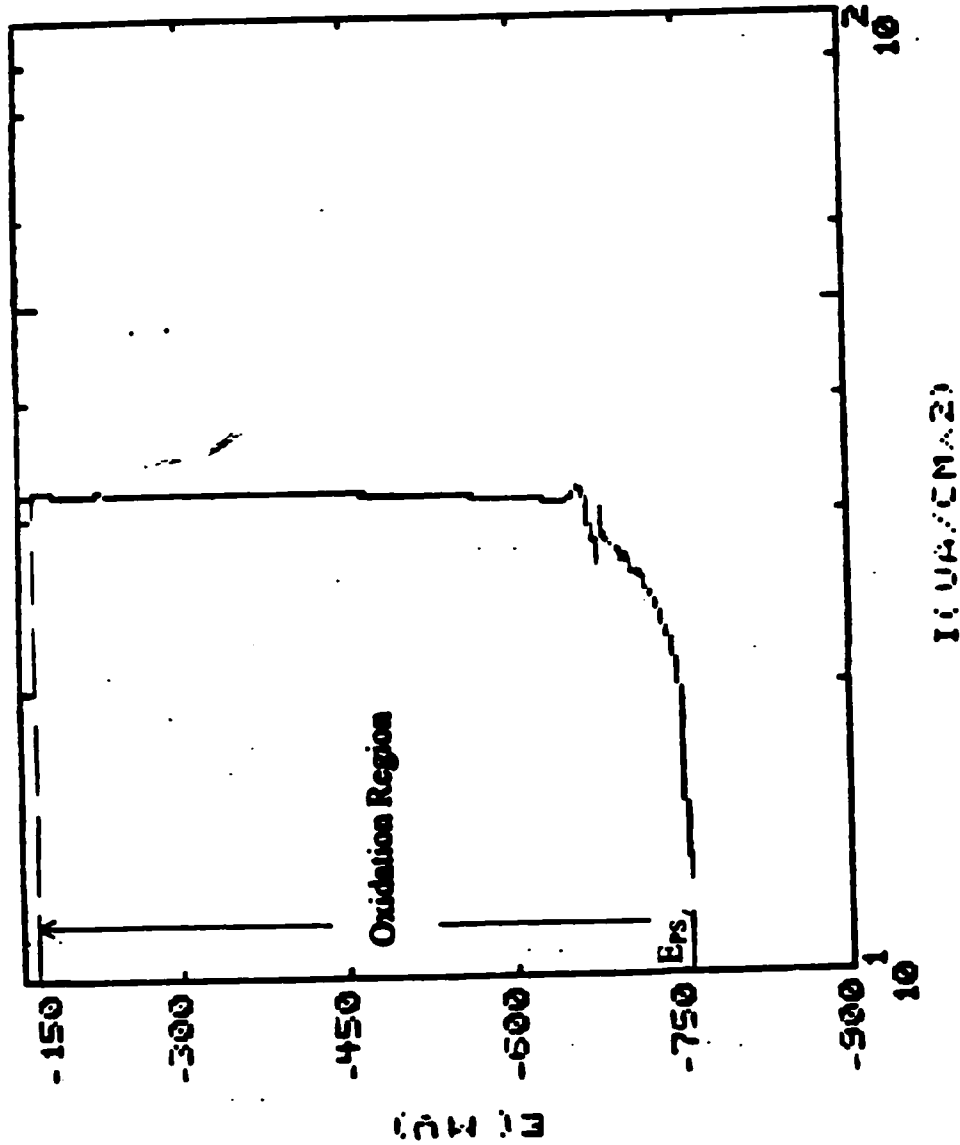Figure 24. Potentiodynamic Scan of SS-304 at 200 ppb dissolve O_2 and 350°F.
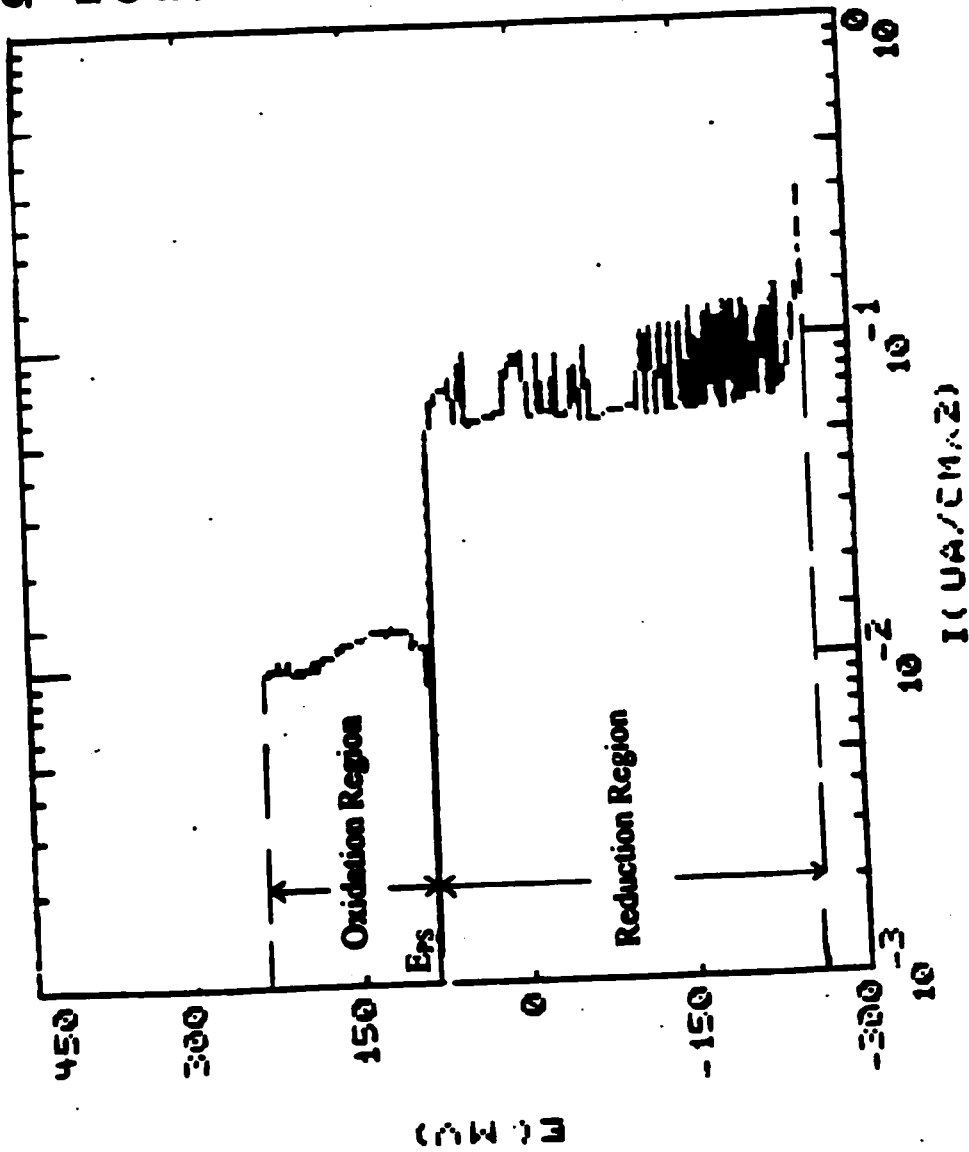
Figure 25. Potentiodynamic Scan of SS-304 at 200 ppb dissolve O_2 and 550°F.

Conditions:

Dissolve O_2 of water: 200 ppb
Conductivity of water: 0.76
Set up temperature: 550°F
Water temperature of water: 550°F
Furnace Temperature: 455°F
Pressure in high pressure loop: 1000 psi
Water Flow : 200 sccm
Nitrogen Pressure: 1000psi
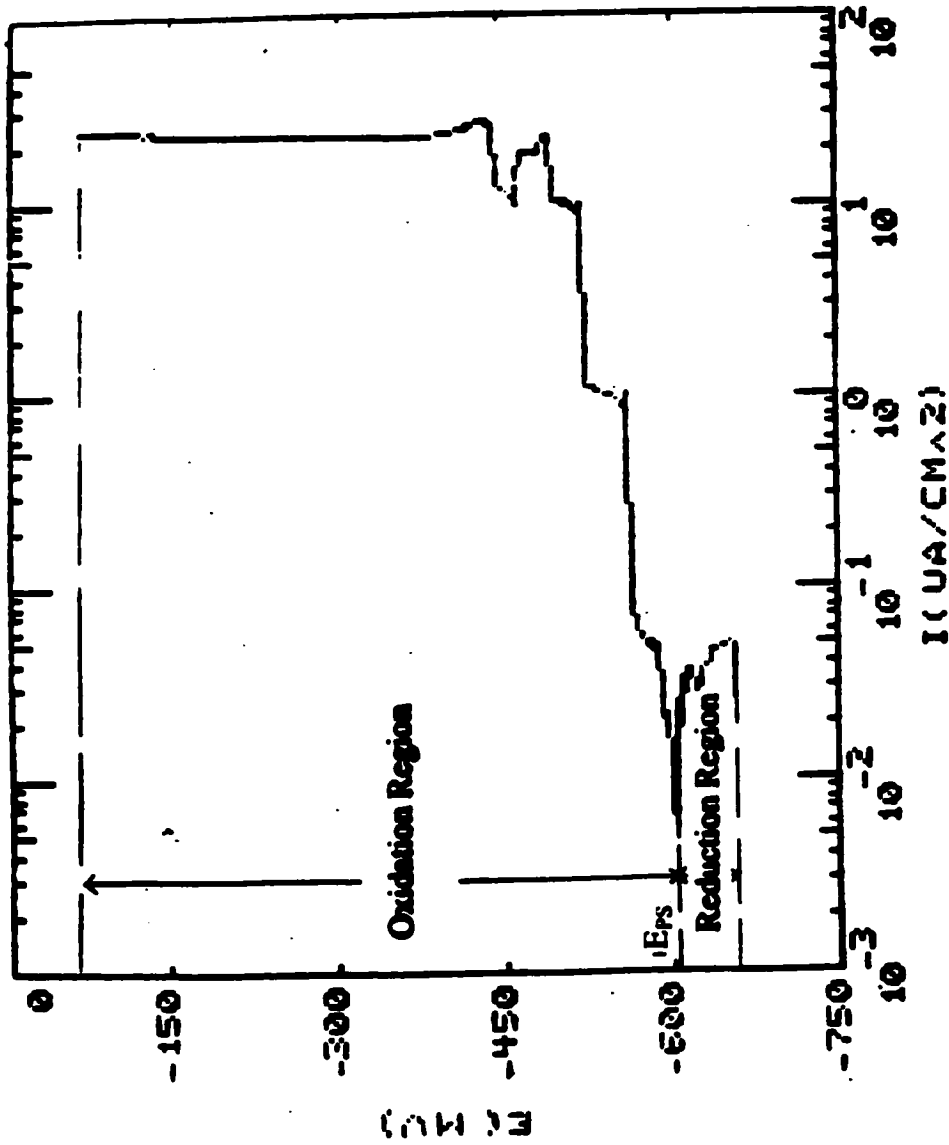Pressure in low pressure loop: 30 psi
Pump Stroke: 18%

64

Conditions:

Dissolve O_2 of water: 8000 ppb
Conductivity of water: 0.76
Set up temperature: 250°F
Water temperature of water: 250°F
Furnace Temperature: 167°F
Pressure in high pressure loop: 1000 psi
Water Flow : 200 sccm
Nitrogen Pressure: 1000psi
Pressure in low pressure loop: 30 psi
Pump Stroke: 18%

Oxidation Region

Reduction Region

E_{rs}

I (UA/CM^2)

E (MV)

500

400

200

0

-200

-400

10^{-3} 10^{-2} 10^{-1} 10^{0}
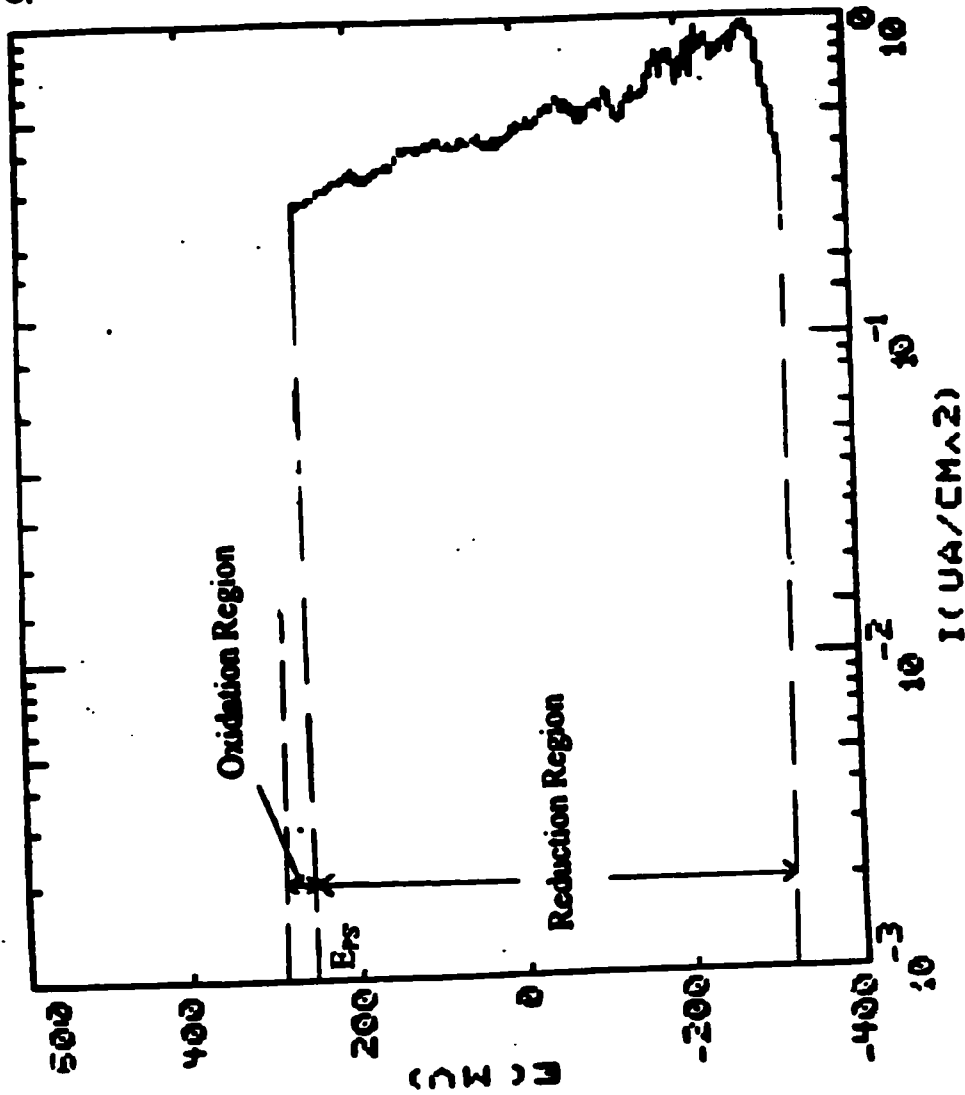
Figure 26. Potentiodynamic Scan of SS-304 at 8000 ppb dissolve O_2 and 250°F.

65

Conditions:

Dissolve O_2 of water: 8000 ppb
Conductivity of water: 0.76
Set up temperature: 350°F
Water temperature of water: 350°F
Furnace Temperature: 217°F
Pressure in high pressure loop: 1000 psi
Water Flow: 200 sccm
Nitrogen Pressure: 1000psi
Pressure in low pressure loop: 30 psi
Pump Stroke: 18%
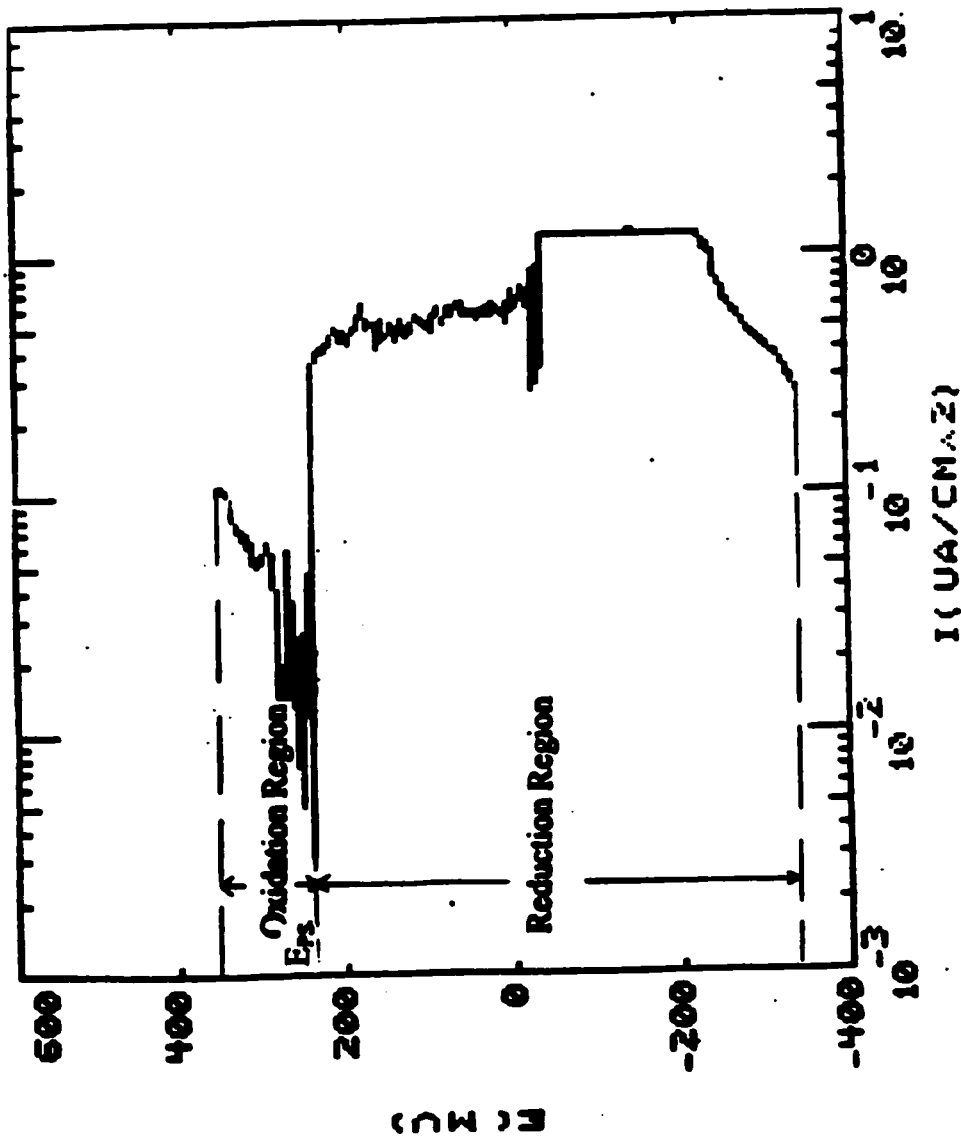
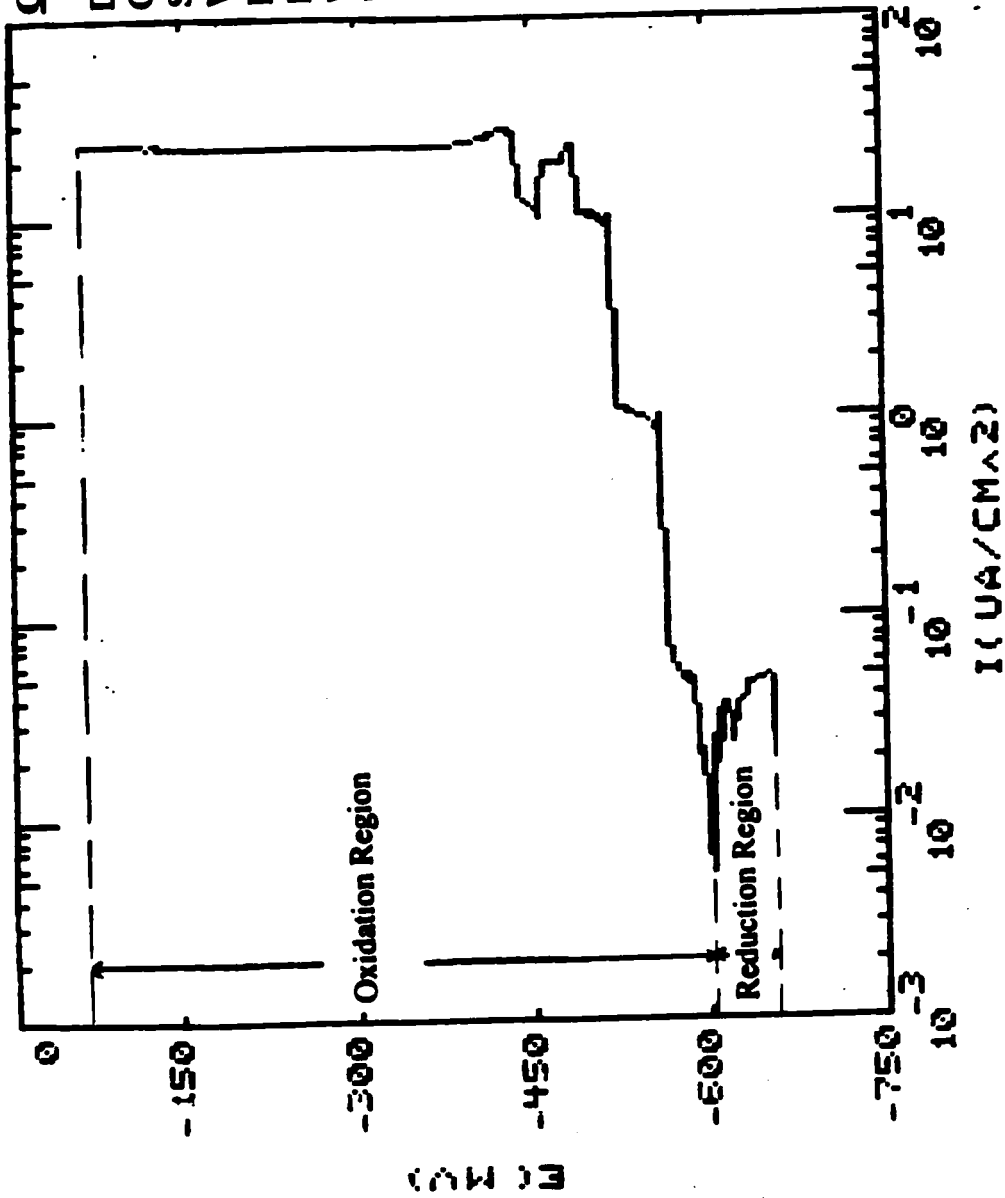Figure 27. Potentiodynamic Scan of SS-304 at 8000 ppb dissolve O_2 and 350°F.

66
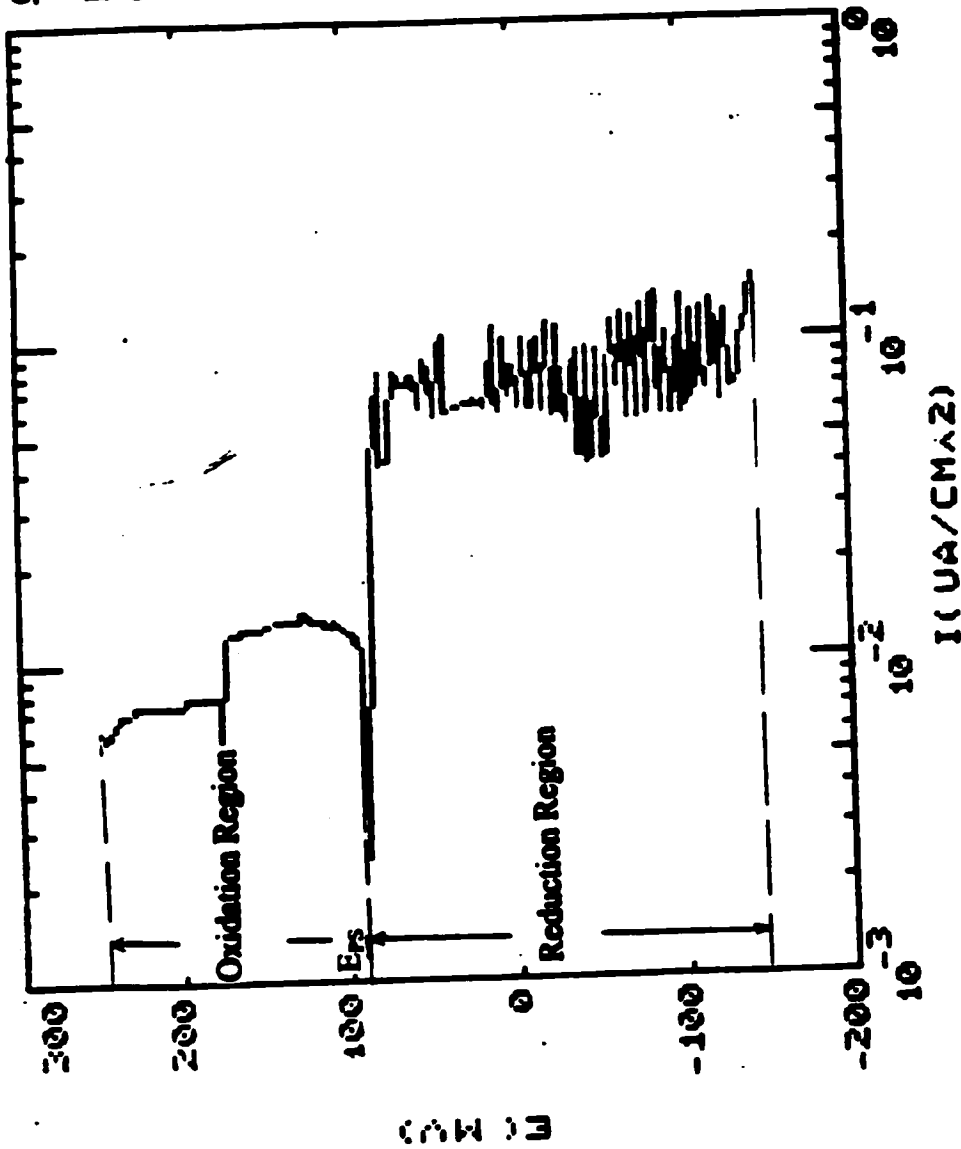
Figure 28. Potentiodynamic Scan of SS-304 at 8000 ppb dissolve O_2 and 550°F.

Conditions:

Dissolve O_2 of water: 8000 ppb
Conductivity of water: 0.76
Set up temperature: 550°F
Water temperature of water: 550°F
Furnace Temperature: 417°F
Pressure in high pressure loop: 1000 psi
Water Flow : 200 sccm
Nitrogen Pressure: 1000psi
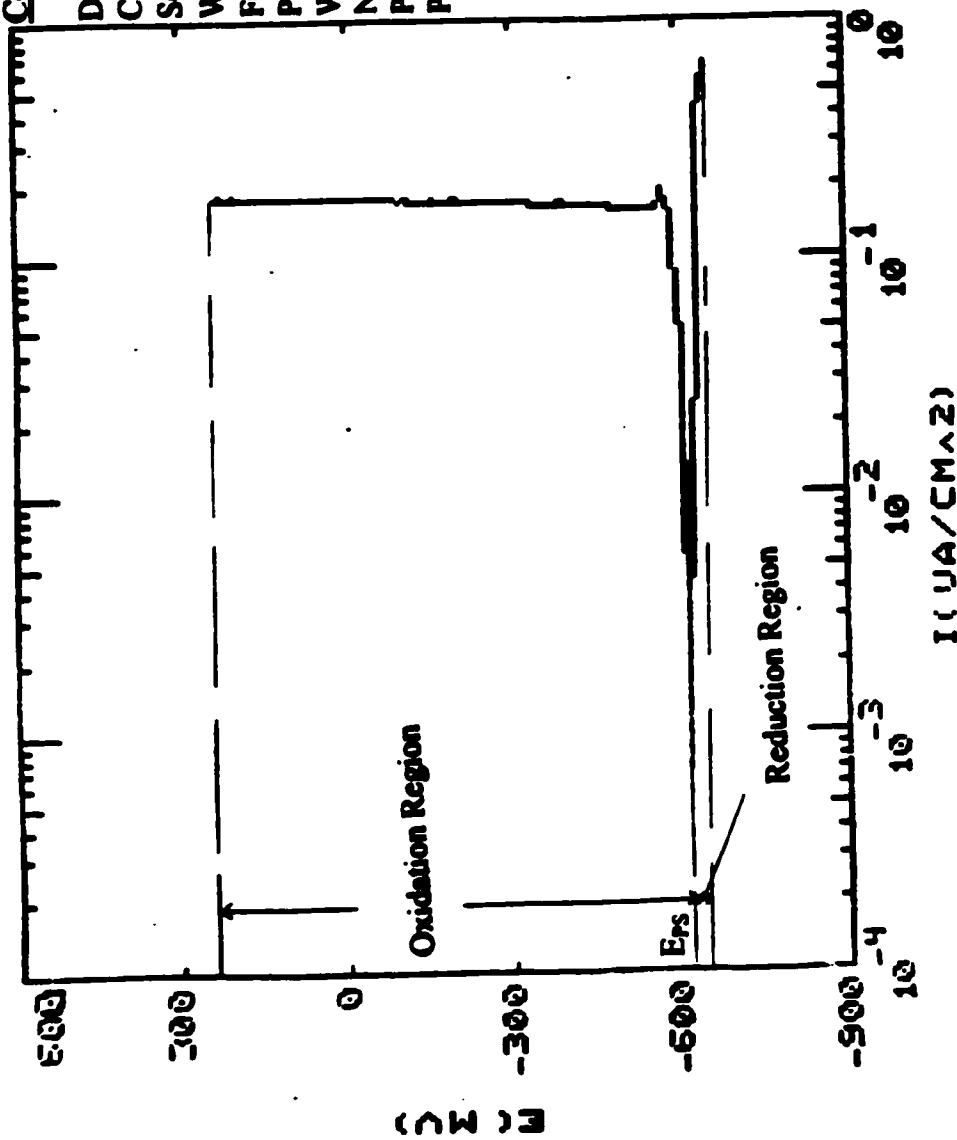Pressure in low pressure loop: 30 psi
Pump Stroke: 18%

67
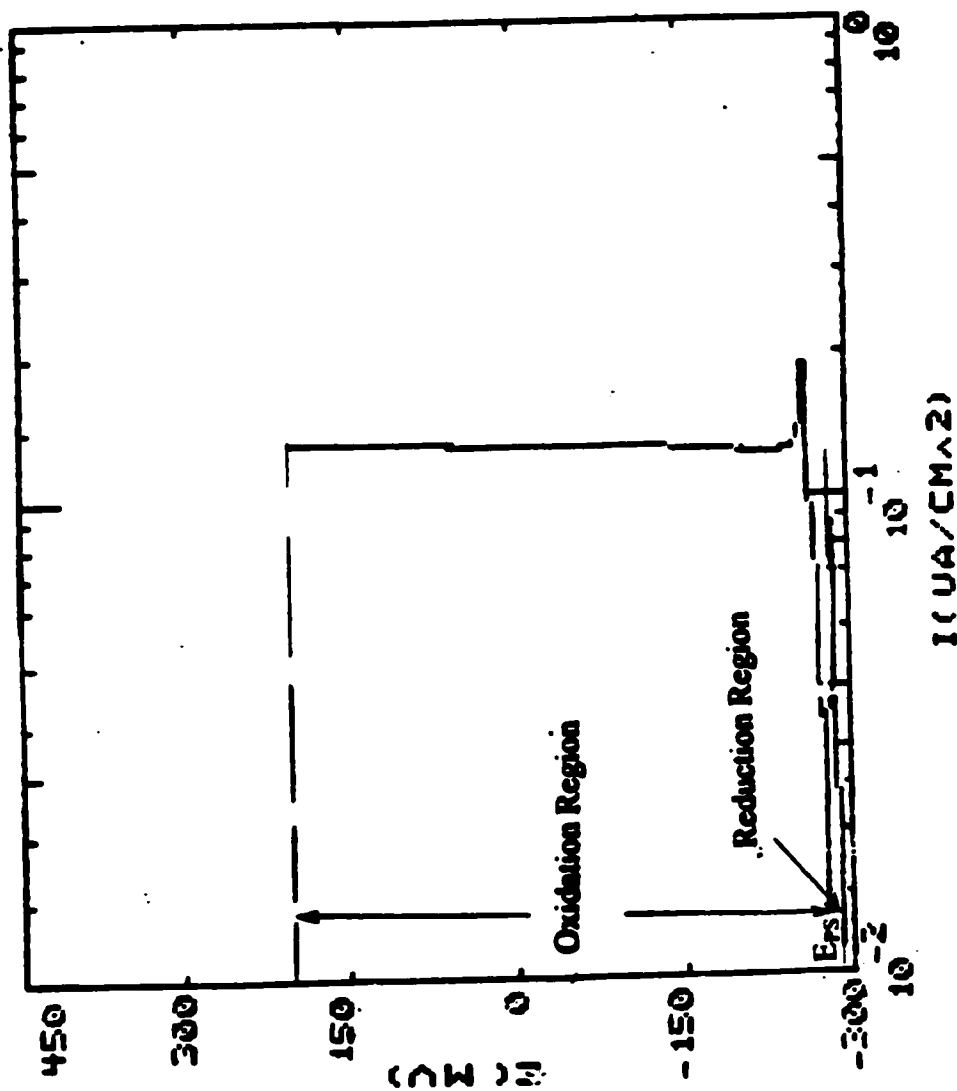
Figure 29. Potentiodynamic Scan of Mg at 50 ppb dissolve O_2 and 250°F.

Conditions:

Dissolve O_2 of water: 50 ppb
Conductivity of water: 0.76
Set up temperature: 250°F
Water temperature of water: 250°F
Furnace Temperature: 167°F
Pressure in high pressure loop: 1000 psi
Water Flow : 200 sccm
Nitrogen Pressure: 1000psi
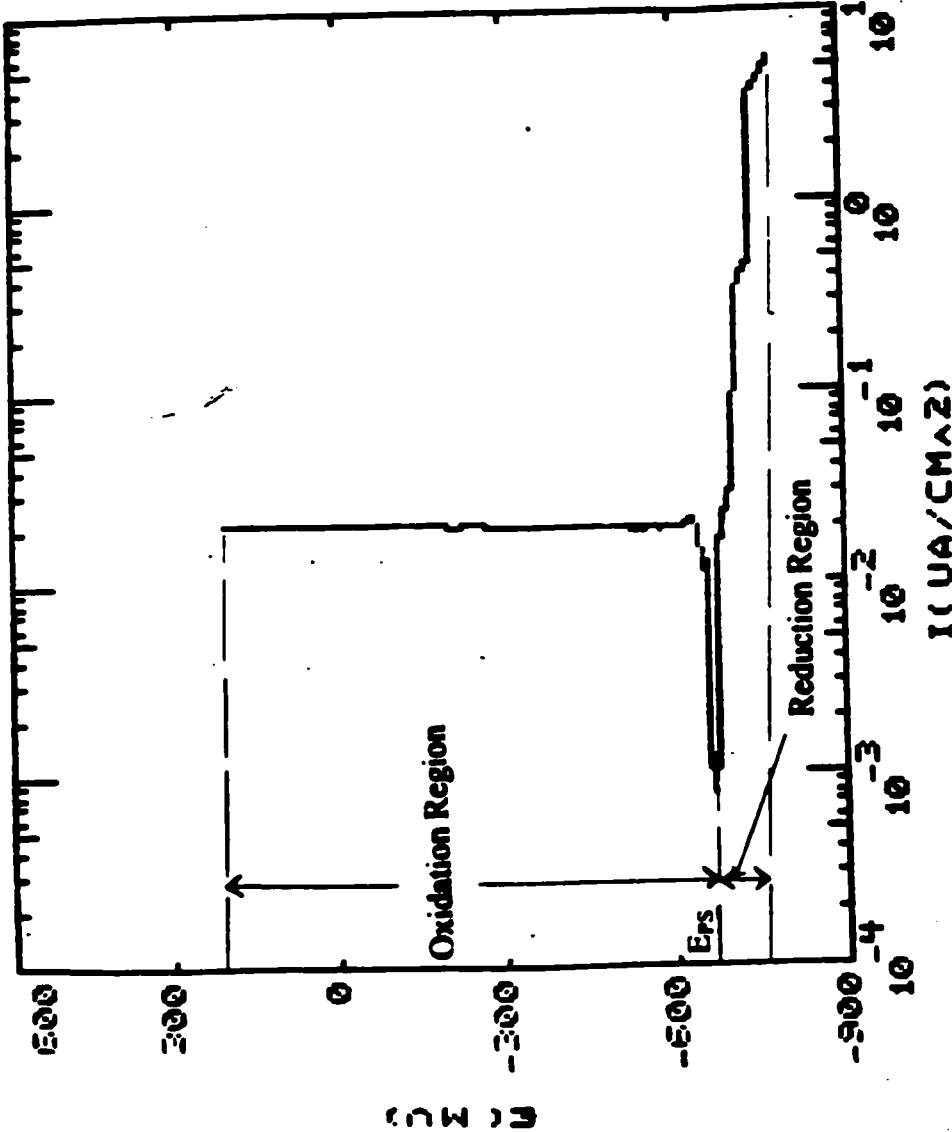Pressure in low pressure loop: 30 psi
Pump Stroke: 18%

68
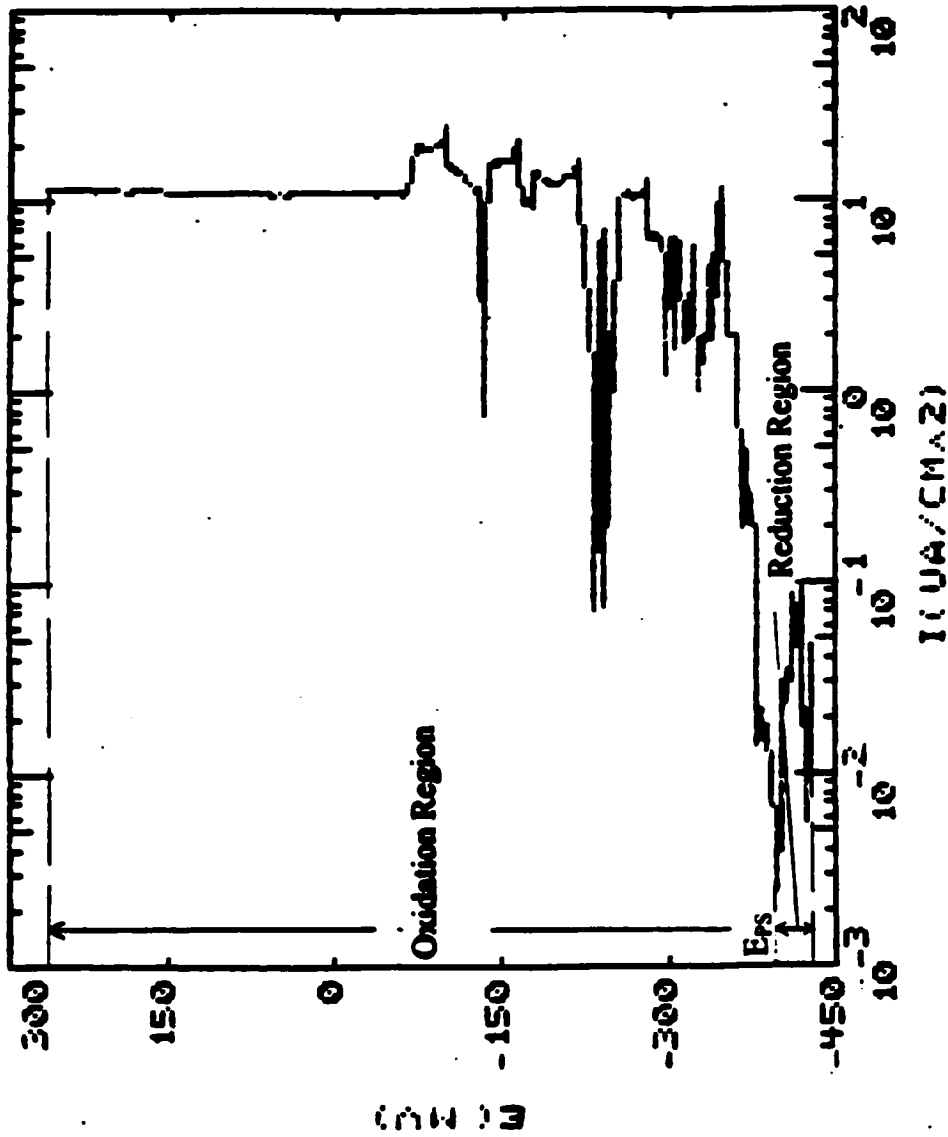
Figure 30. Potentiodynamic Scan of Mg at 50 ppb dissolve O₂ and 350°F.

Conditions:

Dissolve O₂ of water: 50 ppb
Conductivity of water: 0.76
Set up temperature: 350°F
Water temperature of water: 350°F
Furnace Temperature: 218°F
Pressure in high pressure loop: 1000 psi
Water Flow : 200 sccm
Nitrogen Pressure: 1000psi
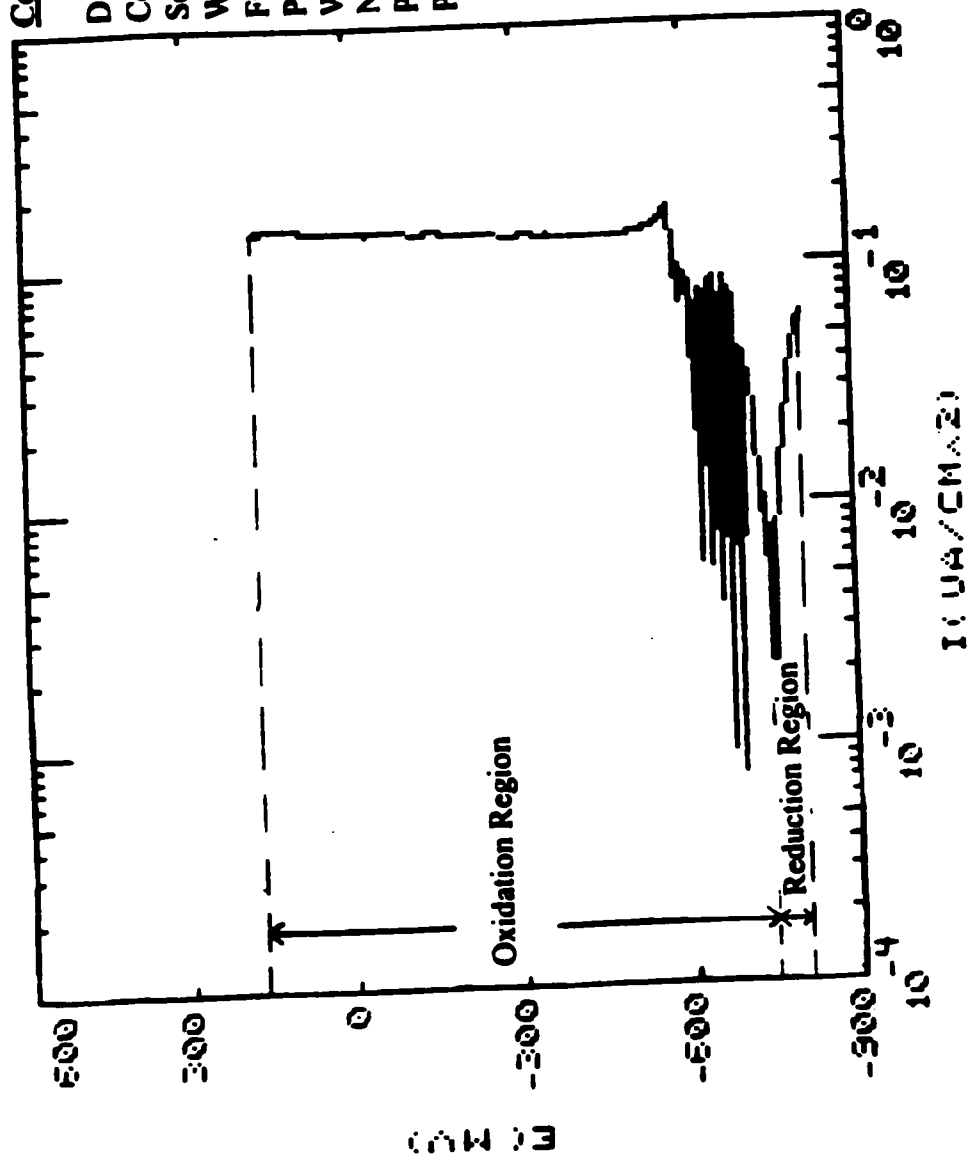Pressure in low pressure loop: 30 psi
Pump Stroke: 18%

69
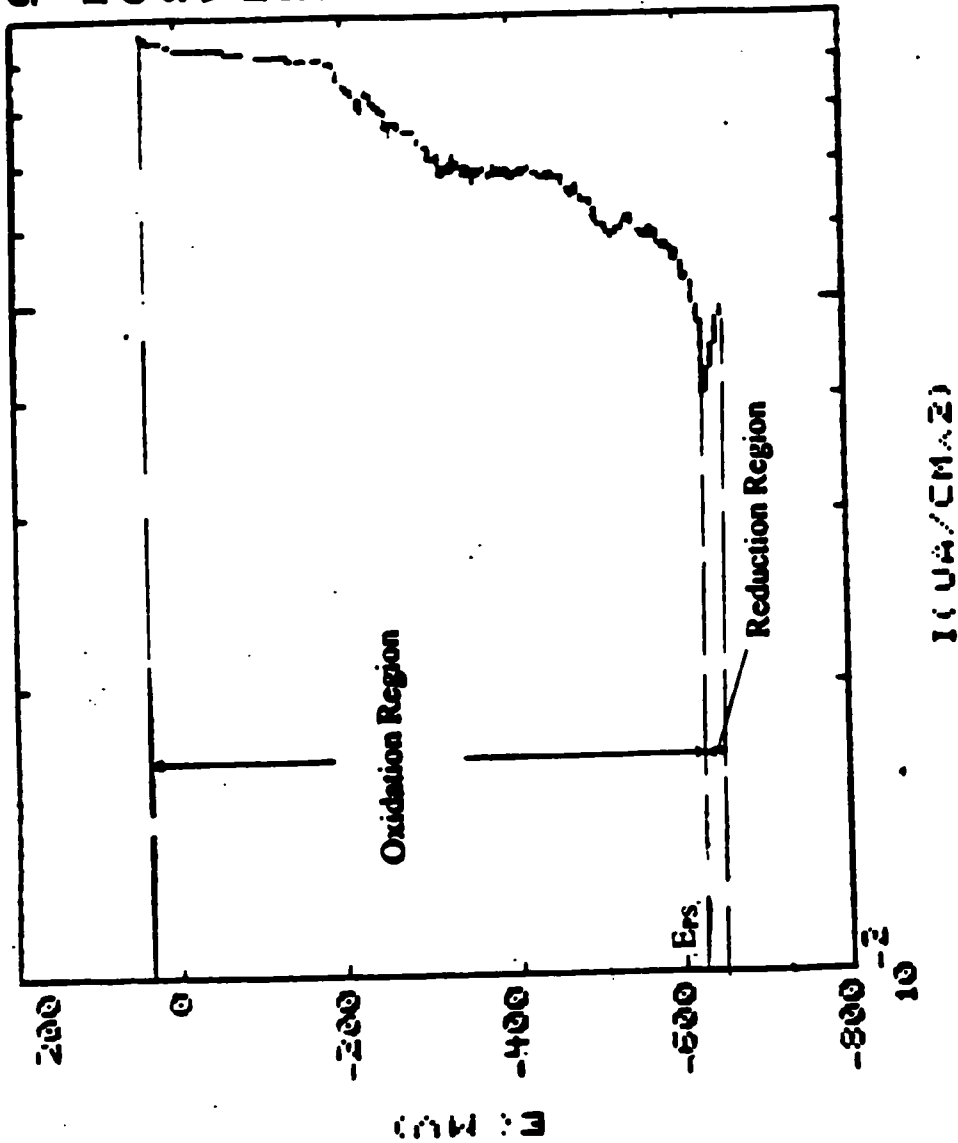
Figure 31. Potentiodynamic Scan of Mg at 50 ppb dissolve O_2 and 550°F.

Conditions:

Dissolve O_2 of water: 50 ppb
Conductivity of water: 0.76
Set up temperature: 550°F
Water temperature of water: 550°F
Furnace Temperature: 418°F
Pressure in high pressure loop: 1000 psi
Water Flow: 200 sccm
Nitrogen Pressure: 1000psi
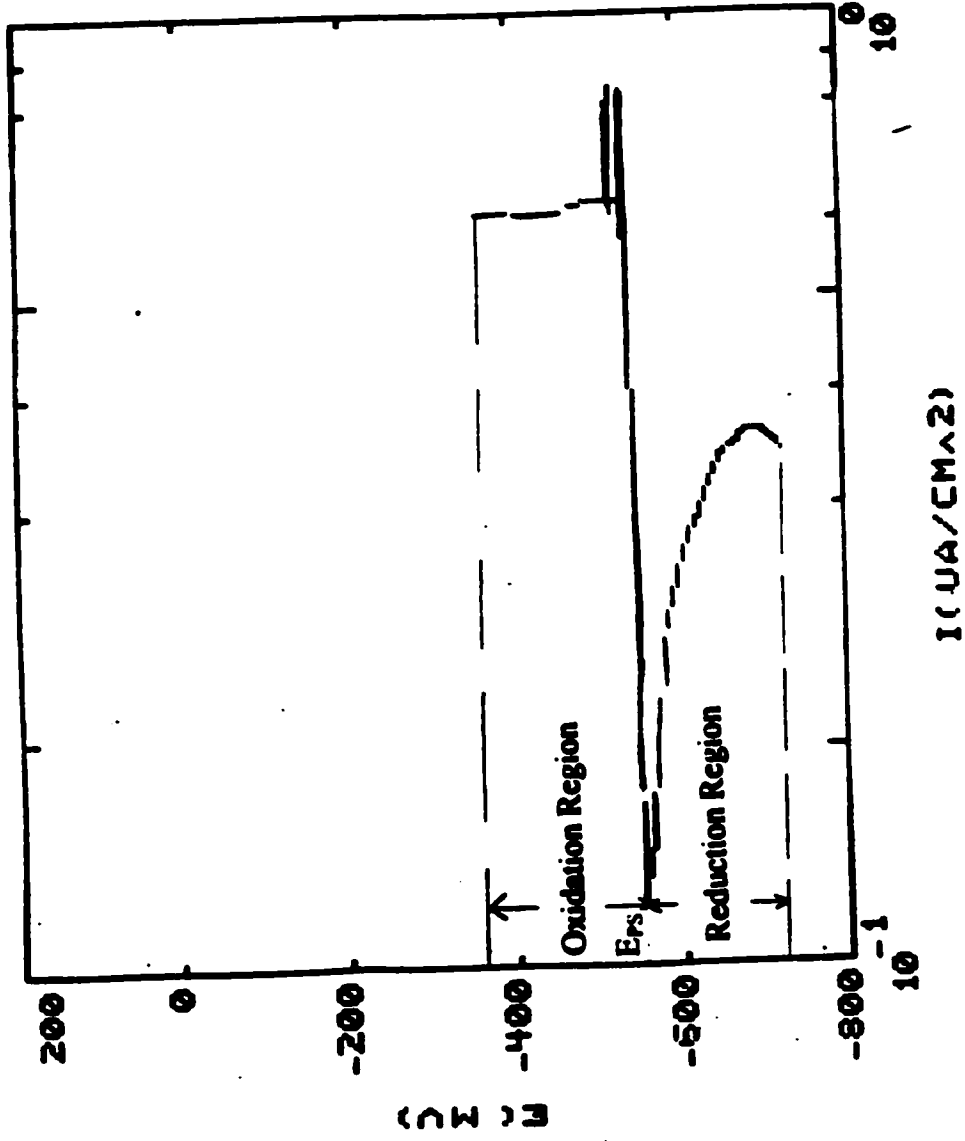Pressure in low pressure loop: 30 psi
Pump Stroke: 18%

Oxidation Region

Reduction Region

70
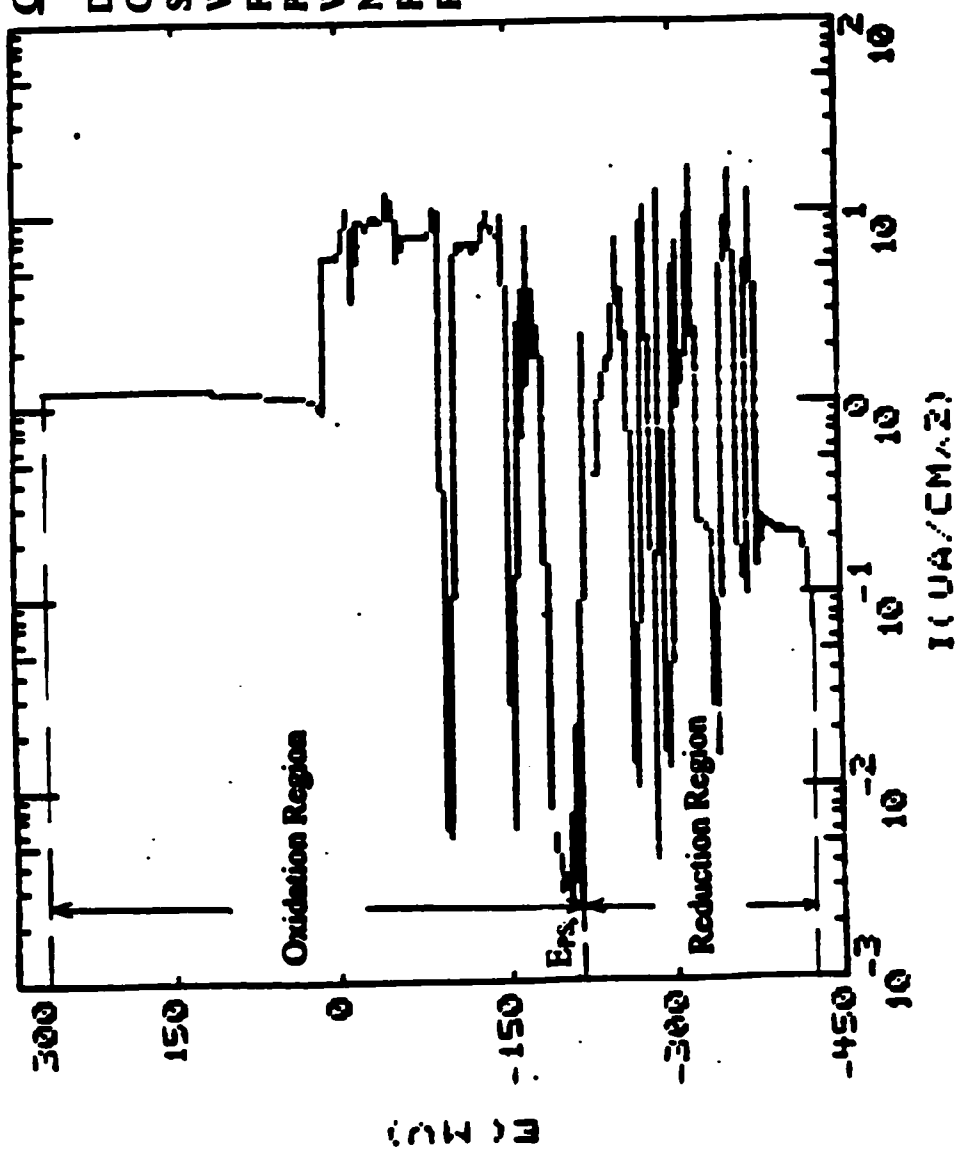
Figure 32. Potentiodynamic Scan of Mg at 200 ppb dissolve O_2 and 250°F.

Conditions:

Dissolve O_2 of water: 200 ppb
Conductivity of water: 0.76
Set up temperature: 350°F
Water temperature of water: 350°F
Furnace Temperature: 214°F
Pressure in high pressure loop: 1000 psi
Water Flow: 200 sccm
Nitrogen Pressure: 1000psi
Pressure in low pressure loop: 30 psi
Pump Stroke: 18%
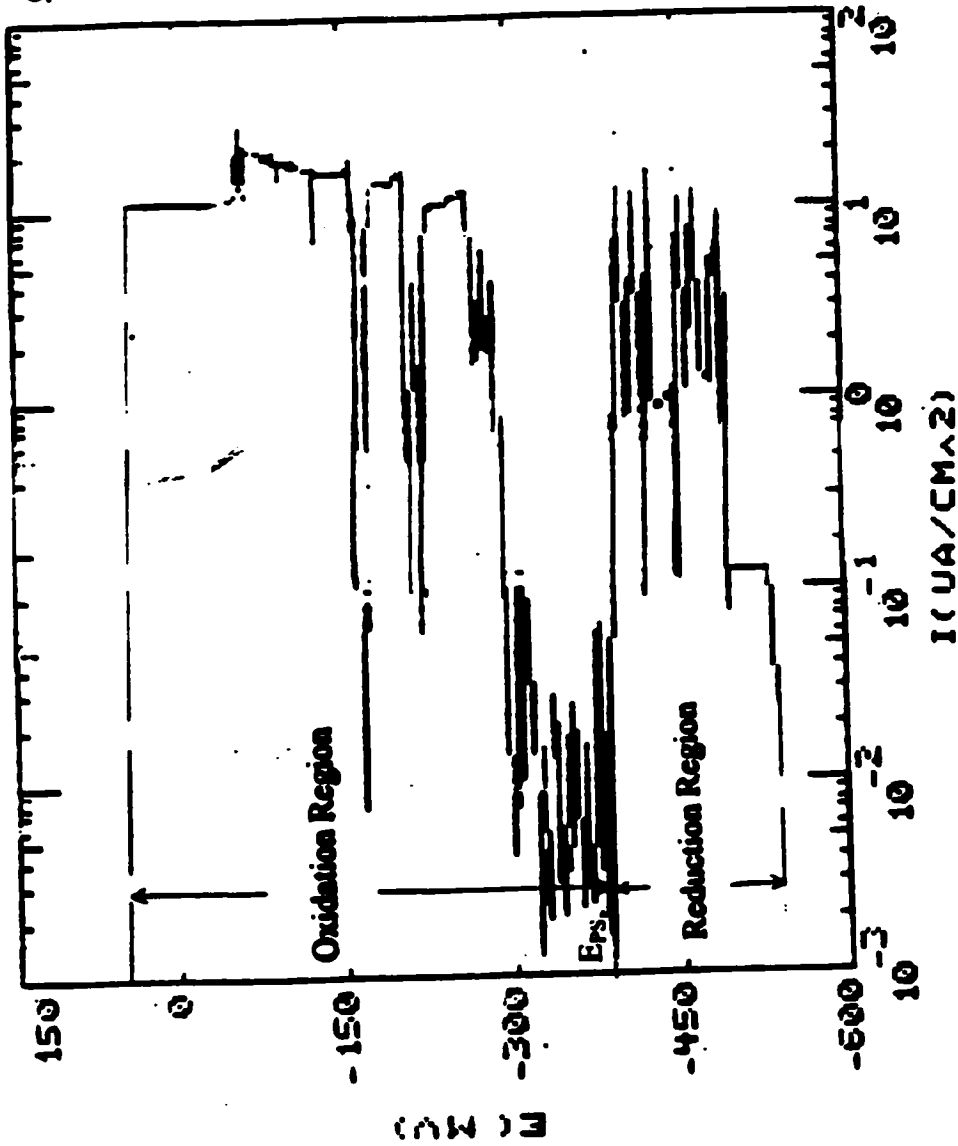
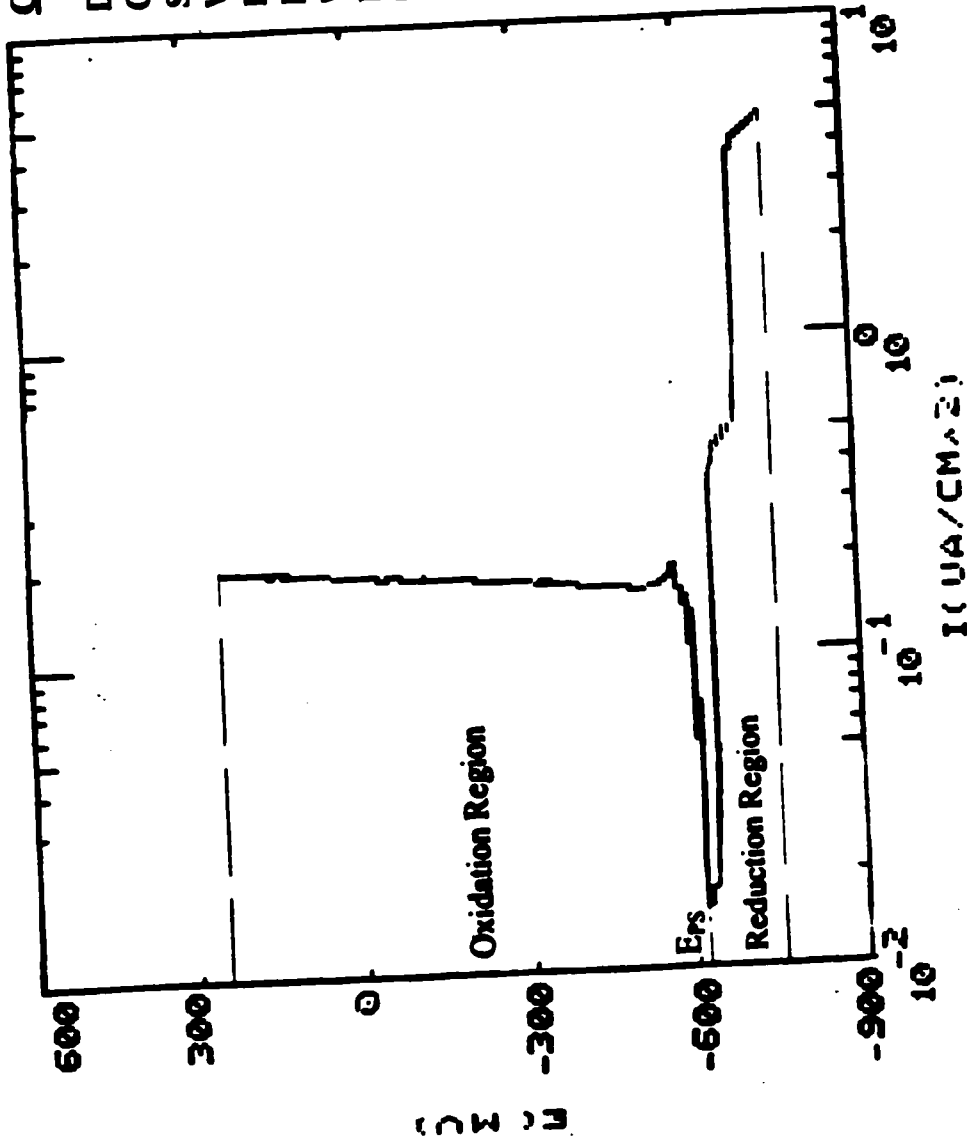Figure 33. Potentiodynamic Scan of Mg at 200 ppb dissolve O_2 and 350°F.

72
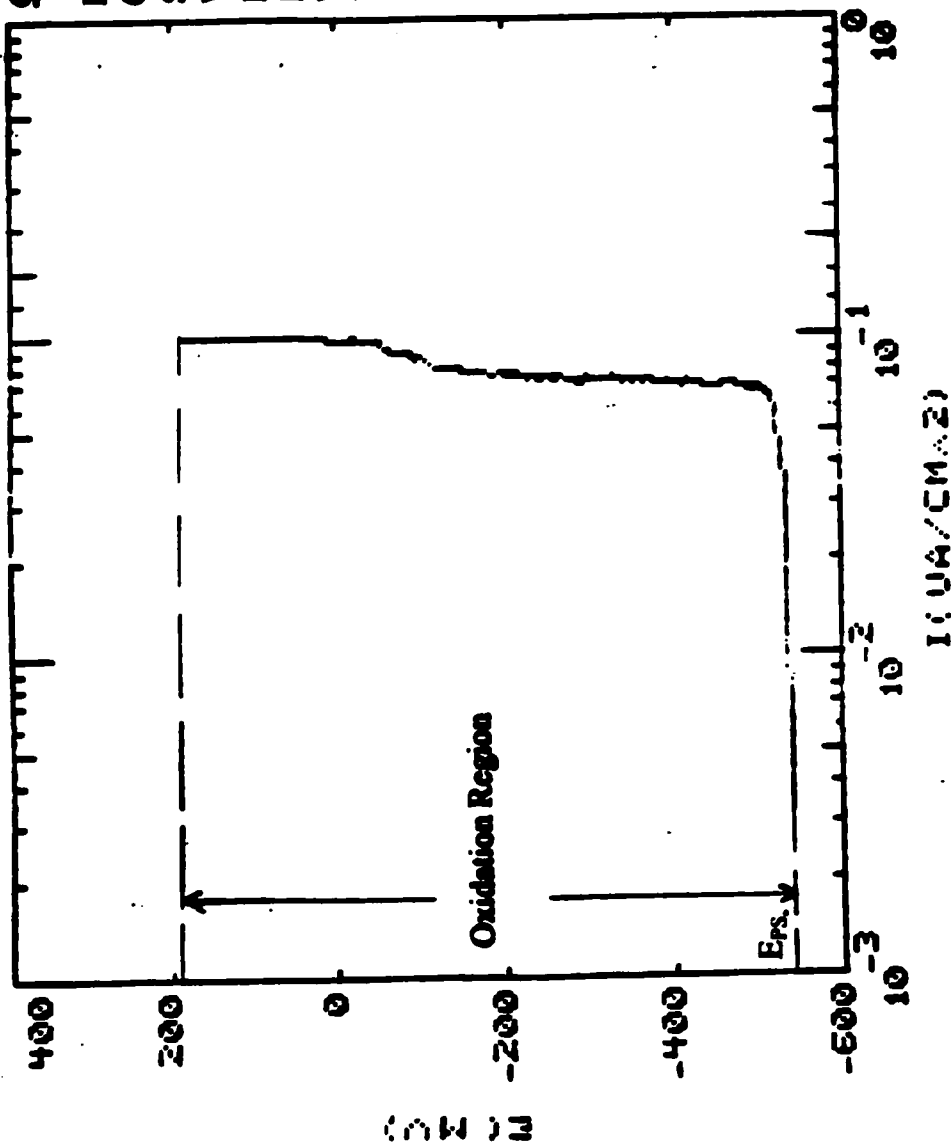
Figure 34. Potentiodynamic Scan of Mg at 200 ppb dissolve O_2 and 550°F.

Conditions:

Dissolve O_2 of water: 200 ppb
Conductivity of water: 0.76
Set up temperature: 550°F
Water temperature of water: 550°F
Furnace Temperature: 455°F
Pressure in high pressure loop: 1000 psi
Water Flow : 200 sccm
Nitrogen Pressure: 1000psi
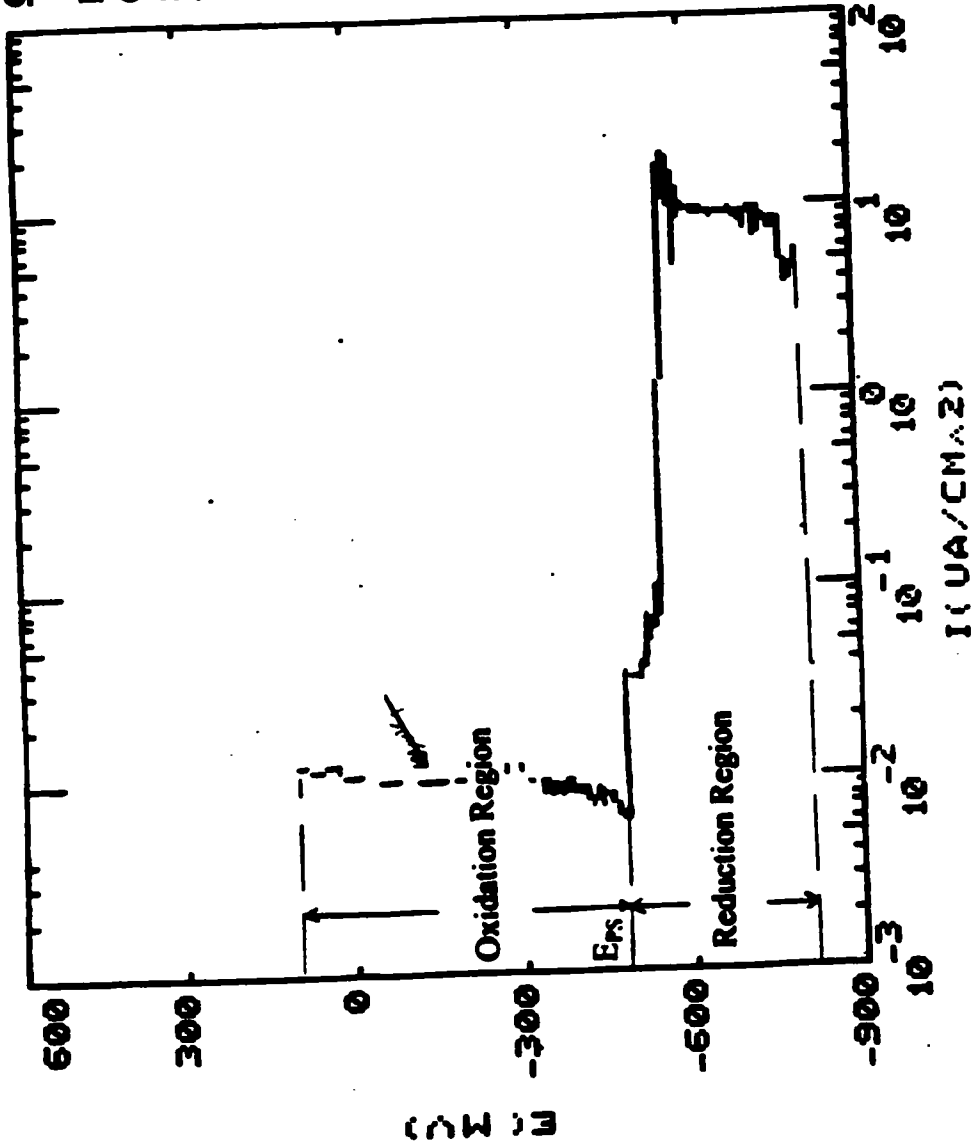Pressure in low pressure loop: 30 psi
Pump Stroke: 18%
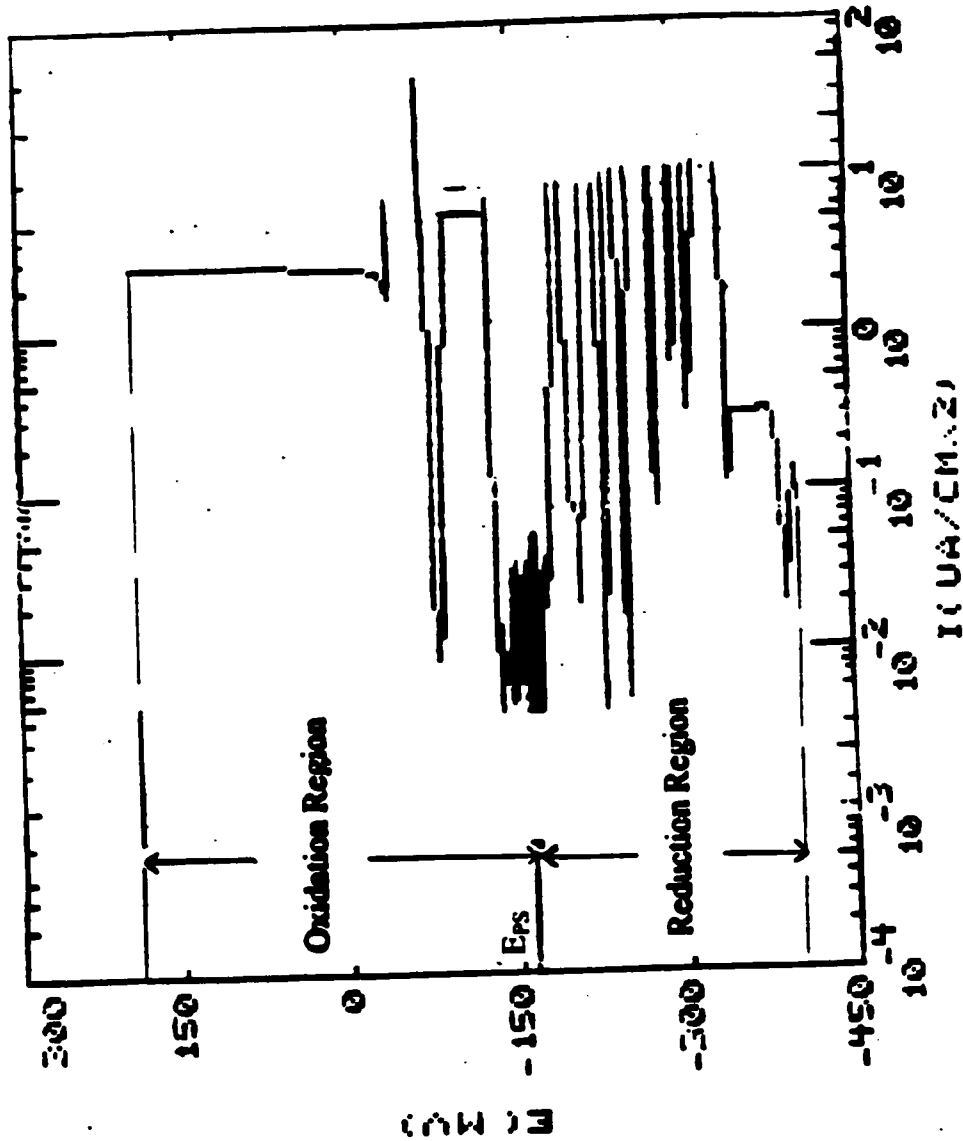
Figure 35. Potentiodynamic Scan of Mg at 8000 ppb dissolve O_2 and 250°F.

Conditions:

Dissolve O_2 of water: 8000 ppb
Conductivity of water: 0.76
Set up temperature: 250°F
Water temperature of water: 250°F
Furnace Temperature: 167°F
Pressure in high pressure loop: 1000 psi
Water Flow : 200 sccm
Nitrogen Pressure: 1000psi
Pressure in low pressure loop: 30 psi
Pump Stroke: 18%

74
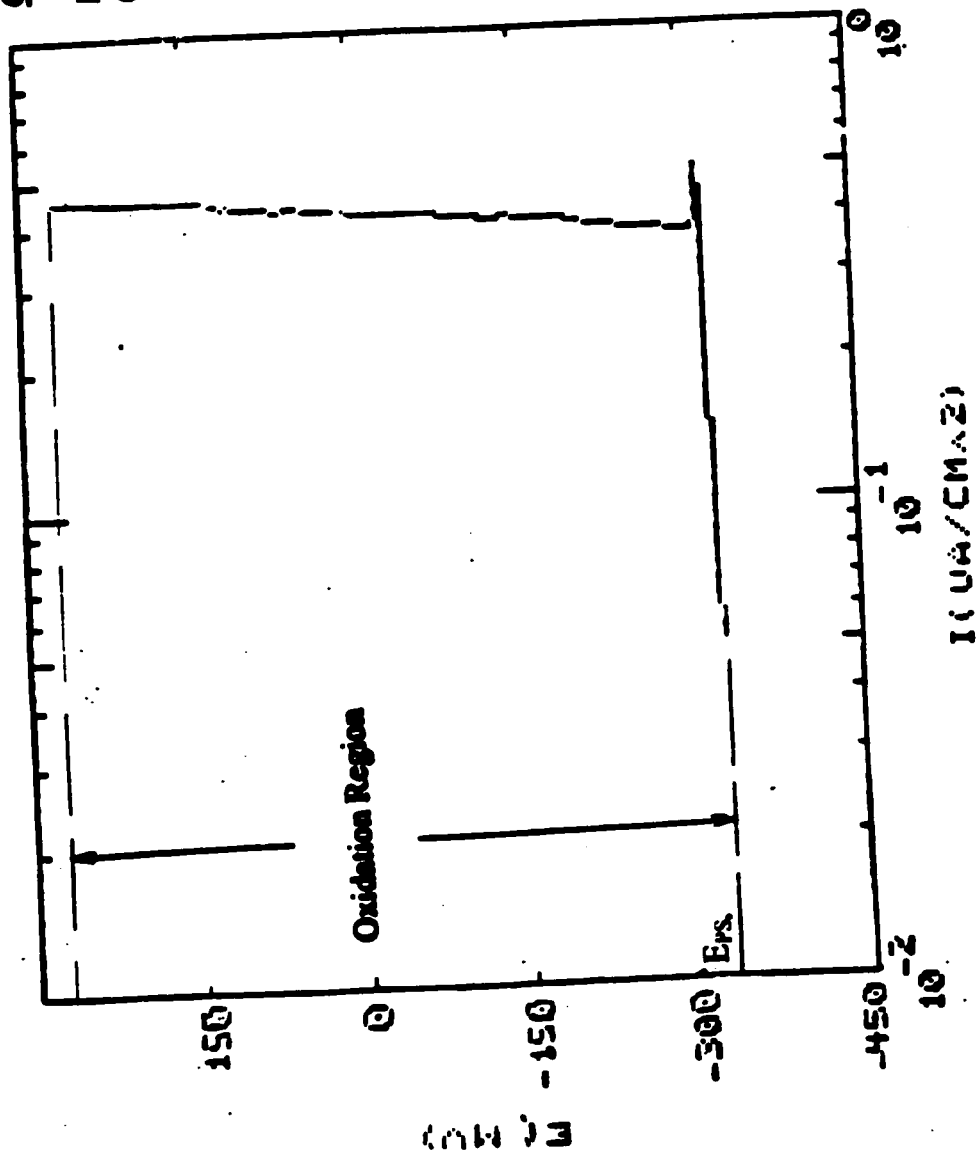
Figure 36. Potentiodynamic Scan of Mg at 8000 ppb dissolve O_2 and 350°F.

Conditions:

Dissolve O_2 of water: 8000 ppb
Conductivity of water: 0.76
Set up temperature: 350°F
Water temperature of water: 350°F
Furnace Temperature: 214°F
Pressure in high pressure loop: 1000 psi
Water Flow : 200 sccm
Nitrogen Pressure: 1000psi
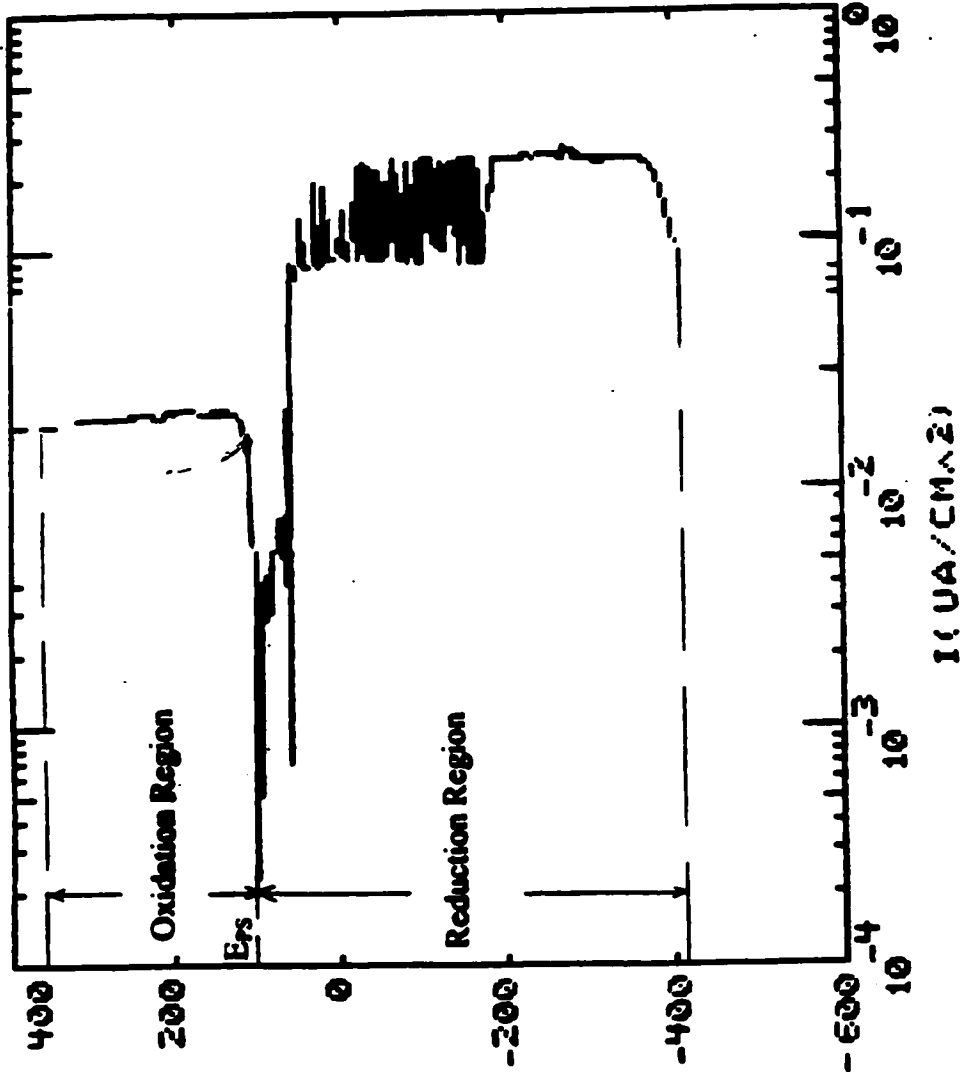Pressure in low pressure loop: 30 psi
Pump Stroke: 18%

75
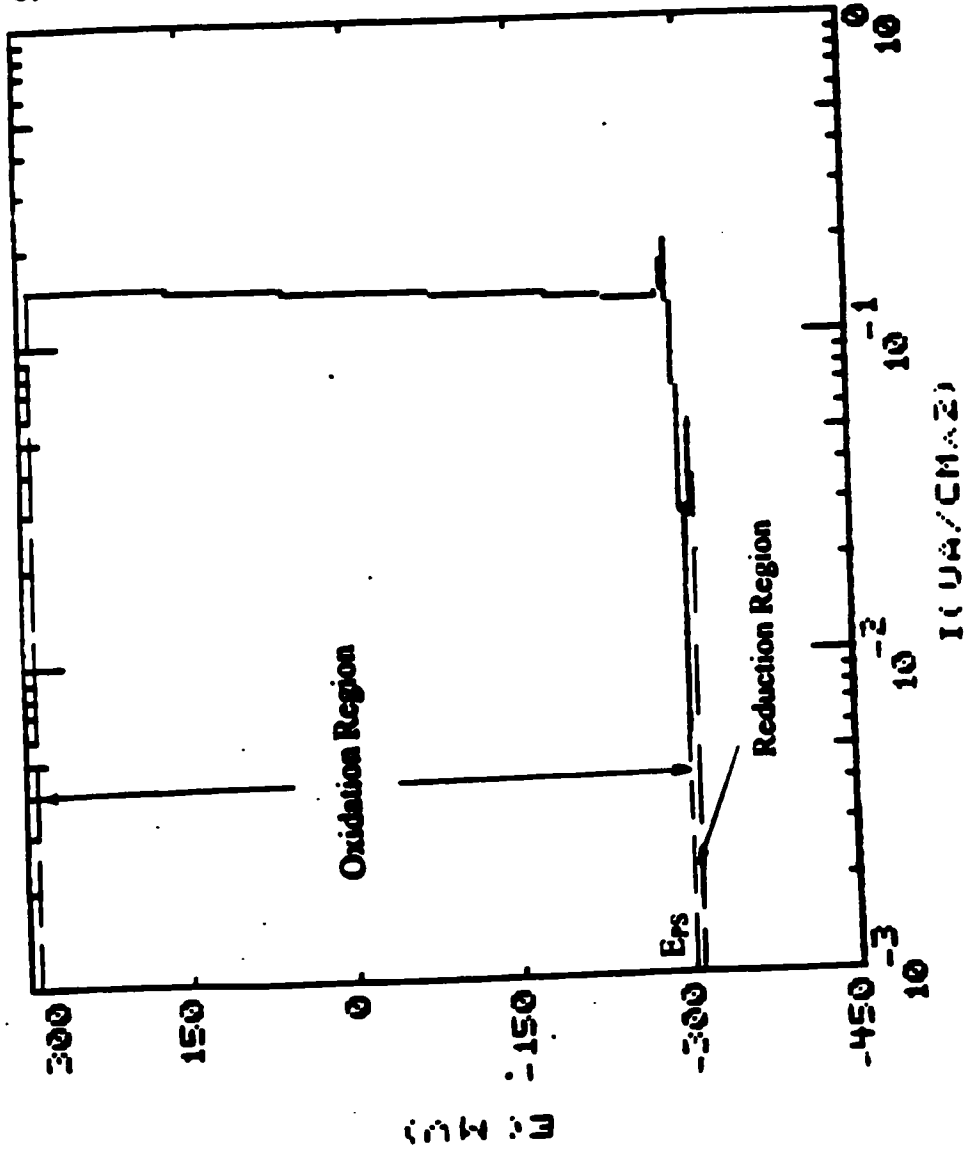
Figure 37. Potentiodynamic Scan of Mg at 8000 ppb dissolve O_2 and 550°F.

Conditions:

Dissolve O_2 of water: 8000 ppb
Conductivity of water: 0.76
Set up temperature: 550°F
Water temperature of water: 550°F
Furnace Temperature: 418°F
Pressure in high pressure loop: 1000 psi
Water Flow : 200 sccm
Nitrogen Pressure: 1000psi
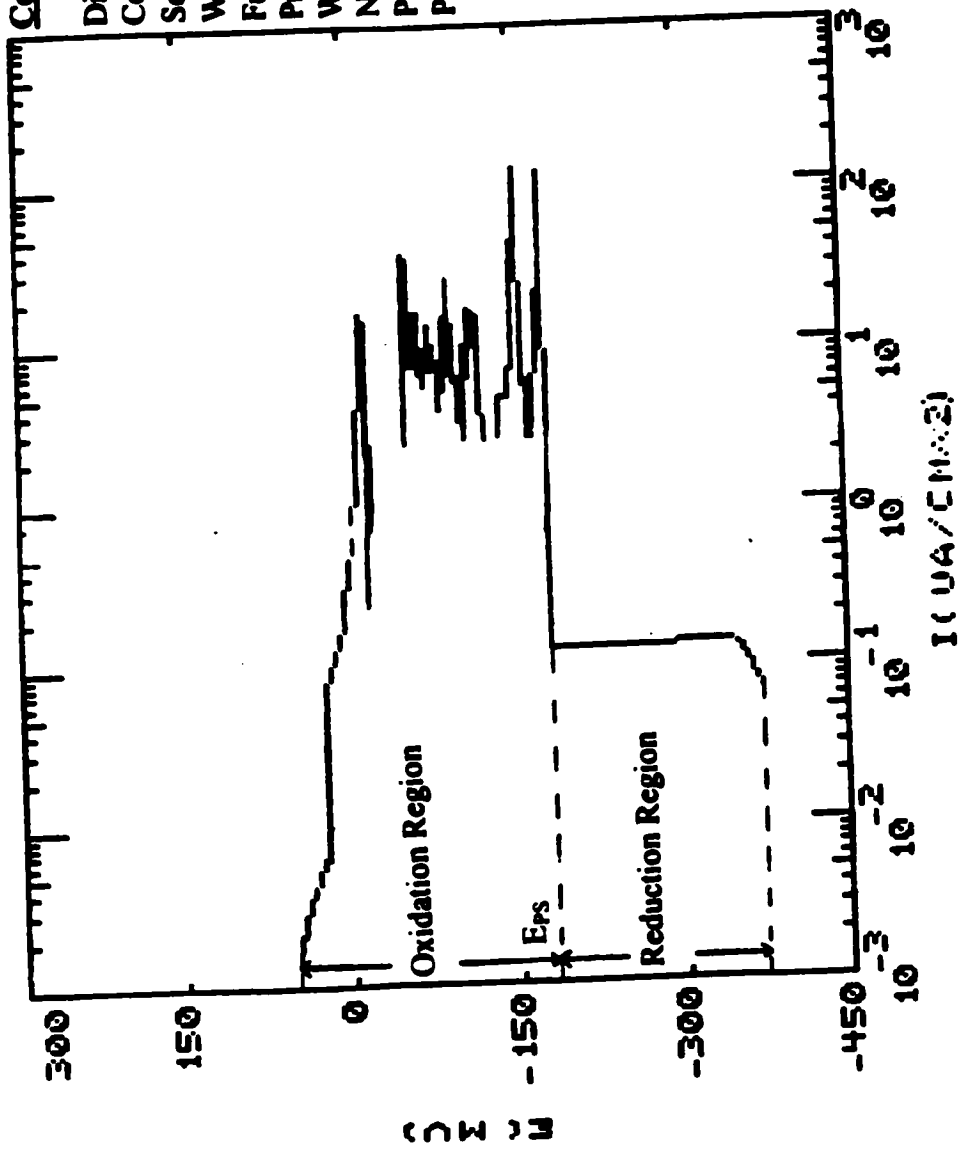Pressure in low pressure loop: 30 psi
Pump Stroke: 18%

76

Conditions:

Dissolve O_2 of water: 50 ppb
Conductivity of water: 0.76
Set up temperature: 250°F
Water temperature of water: 250°F
Furnace Temperature: 167°F
Pressure in high pressure loop: 1000 psi
Water Flow : 200 sccm
Nitrogen Pressure: 1000psi
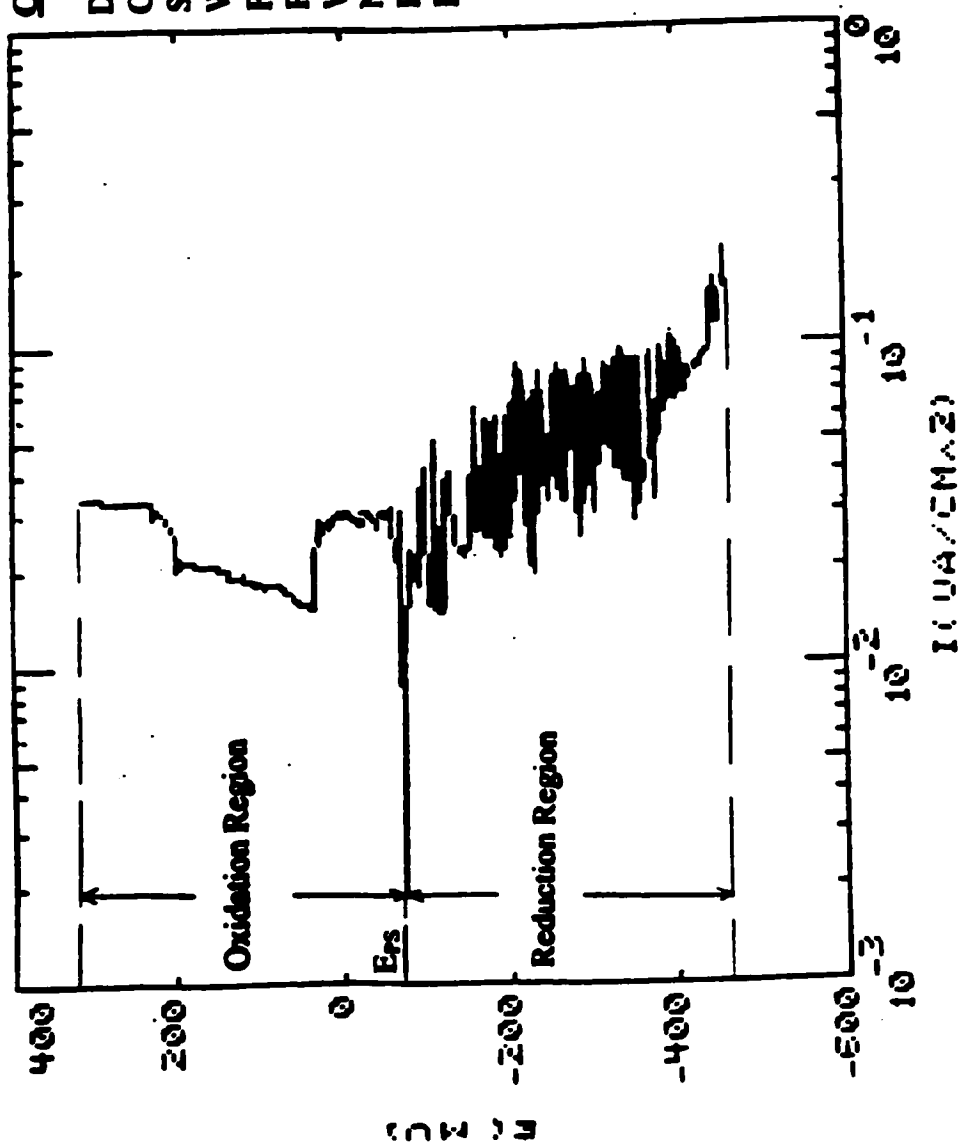Pressure in low pressure loop: 30 psi
Pump Stroke: 18%
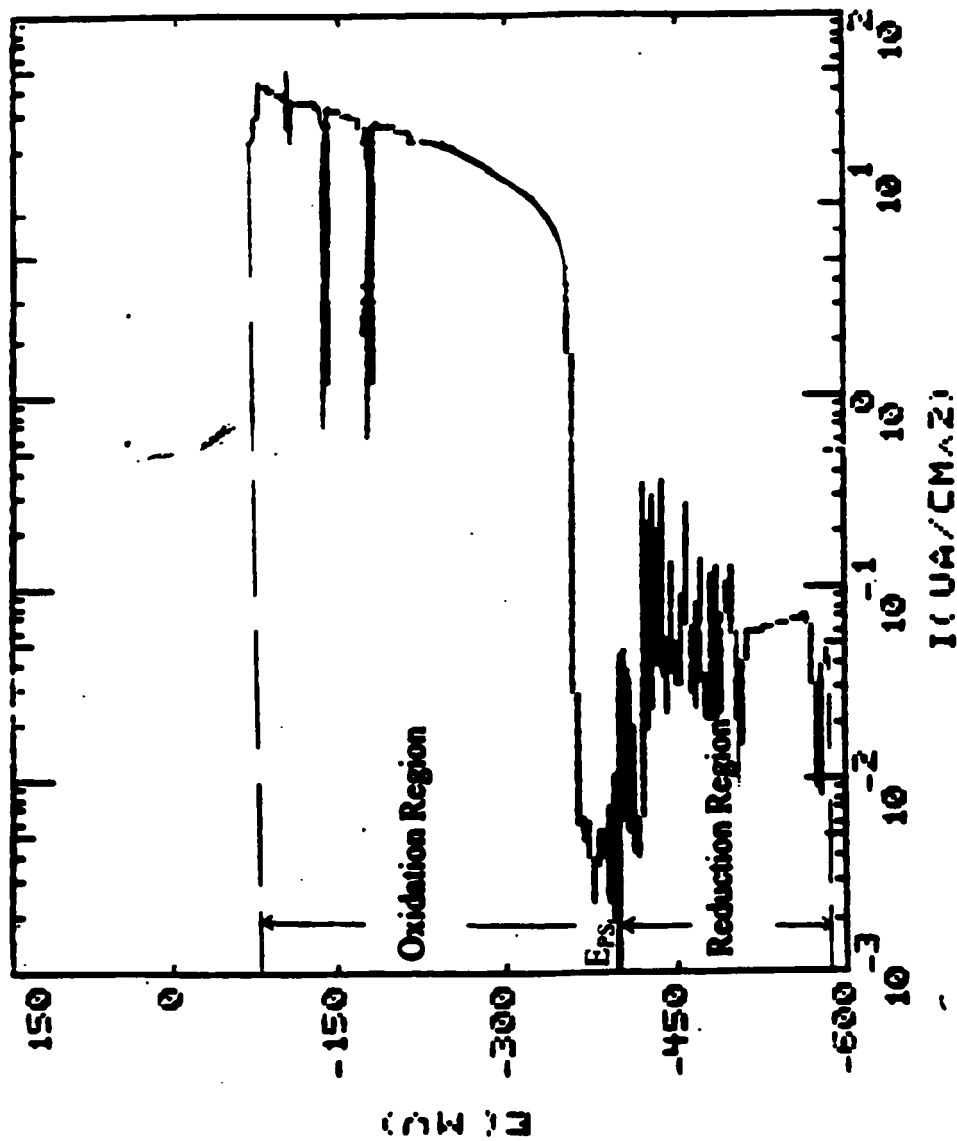
Figure 38. Potentiodynamic Scan of Zn at 50 ppb dissolve O_2 and 250°F.

77
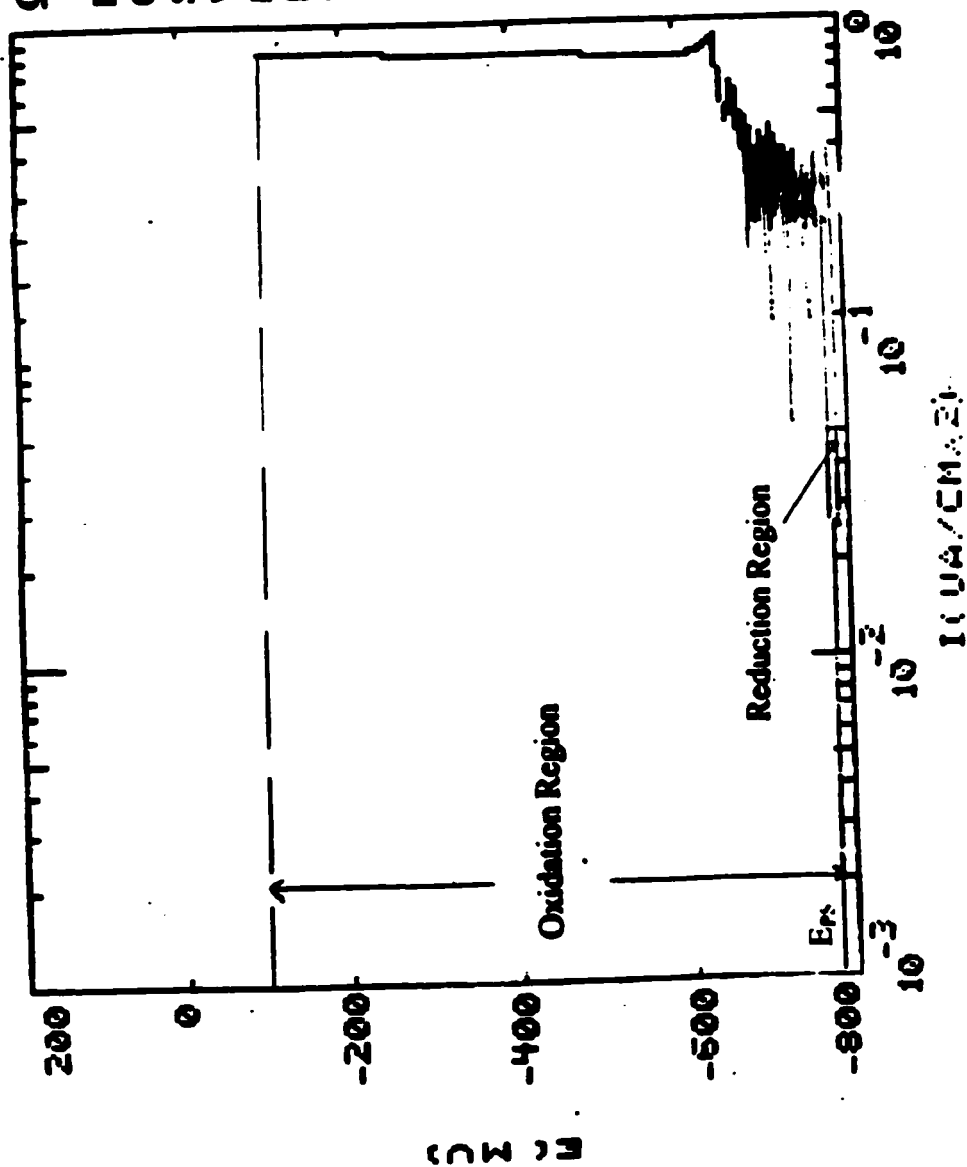
Figure 39. Potentiodynamic Scan of Zn at 50 ppb dissolve O_2 and 350°F.
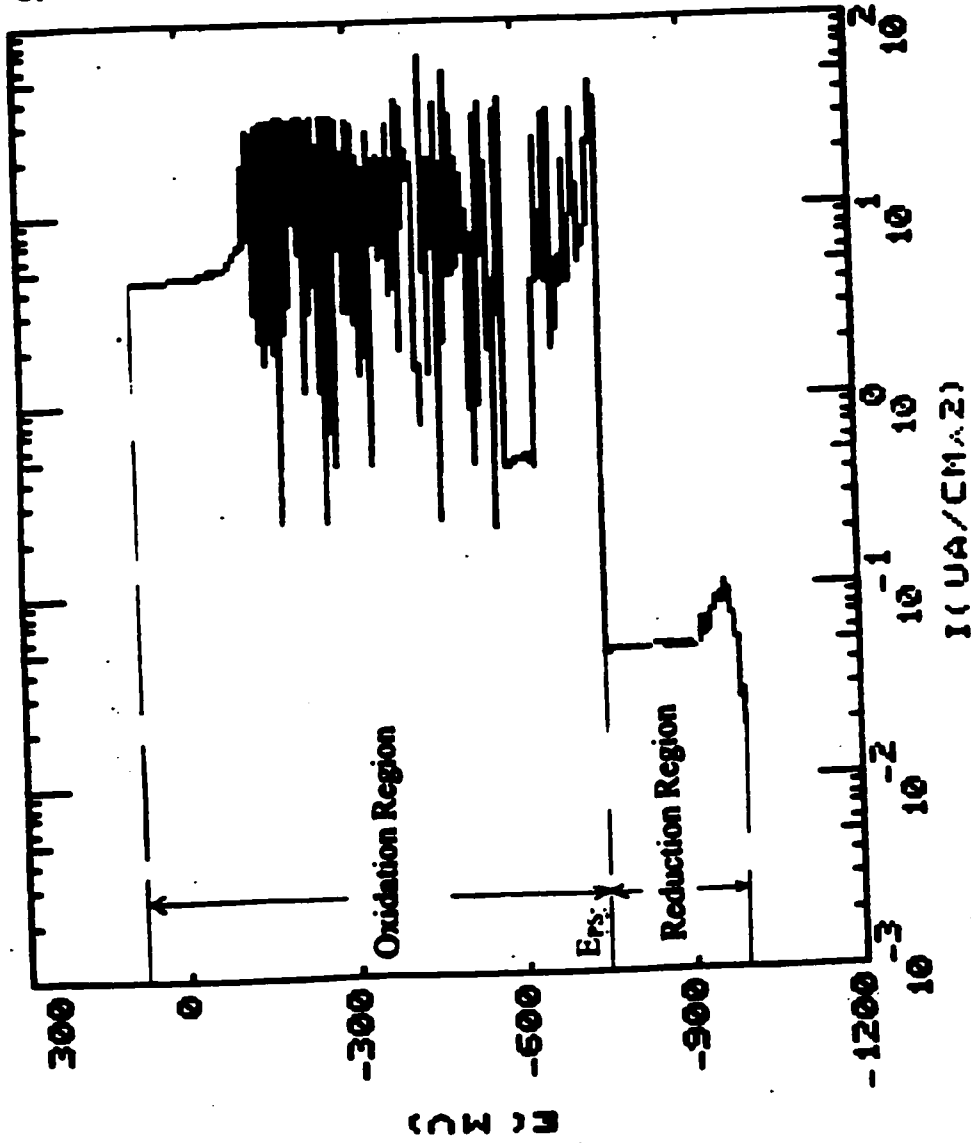
78

Figure 40. Potentiodynamic Scan of Zn at 50 ppb dissolve O₂ and 550°F.

Conditions:

Dissolve O₂ of water: 50 ppb
Conductivity of water: 0.76
Set up temperature: 550°F
Water temperature of water: 550°F
Furnace Temperature: 418°F
Pressure in high pressure loop: 1000 psi
Water Flow: 200 sccm
Nitrogen Pressure: 1000psi
Pressure in low pressure loop: 30 psi
Pump Stroke: 18%

79

Figure 41. Potentiodynamic Scan of Zn at 200 ppb dissolve O_2 and 250°F.

Conditions:

Dissolve O_2 of water: 200 ppb
Conductivity of water: 0.76
Set up temperature: 250°F
Water temperature of water: 250°F
Furnace Temperature: 168°F
Pressure in high pressure loop: 1000 psi
Water Flow : 200 sccm
Nitrogen Pressure: 1000psi
Pressure in low pressure loop: 30 psi
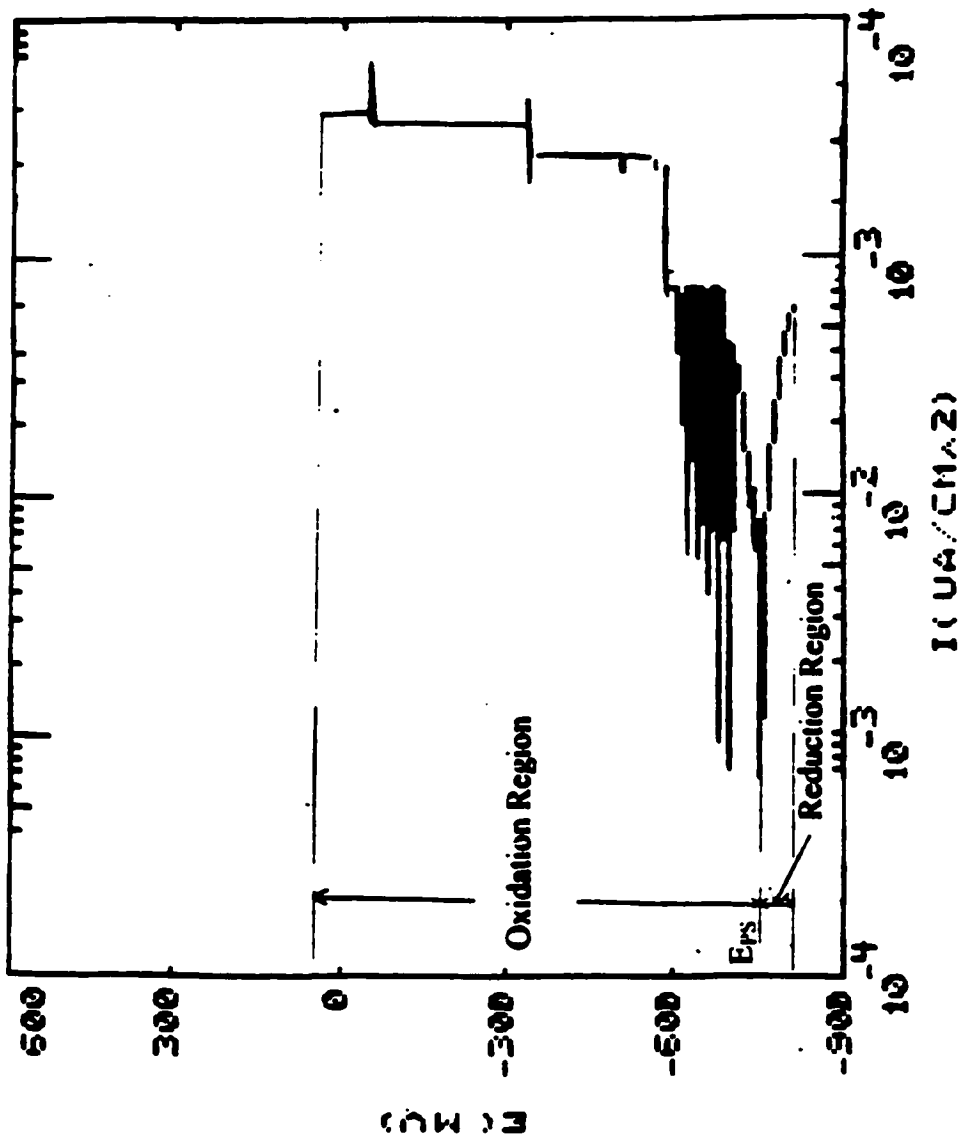Pump Stroke: 18%

80

Figure 42. Potentiodynamic Scan of Zn at 200 ppb dissolve O_2 and 350°F.

Conditions:

Dissolve O_2 of water: 200 ppb
Conductivity of water: 0.76
Set up temperature: 550°F
Water temperature of water: 550°F
Furnace Temperature: 455°F
Pressure in high pressure loop: 1000 psi
Water Flow : 200 sccm
Nitrogen Pressure: 1000psi
Pressure in low pressure loop: 30 psi
Pump Stroke: 18%

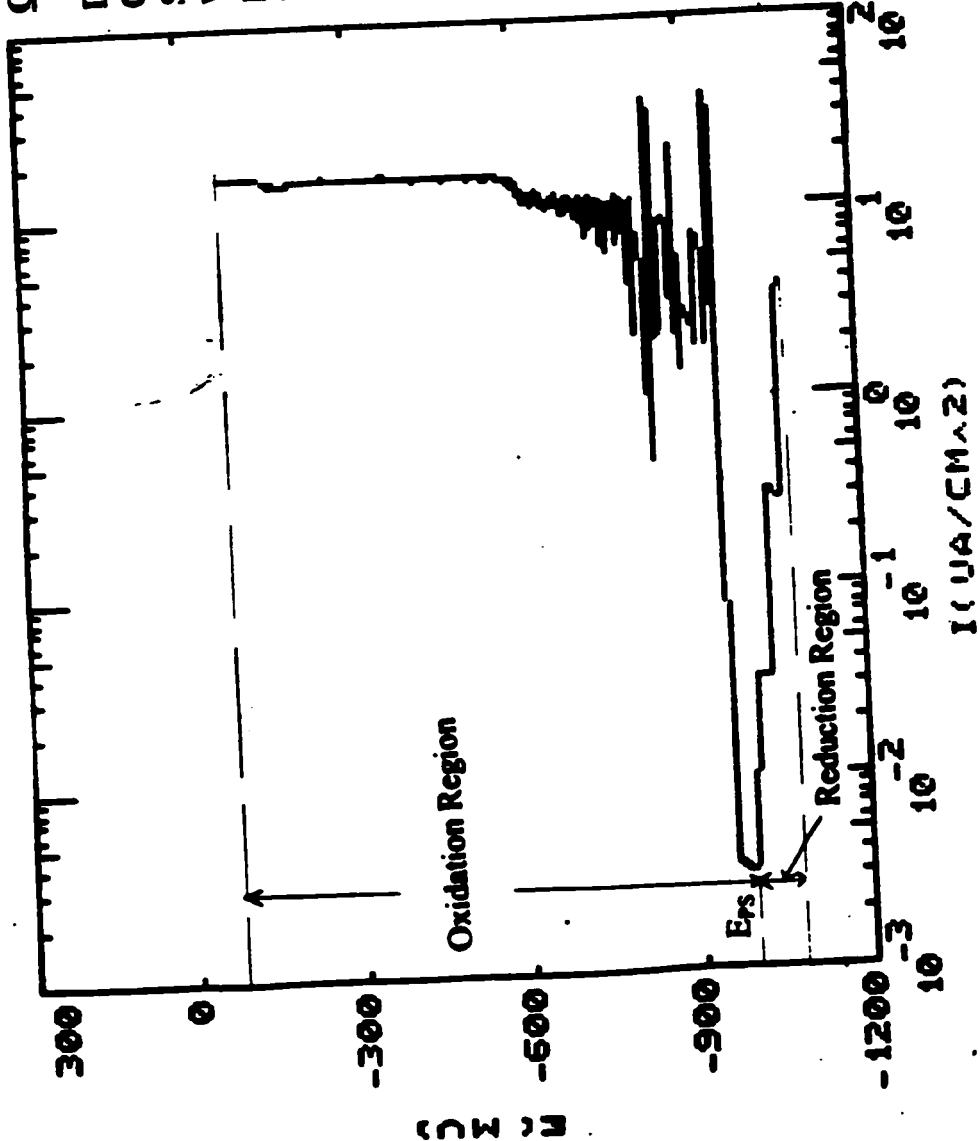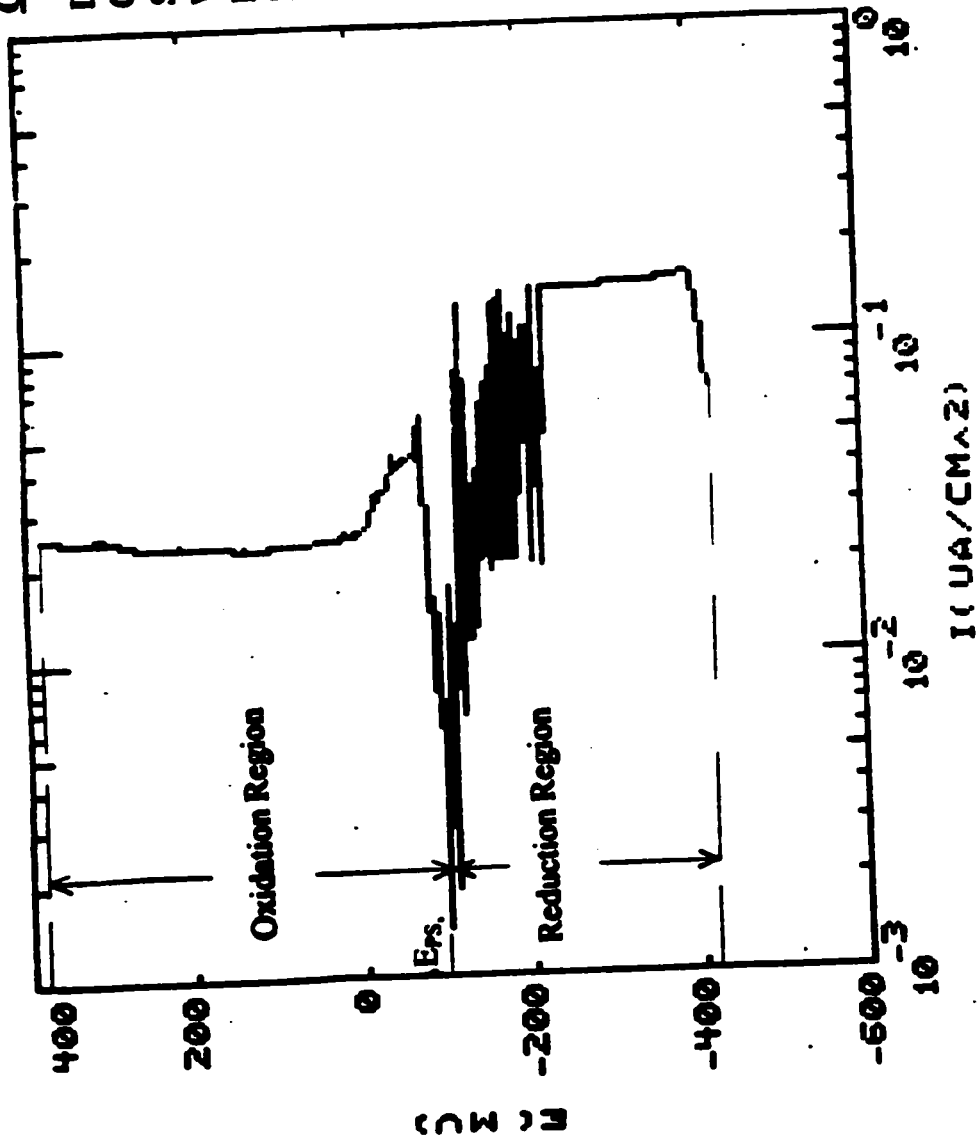Figure 43. Potentiodynamic Scan of Zn at 200 ppb dissolve O_2 and 550°F.

82

Figure 44. Potentiodynamic Scan of Zn at 8000 ppb dissolve O_2 and 250°F.

83
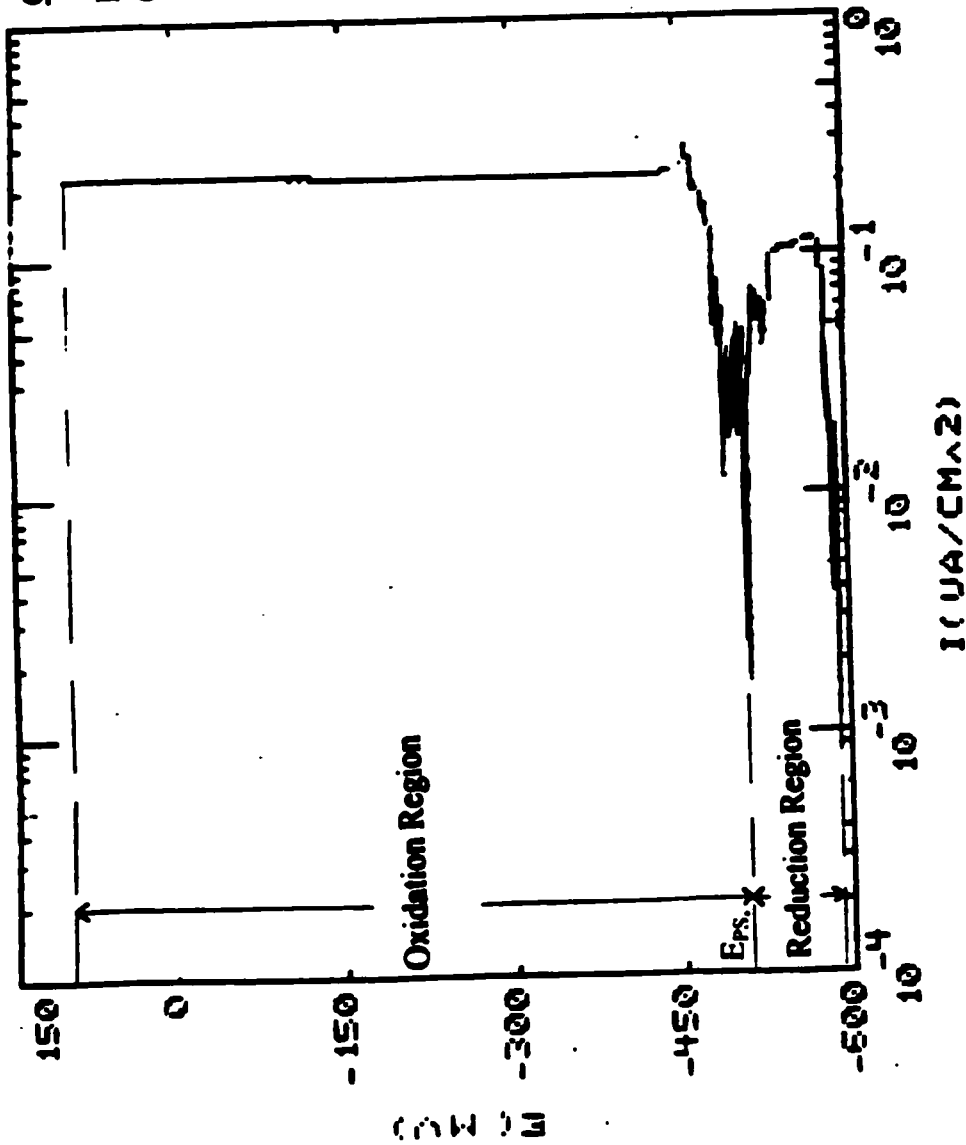
Figure 45. Potentiodynamic Scan of Zn at 8000 ppb dissolve O_2 and 350°F.

84

Figure 46. Potentiodynamic Scan of Zn at 8000 ppb dissolve O_2 and 550°F.

Conditions:

Dissolve O_2 of water: 8000 ppb
Conductivity of water: 0.76
Set up temperature: 550°F
Water temperature of water: 550°F
Furnace Temperature: 417°F
Pressure in high pressure loop: 1000 psi
Water Flow : 200 sccm
Nitrogen Pressure: 1000psi
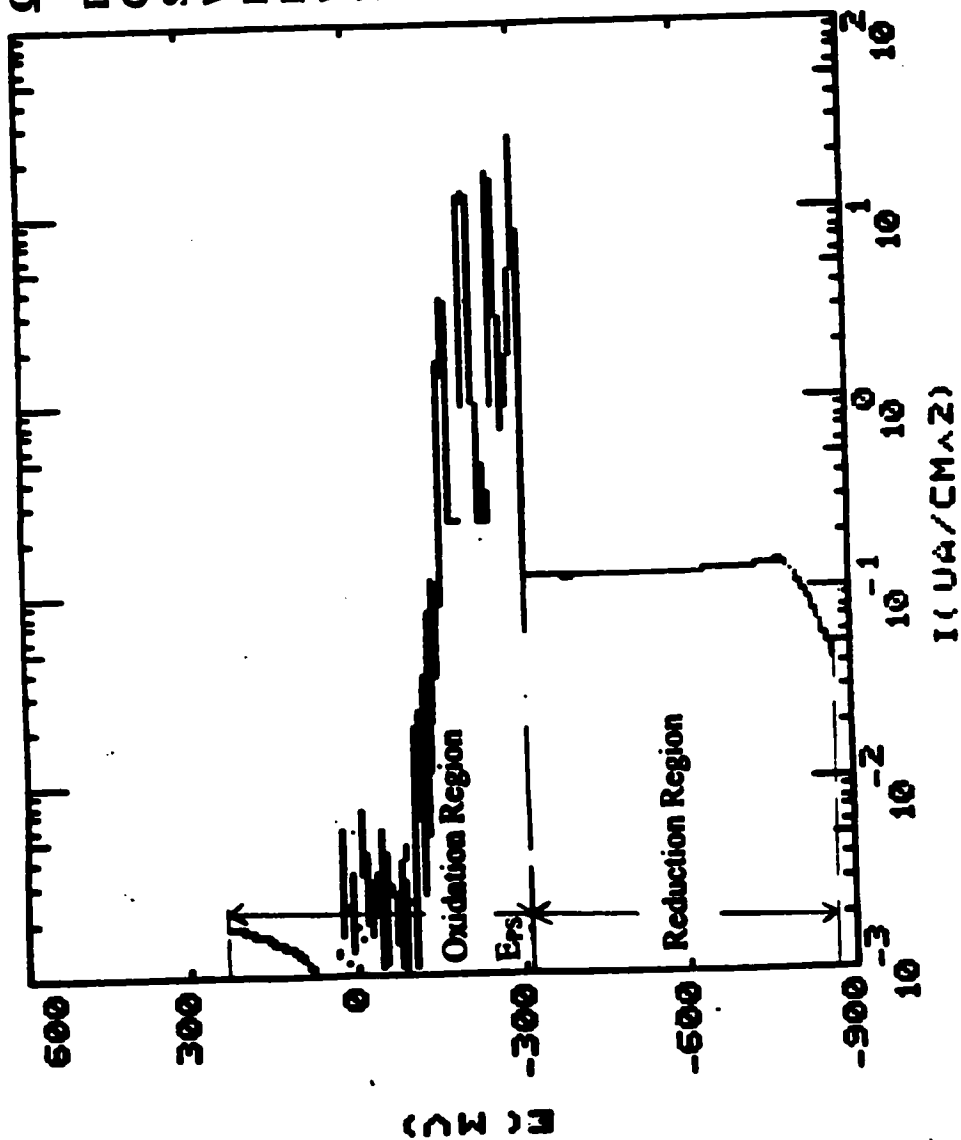Pressure in low pressure loop: 30 psi
Pump Stroke: 18%

85

Figure 47. Potentiodynamic Scan of Zr-alloy at 50 ppb dissolve O_2 and 250°F.

Figure 48. Potentiodynamic Scan of Zr-alloy at 50 ppb dissolve O₂ and 350°F.

Figure 49. Potentiodynamic Scan of Zr-alloy at 50 ppb dissolve O_2 and 550°F.

Conditions:

Dissolve O_2 of water: 50 ppb
Conductivity of water: 0.76
Set up temperature: 550°F
Water temperature of water: 550°F
Furnace Temperature: 167°F
Pressure in high pressure loop: 1000 psi
Water Flow : 200 sccm
Nitrogen Pressure: 1000psi
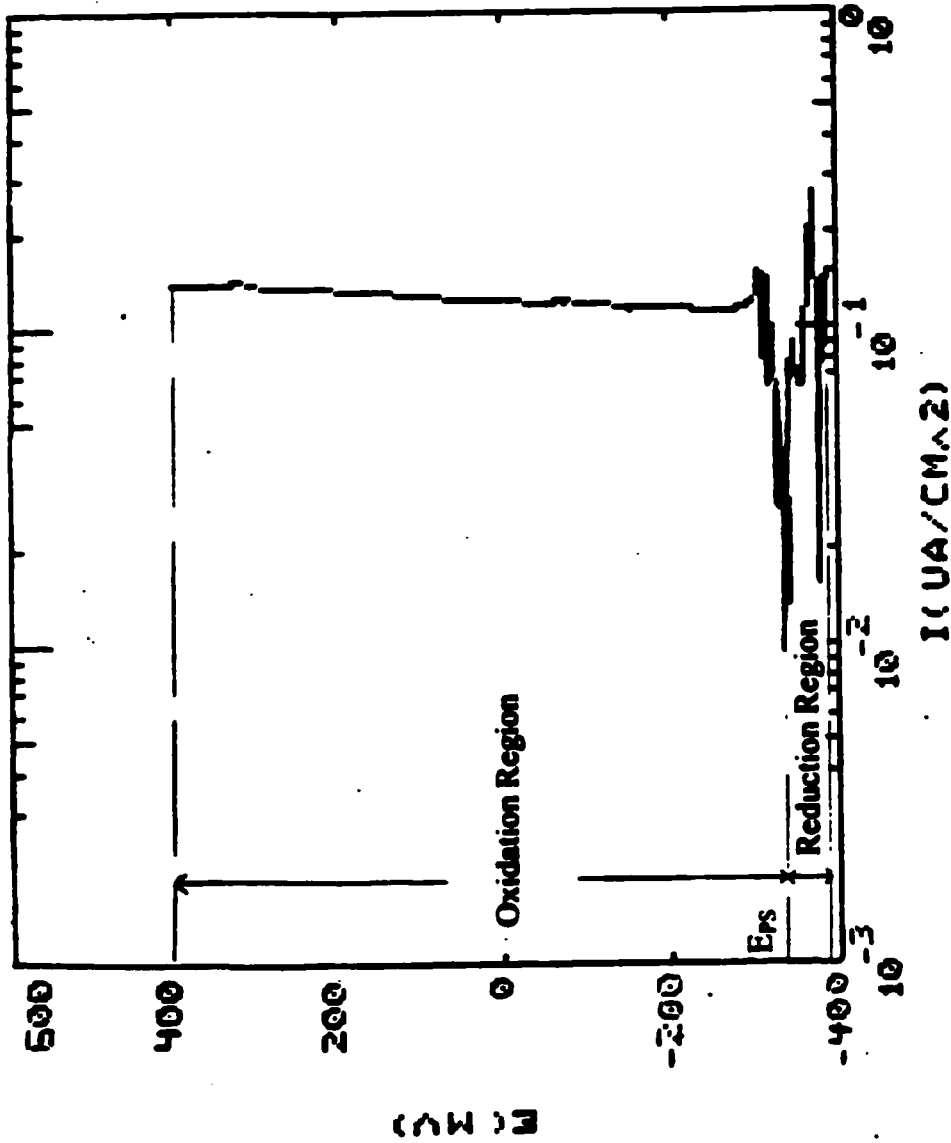Pressure in low pressure loop: 30 psi
Pump Stroke: 18%

88

Figure 50. Potentiodynamic Scan of Zr-alloy at 200 ppb dissolve O_2 and 250°F.

89

Figure 51. Potentiodynamic Scan of Zr-alloy at 200 ppb dissolve O_2 and 350°F.

Conditions:

Dissolve O_2 of water: 200 ppb
Conductivity of water: 0.76
Set up temperature: 350°F
Water temperature of water: 350°F
Furnace Temperature: 217°F
Pressure in high pressure loop: 1000 psi
Water Flow : 200 sccm
Nitrogen Pressure: 1000psi
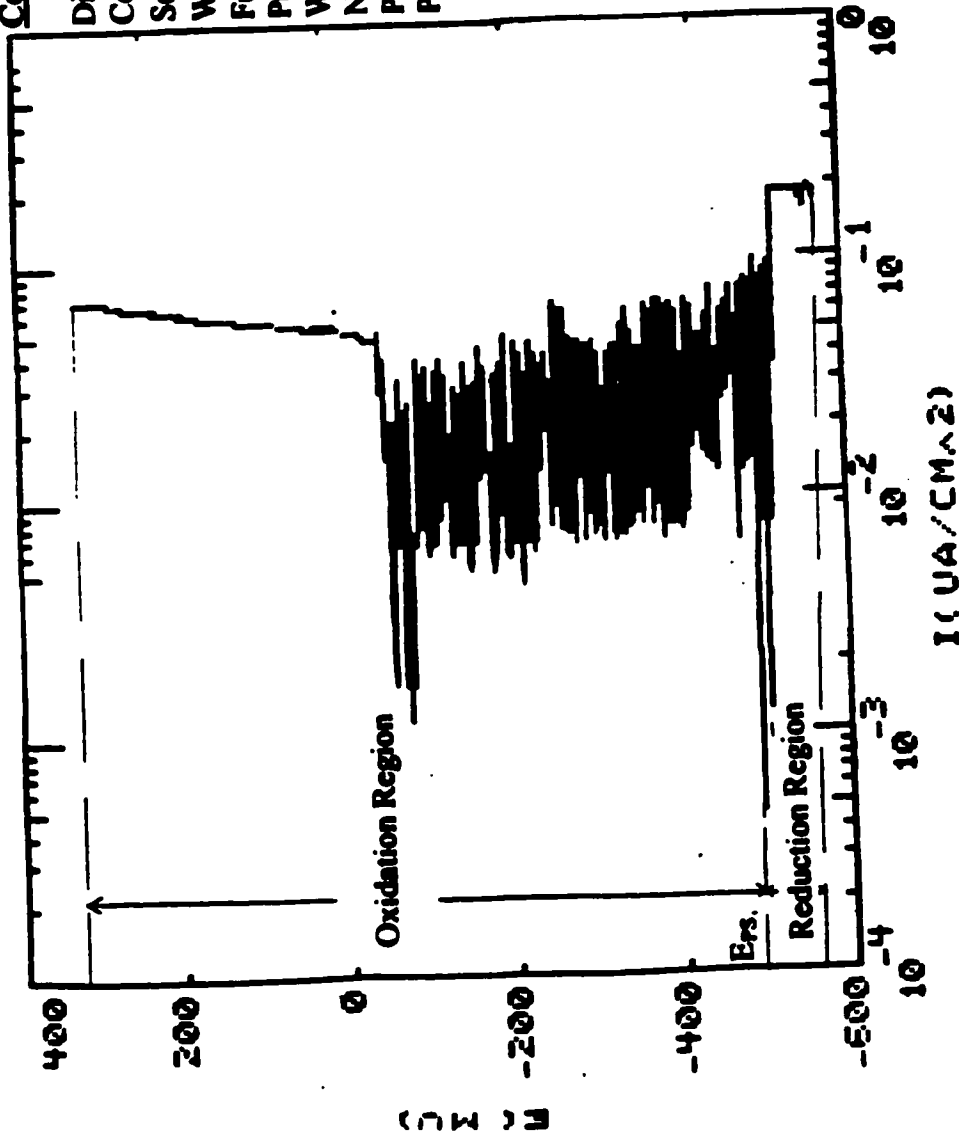Pressure in low pressure loop: 30 psi
Pump Stroke: 18%

Figure 52. Potentiodynamic Scan of Zr-alloy at 200 ppb dissolve O₂ and 550°F.

91

Conditions:

Dissolve O_2 of water: 8000 ppb
Conductivity of water: 0.76
Set up temperature: 250°F
Water temperature of water: 250°F
Furnace Temperature: 168°F
Pressure in high pressure loop: 1000 psi
Water Flow : 200 sccm
Nitrogen Pressure: 1000psi
Pressure in low pressure loop: 30 psi
Pump Stroke: 18%

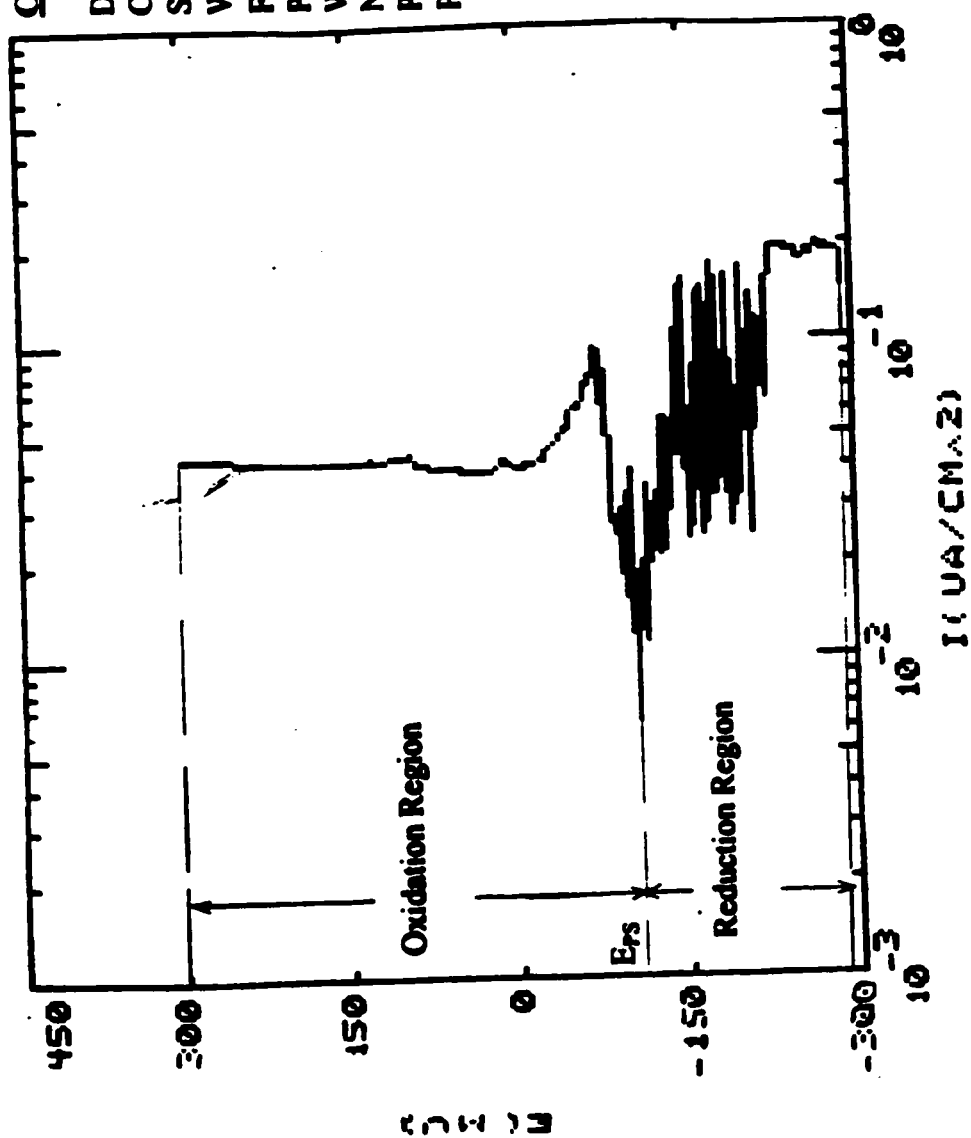Figure 53. Potentiodynamic Scan of Zr-alloy at 8000 ppb dissolve O_2 and 250°F.

92

Conditions:

Dissolve O_2 of water: 8000 ppb
Conductivity of water: 0.76
Set up temperature: 350°F
Water temperature of water: 350°F
Furnace Temperature: 217°F
Pressure in high pressure loop: 1000 psi
Water Flow : 200 sccm
Nitrogen Pressure: 1000psi
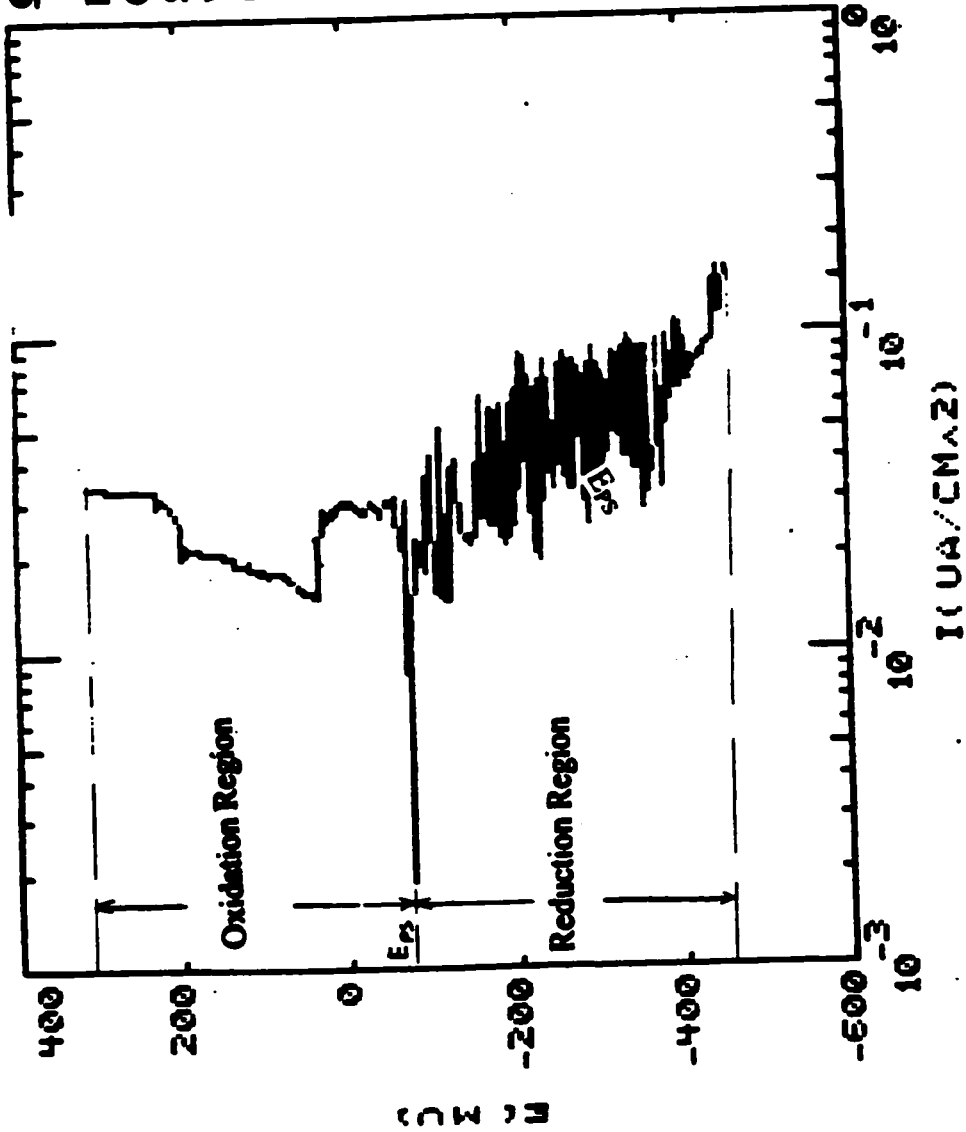Pressure in low pressure loop: 30 psi
Pump Stroke: 18%

Figure 54. Potentiodynamic Scan of Zr-alloy at 8000 ppb dissolve O_2 and 350°F.

93

Figure 55. Potentiodynamic Scan of Zr-alloy at 8000 ppb dissolve O_2 and 550°F.

Conditions:

Dissolve O_2 of water: 8000 ppb
Conductivity of water: 0.76
Set up temperature: 550°F
Water temperature of water: 550°F
Furnace Temperature: 455°F
Pressure in high pressure loop: 1000 psi
Water Flow : 200 sccm
Nitrogen Pressure: 1000psi
Pressure in low pressure loop: 30 psi
Pump Stroke: 18%

Figure 56. Potentiodynamic Scan of Zr at 50 ppb dissolve O_2 and 250°F.

95

Conditions:

Dissolve O_2 of water: 50 ppb
Conductivity of water: 0.76
Set up temperature: 350°F
Water temperature of water: 350°F
Furnace Temperature: 218°F
Pressure in high pressure loop: 1000 psi
Water Flow: 200 sccm
Nitrogen Pressure: 1000psi
Pressure in low pressure loop: 30 psi
Pump Stroke: 18%

Figure 57: Potentiodynamic Scan of Zr at 50 ppb dissolve O_2 and 350°F.

Figure 58. Potentiodynamic Scan of Zr at 50 ppb dissolve O₂ and 550°F.

Conditions:

Dissolve O₂ of water: 50 ppb
Conductivity of water: 0.76
Set up temperature: 550°F
Water temperature of water: 550°F
Furnace Temperature: 455°F
Pressure in high pressure loop: 1000 psi
Water Flow : 200 sccm
Nitrogen Pressure: 1000psi
Pressure in low pressure loop: 30 psi
Pump Stroke: 18%

97

Figure 59. Potentiodynamic Scan of Zr at 200 ppb dissolve O_2 and 250°F.

Figure 60. Potentiodynamic Scan of Zr at 200 ppb dissolve O_2 and 350°F.

Conditions:

Dissolve O_2 of water: 200 ppb
Conductivity of water: 0.76
Set up temperature: 350°F
Water temperature of water: 350°F
Furnace Temperature: 217°F
Pressure in high pressure loop: 1000 psi
Water Flow: 200 sccm
Nitrogen Pressure: 1000psi
Pressure in low pressure loop: 30 psi
Pump Stroke: 18%

Conditions:

Dissolve O_2 of water: 200 ppb
Conductivity of water: 0.76
Set up temperature: 550°F
Water temperature of water: 550°F
Furnace Temperature: 455°F
Pressure in high pressure loop: 1000 psi
Water Flow : 200 sccm
Nitrogen Pressure: 1000psi
Pressure in low pressure loop: 30 psi
Pump Stroke: 18%

Figure 61. Potentiodynamic Scan of Zr at 200 ppb dissolve O_2 and 550°F.

100

Figure 62. Potentiodynamic Scan of Zr at 8000 ppb dissolve O_2 and 250°F.

Conditions:

Dissolve O_2 of water: 8000 ppb
Conductivity of water: 0.76
Set up temperature: 250°F
Water temperature of water: 250°F
Furnace Temperature: 167°F
Pressure in high pressure loop: 1000 psi
Water Flow : 200 sccm
Nitrogen Pressure: 1000psi
Pressure in low pressure loop: 30 psi
Pump Stroke: 18%

Conditions:

Dissolve O_2 of water: 8000 ppb
Conductivity of water: 0.76
Set up temperature: 350°F
Water temperature of water: 350°F
Furnace Temperature: 217°F
Pressure in high pressure loop: 1000 psi
Water Flow : 200 sccm
Nitrogen Pressure: 1000psi
Pressure in low pressure loop: 30 psi
Pump Stroke: 18%

Figure 63. Potentiodynamic Scan of Zr at 8000 ppb dissolve O_2 and 350°F.

102

Figure 64. Potentiodynamic Scan of Zr at 8000 ppb dissolve O_2 and 550°F.

Conditions:

Dissolve O_2 of water: 8000 ppb
Conductivity of water: 0.76
Set up temperature: 550°F
Water temperature of water: 550°F
Furnace Temperature: 455°F
Pressure in high pressure loop: 1000 psi
Water Flow : 200 sccm
Nitrogen Pressure: 1000psi
Pressure in low pressure loop: 30 psi
Pump Stroke: 18%

103

APPENDIX C

Superimposed Voltammograms of SS-304 vs the other metals for the determination of E_{corr}.

Corrosion Potentials are denoted by E_{corr} from Figure 65 to 99. Electrochemical Potentials are denoted by E_{ss}, E_{MG}, E_{ZN}, E_{ZRA} and E_{ZR} for SS-304, Mg, Zn, Zr-alloy and Zr respectively.
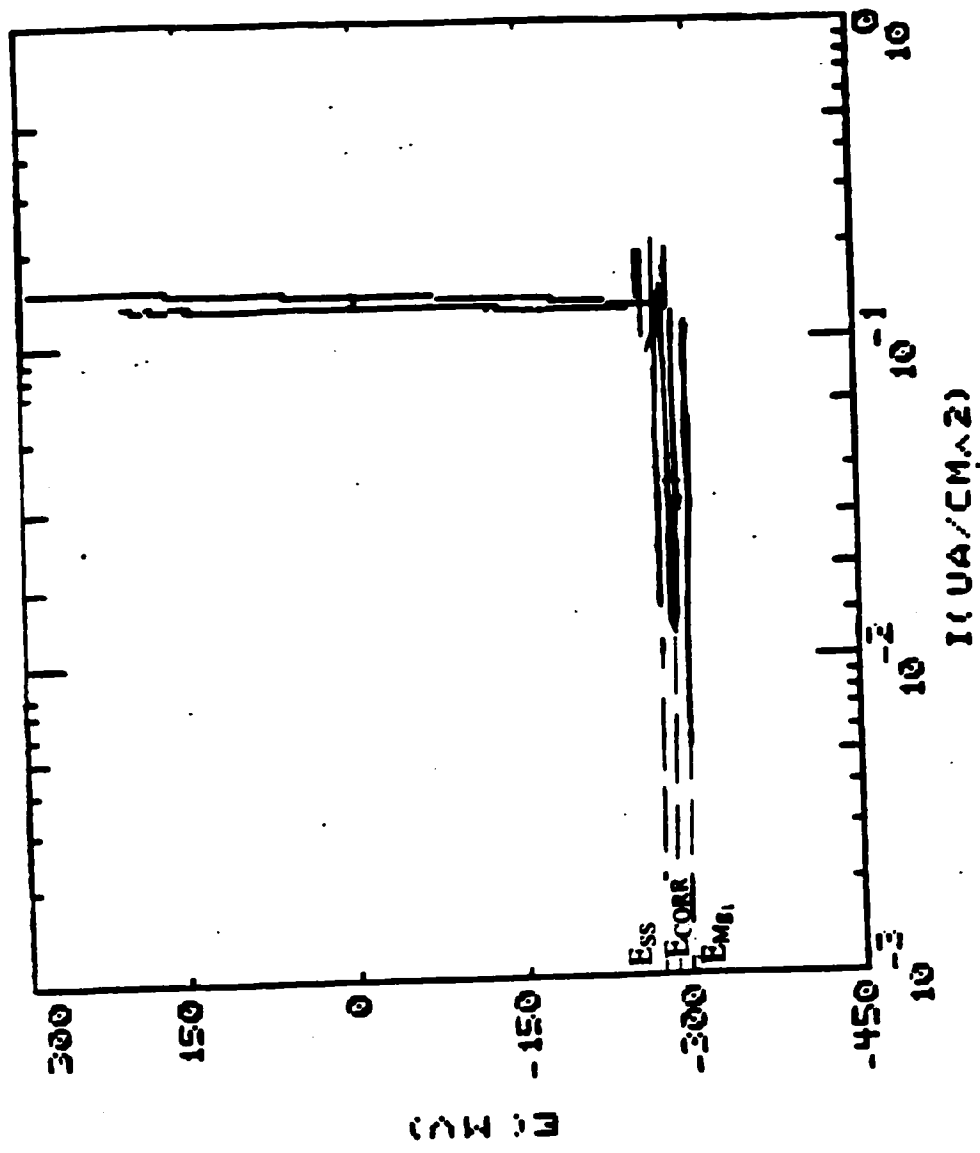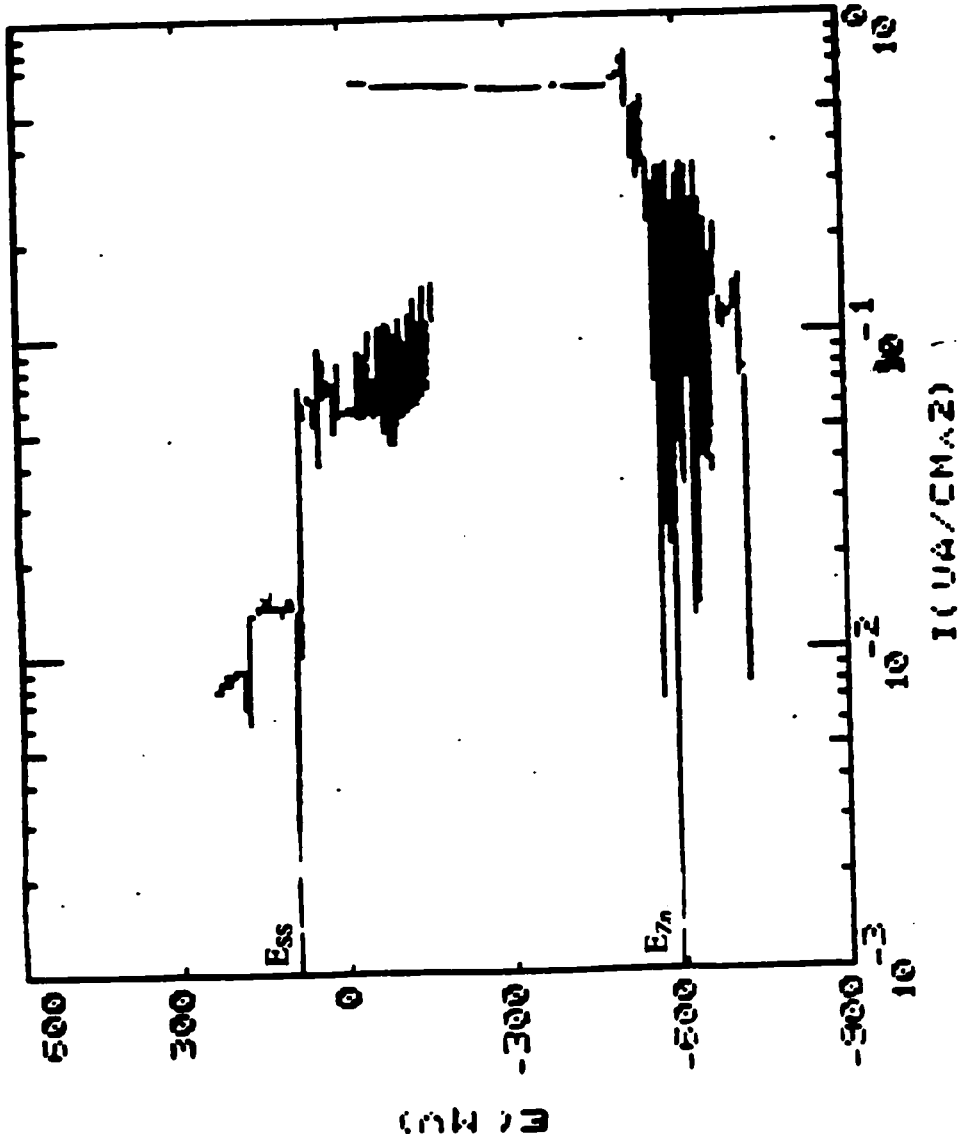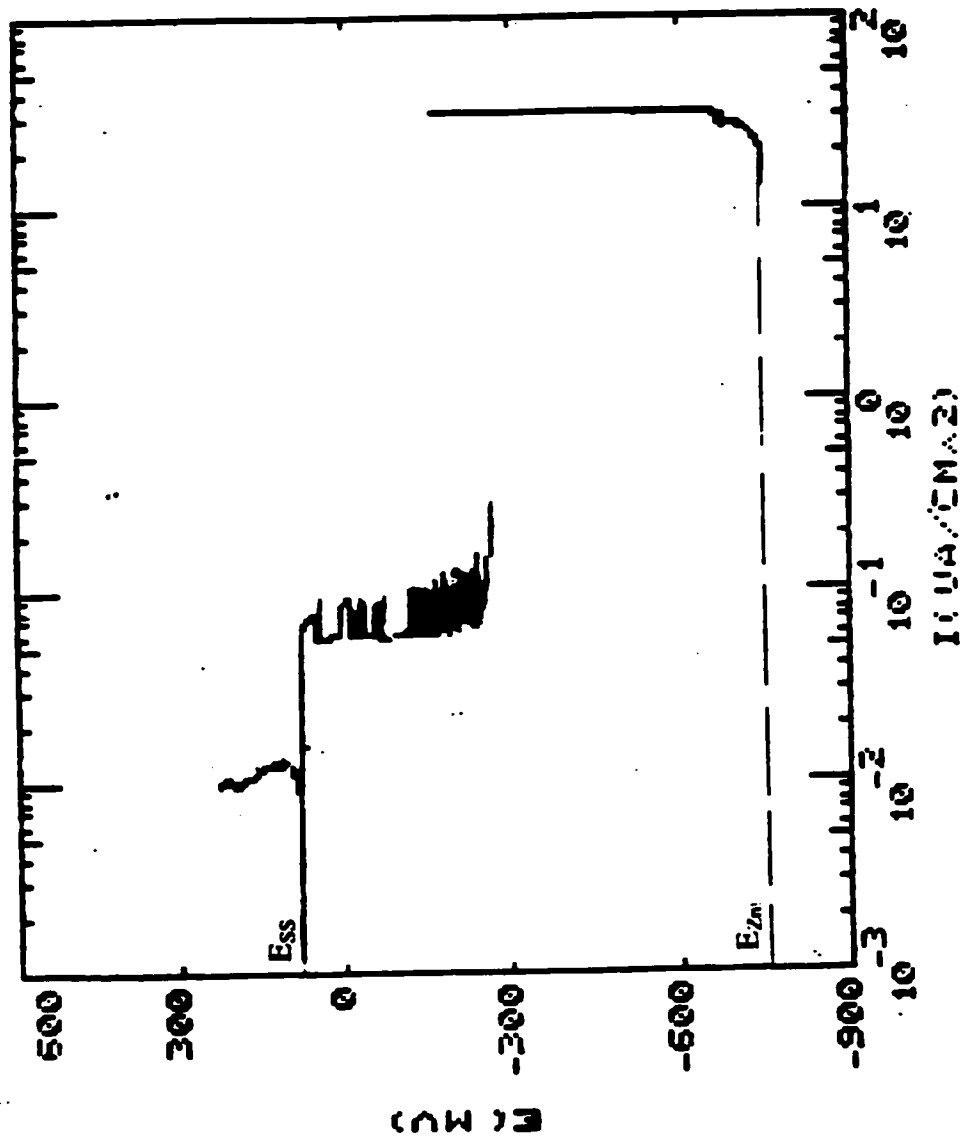
Figure 65. E_{corr} determination from SS-304 and Mg potentiodynamic Scan at 250°F and 50 ppb dissolve oxygen.
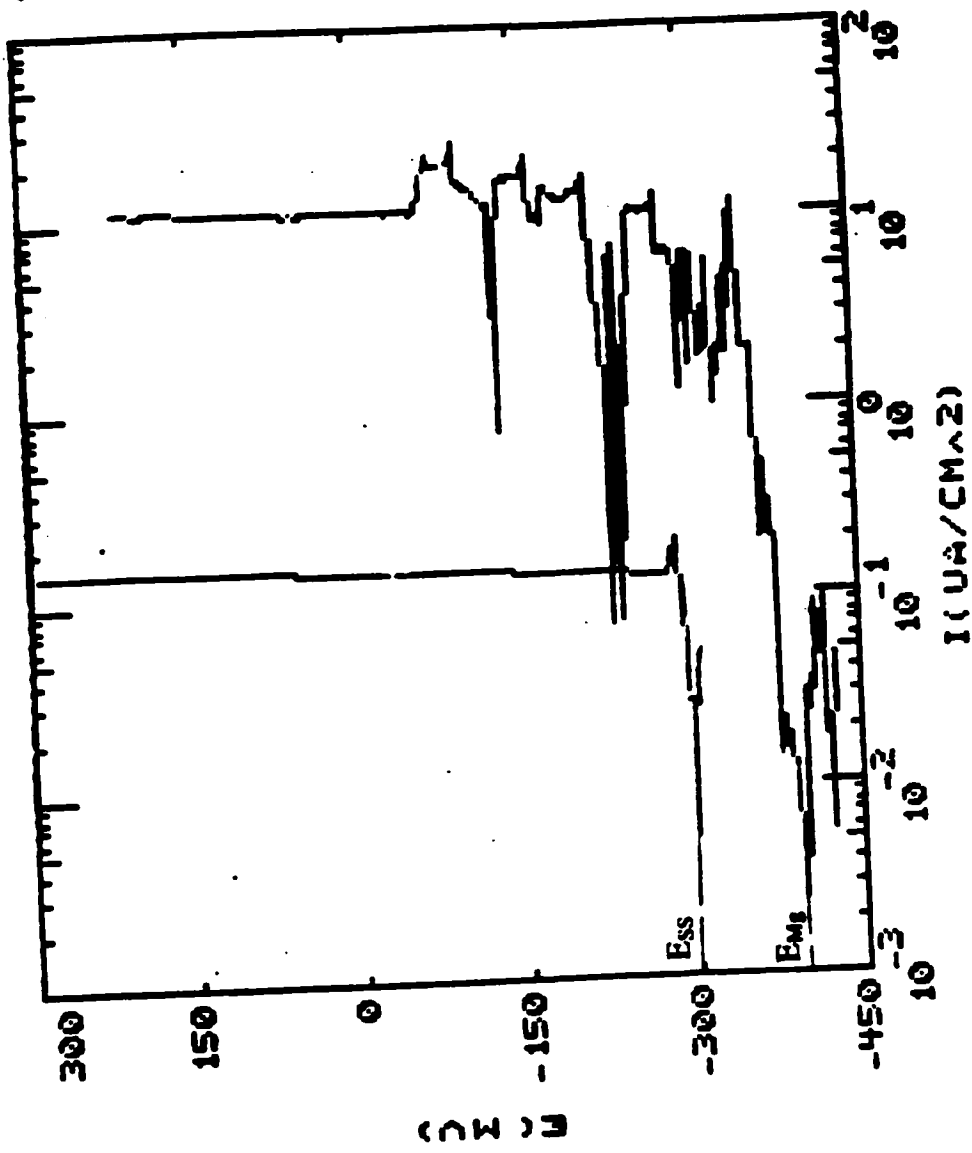
Figure 66. E_{corr} determination from SS-304 and Mg potentiodynamic Scan at 350°F and 50 ppb dissolve oxygen.
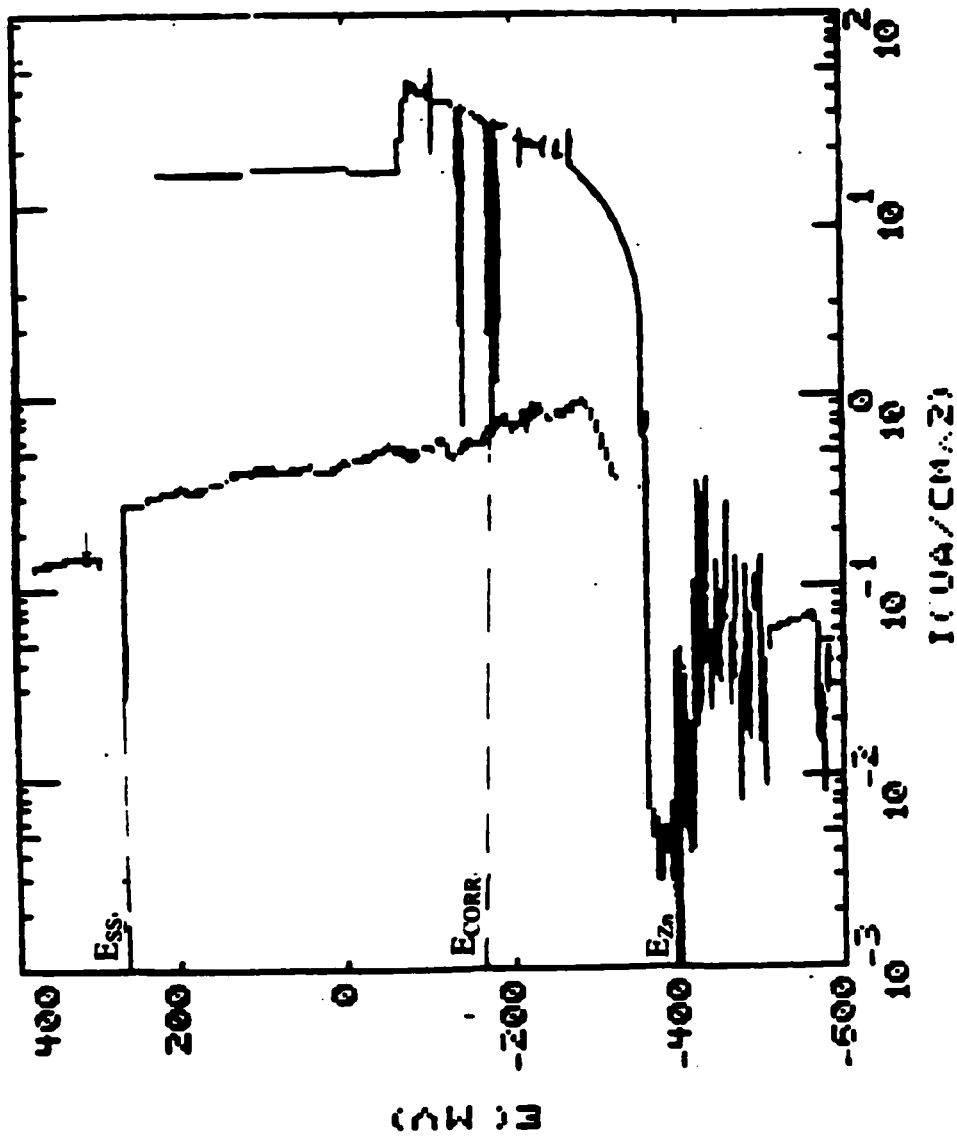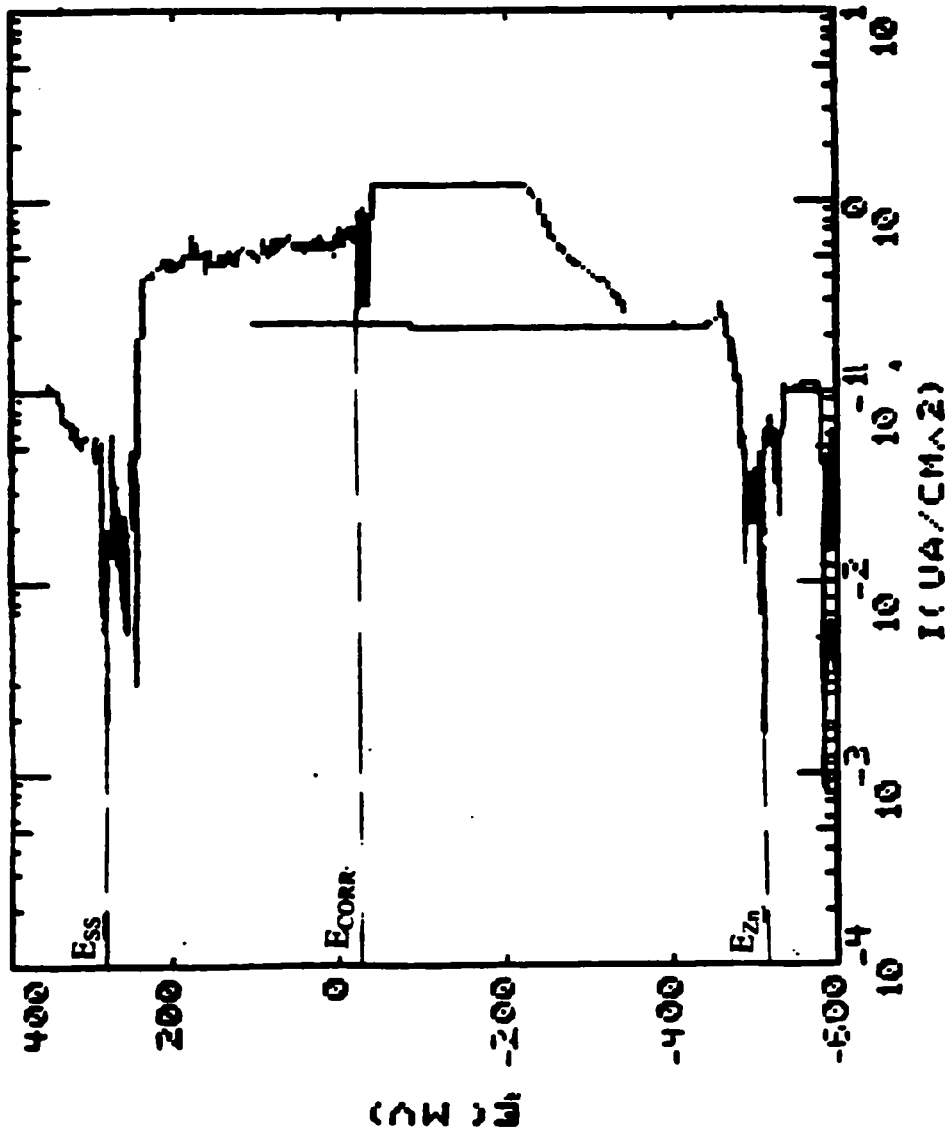
106
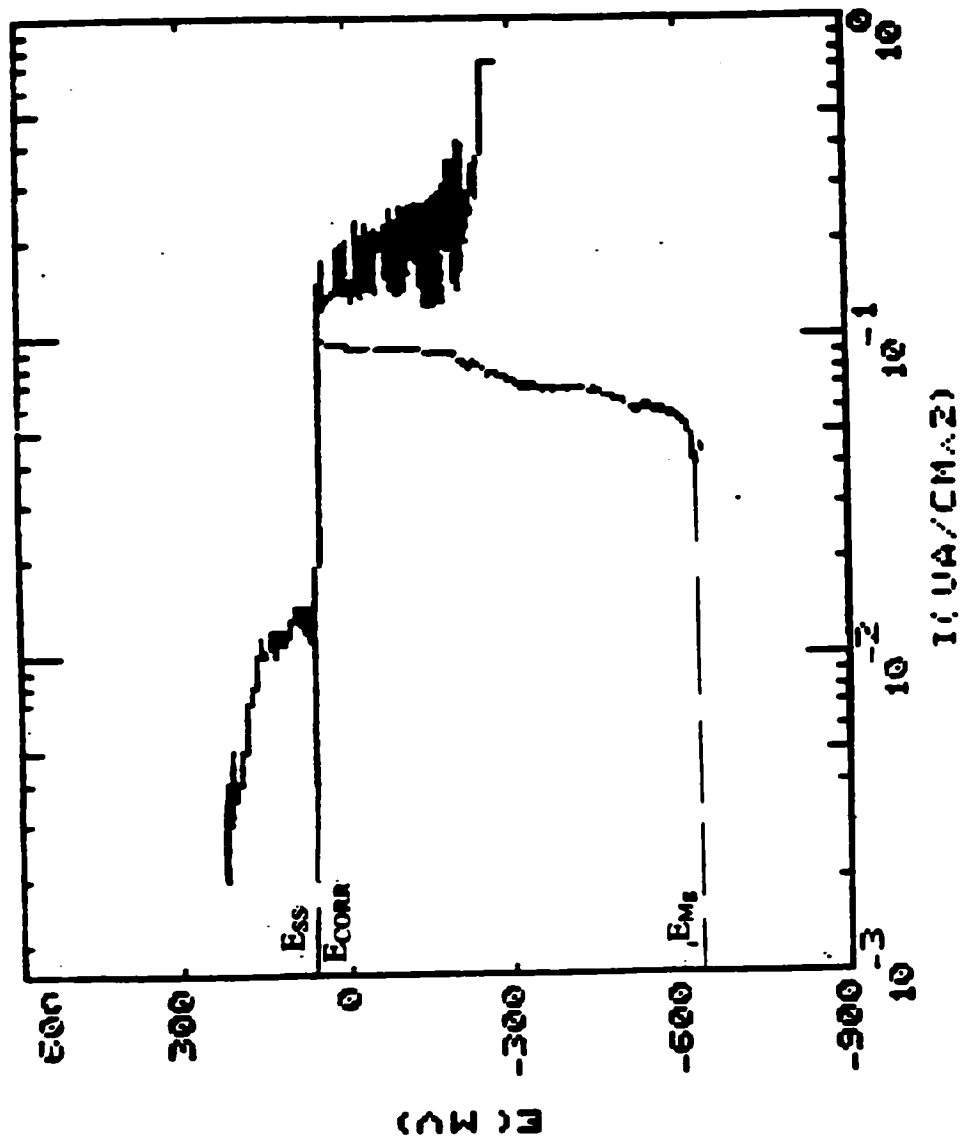
Figure 67. E_{corr} determination from SS-304 and Mg potentiodynamic Scan at 550°F and 50 ppb dissolve oxygen.
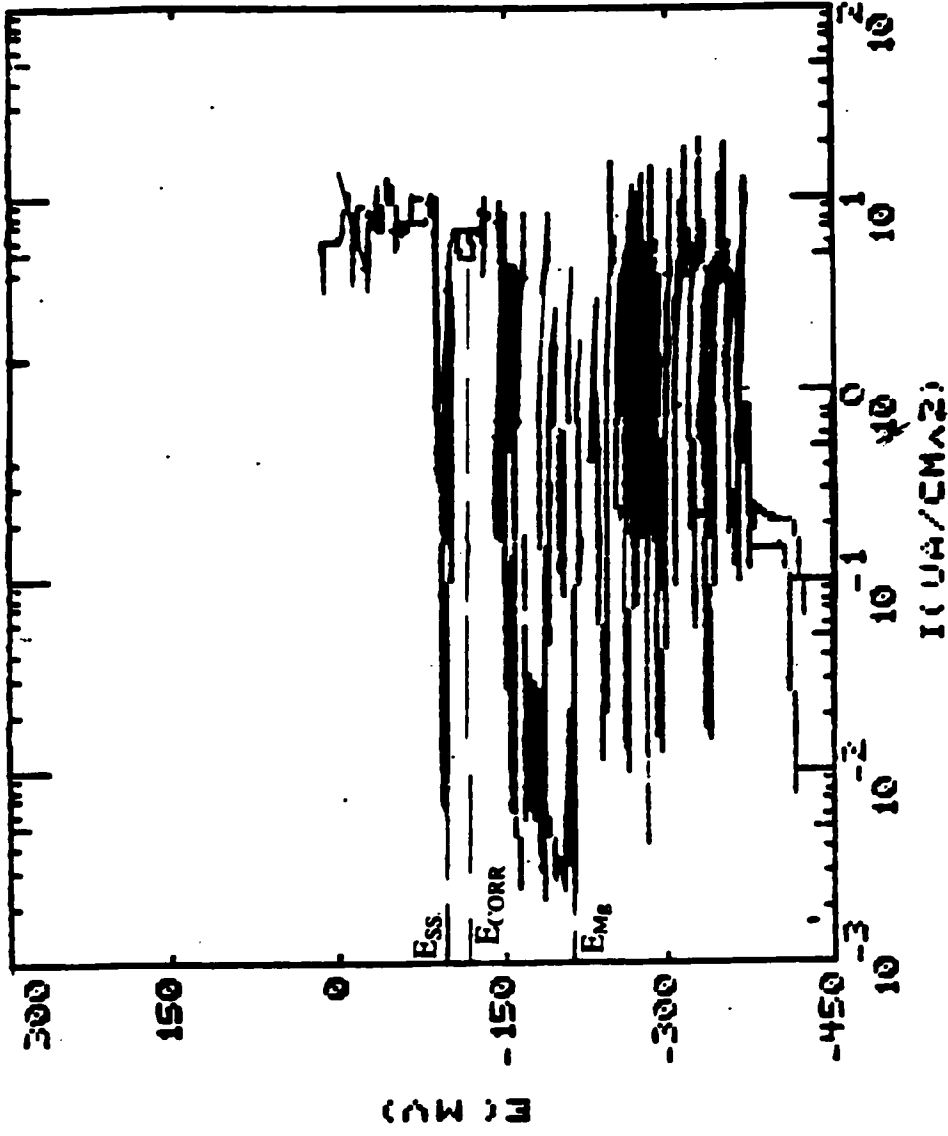
Figure 68. E$_{corr}$ determination from SS-304 and Mg potentiodynamic Scan at 250°F and 200 ppb dissolve oxygen.
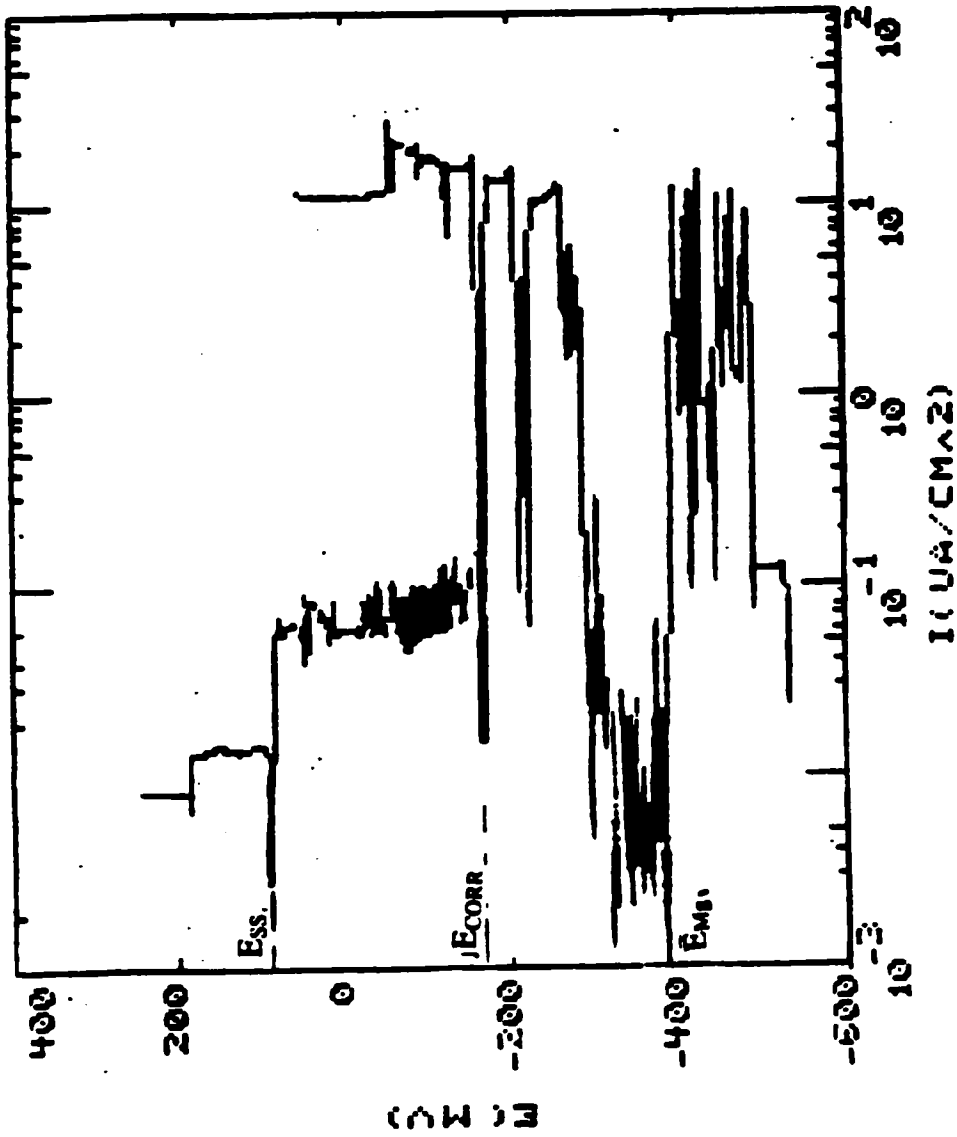
Figure 69. E_{corr} determination from SS-304 and Mg potentiodynamic Scan at 350°F and 200 ppb dissolve oxygen.
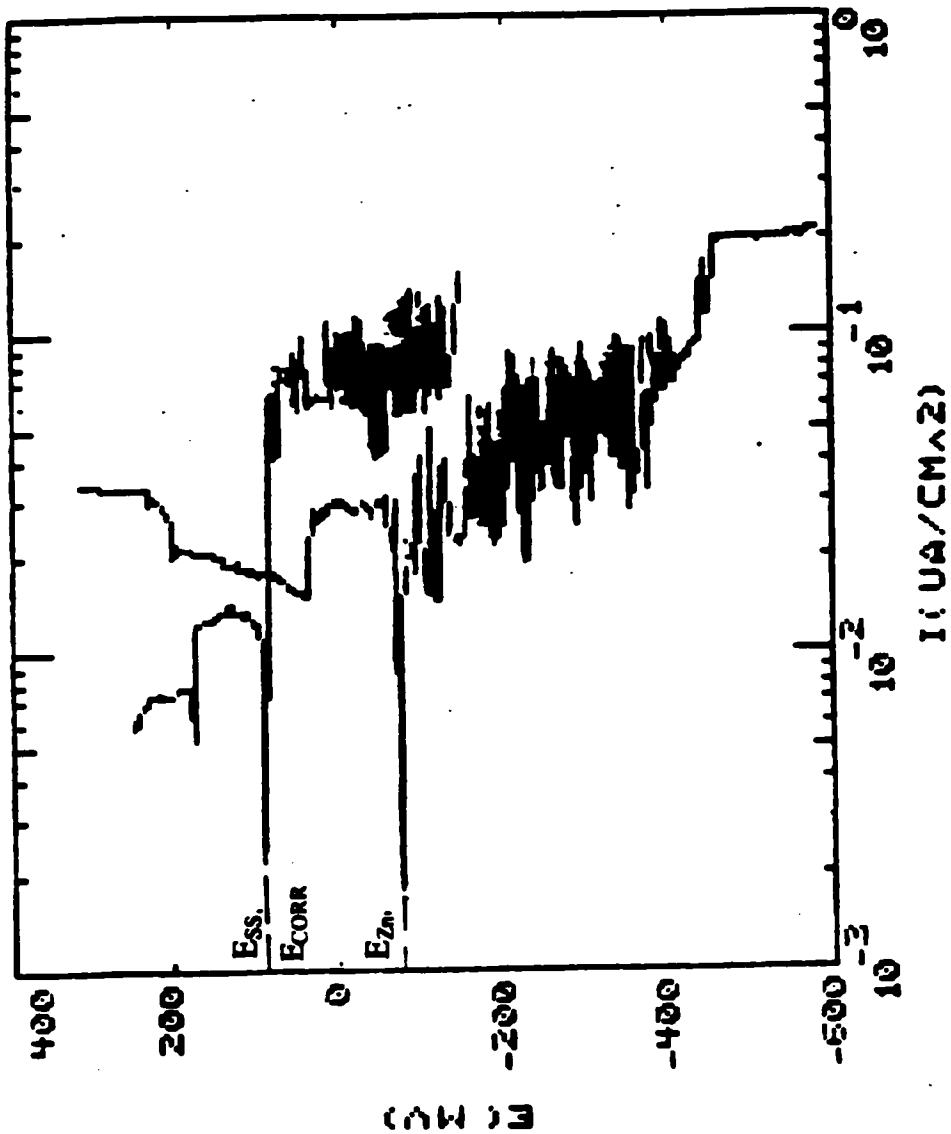
109
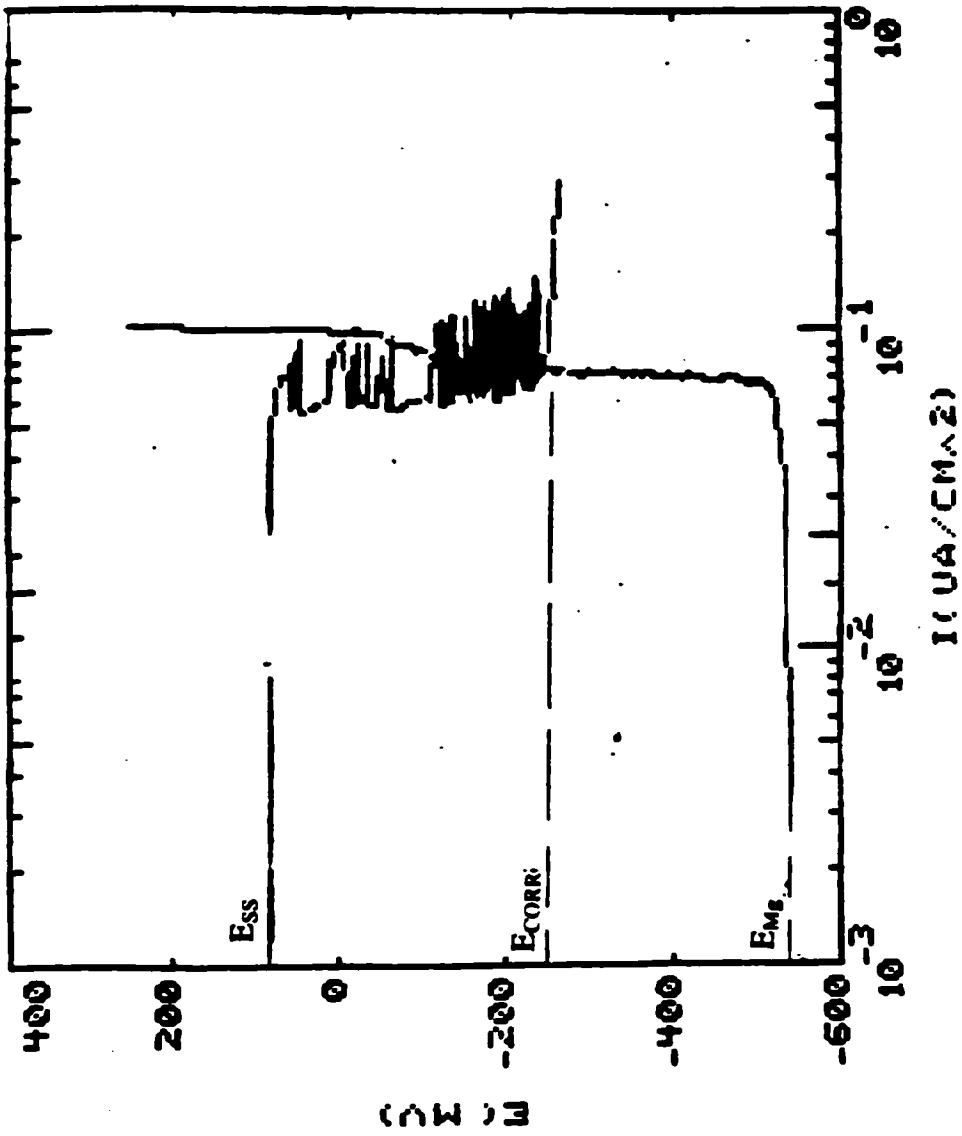
Figure 70. E$_{corr}$ determination from SS-304 and Mg potentiodynamic Scan at 550°F and 200 ppb dissolve oxygen.
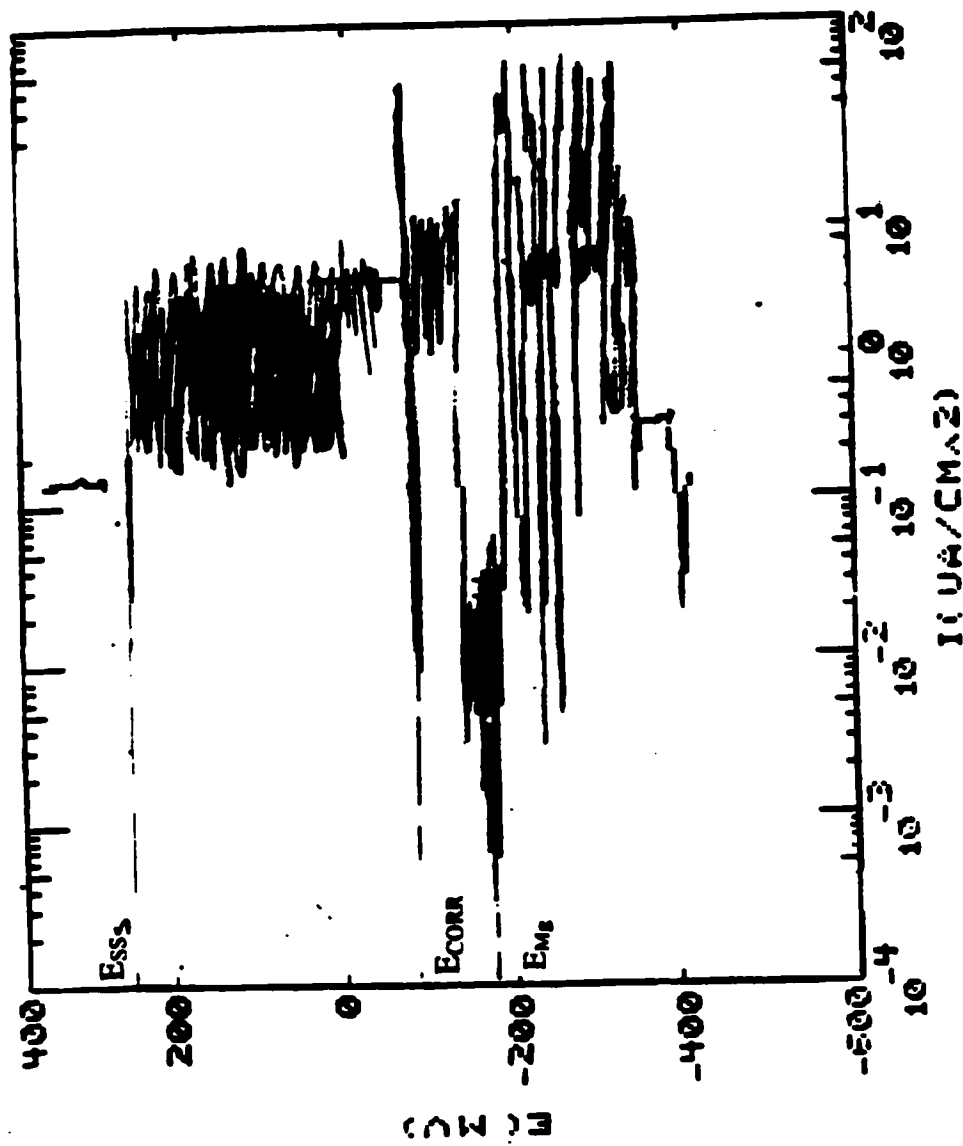
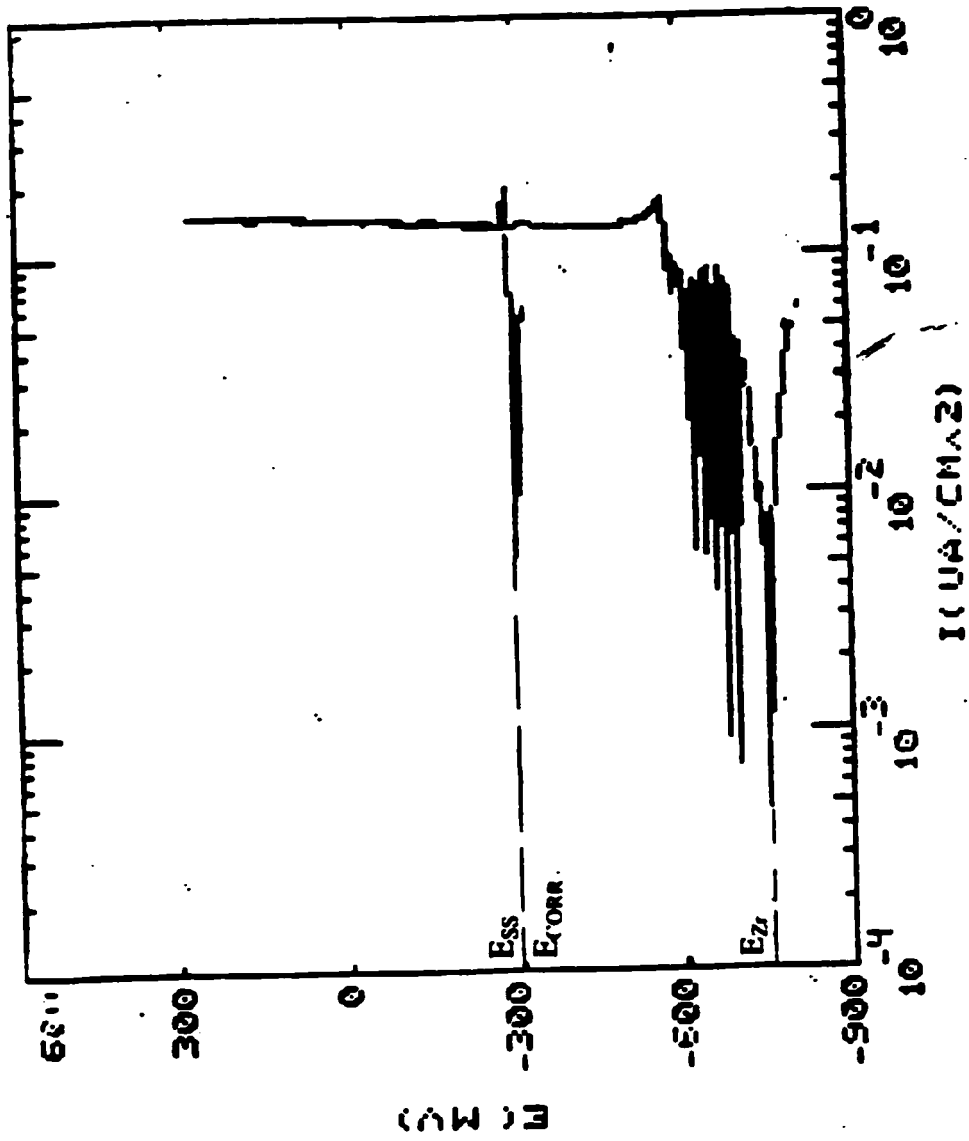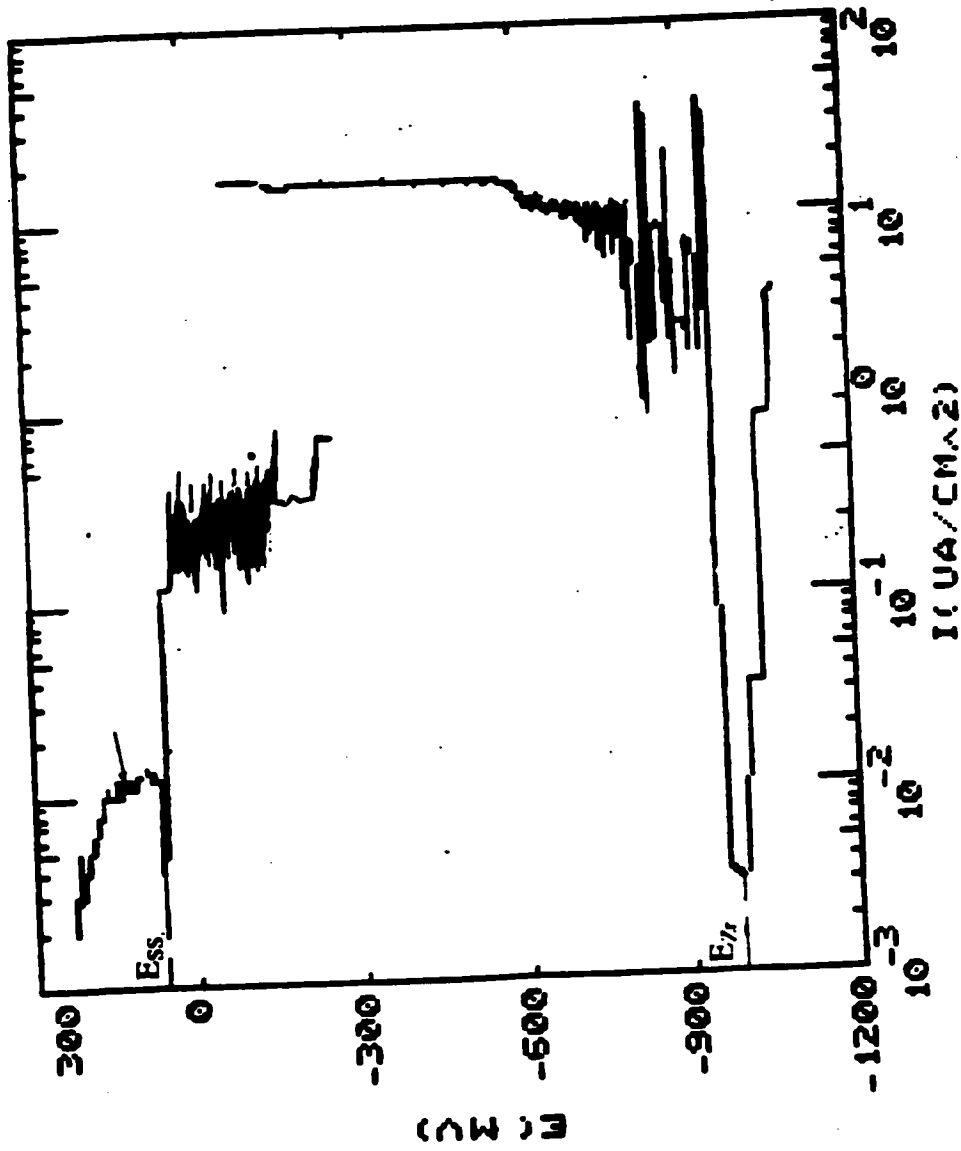Figure 71. E_{corr} determination from SS-304 and Mg potentiodynamic Scan at 250°F and 8000 ppb dissolve oxygen.

111
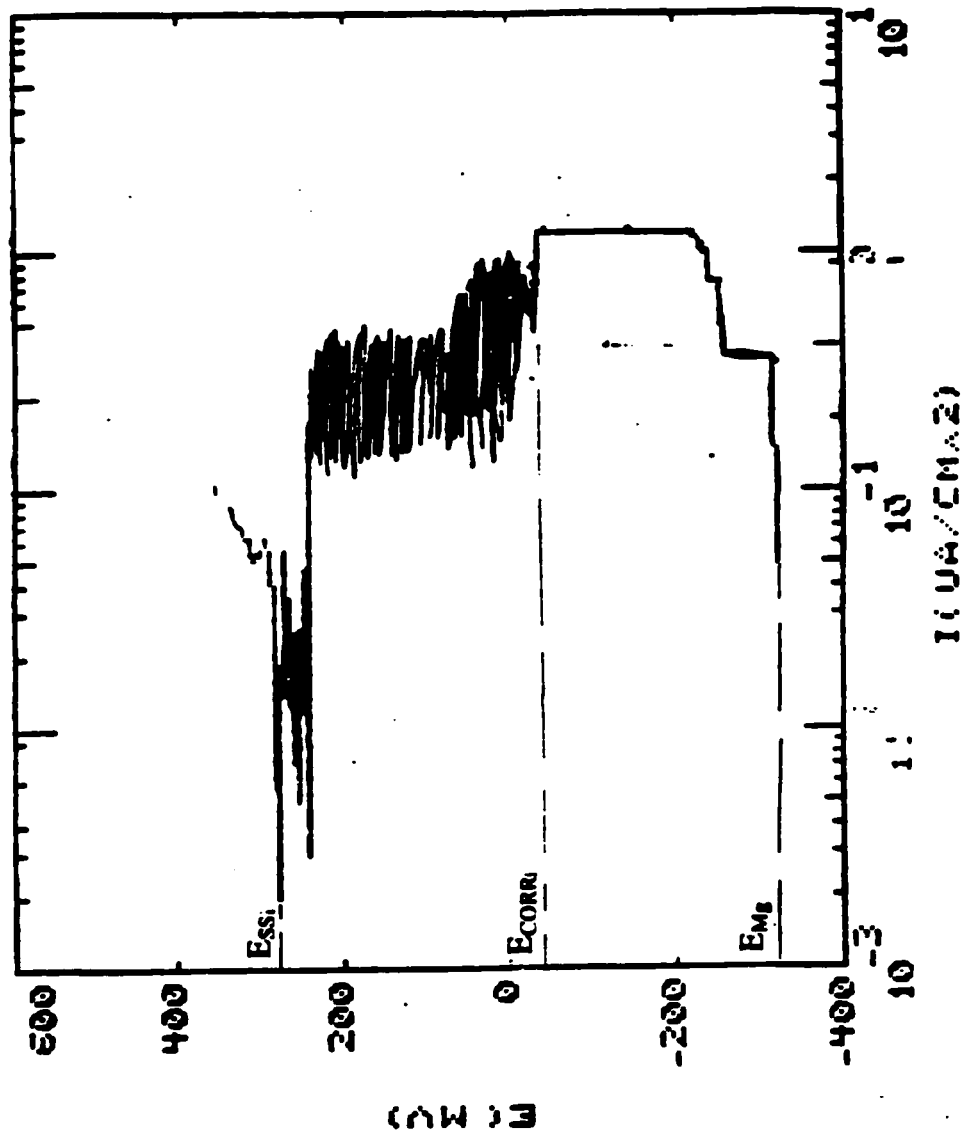
Figure 72. E_{corr} determination from SS-304 and Mg potentiodynamic Scan at 350°F and 8000 ppb dissolve oxygen.

112
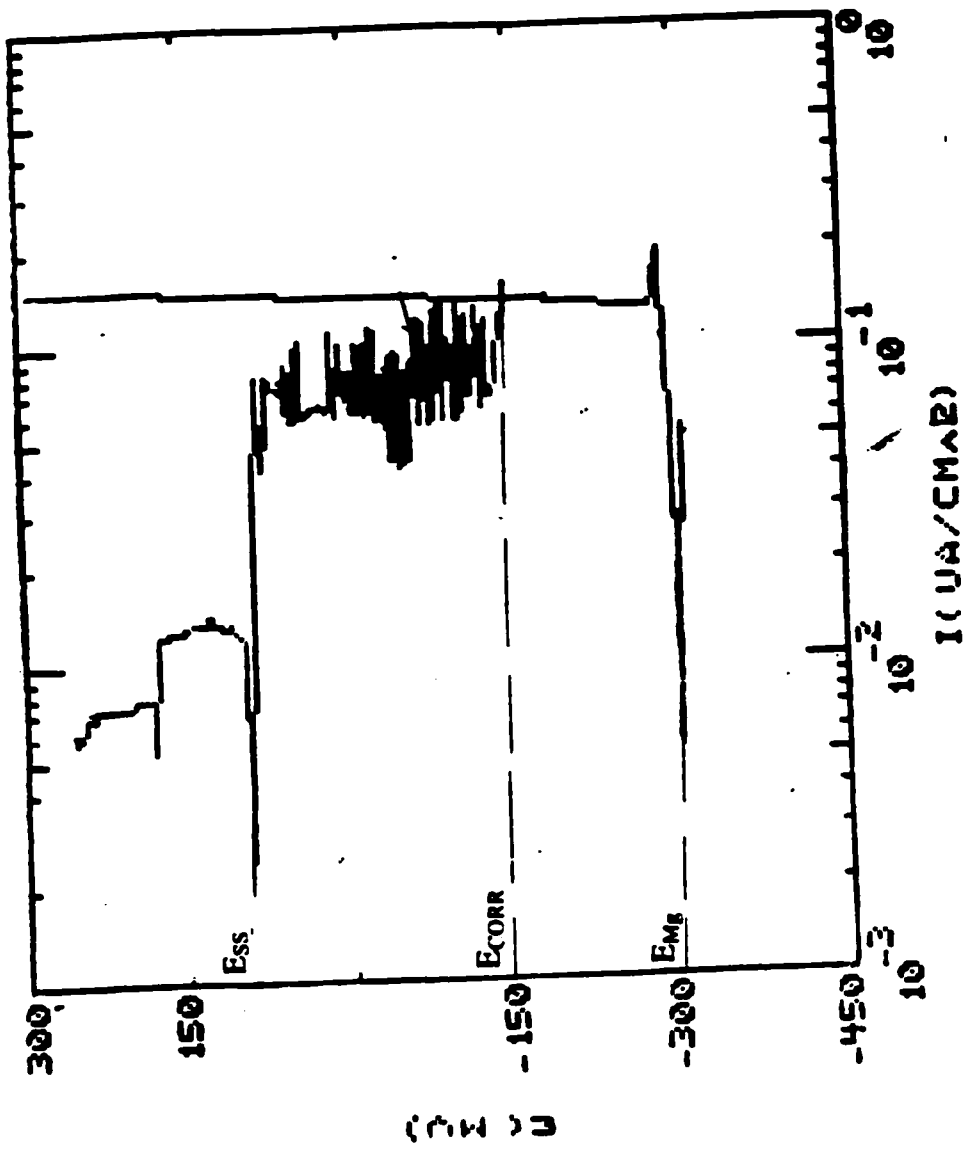
Figure 73. E_{corr} determination from SS-304 and Mg potentiodynamic Scan at 550°F and 8000 ppb dissolve oxygen.

113
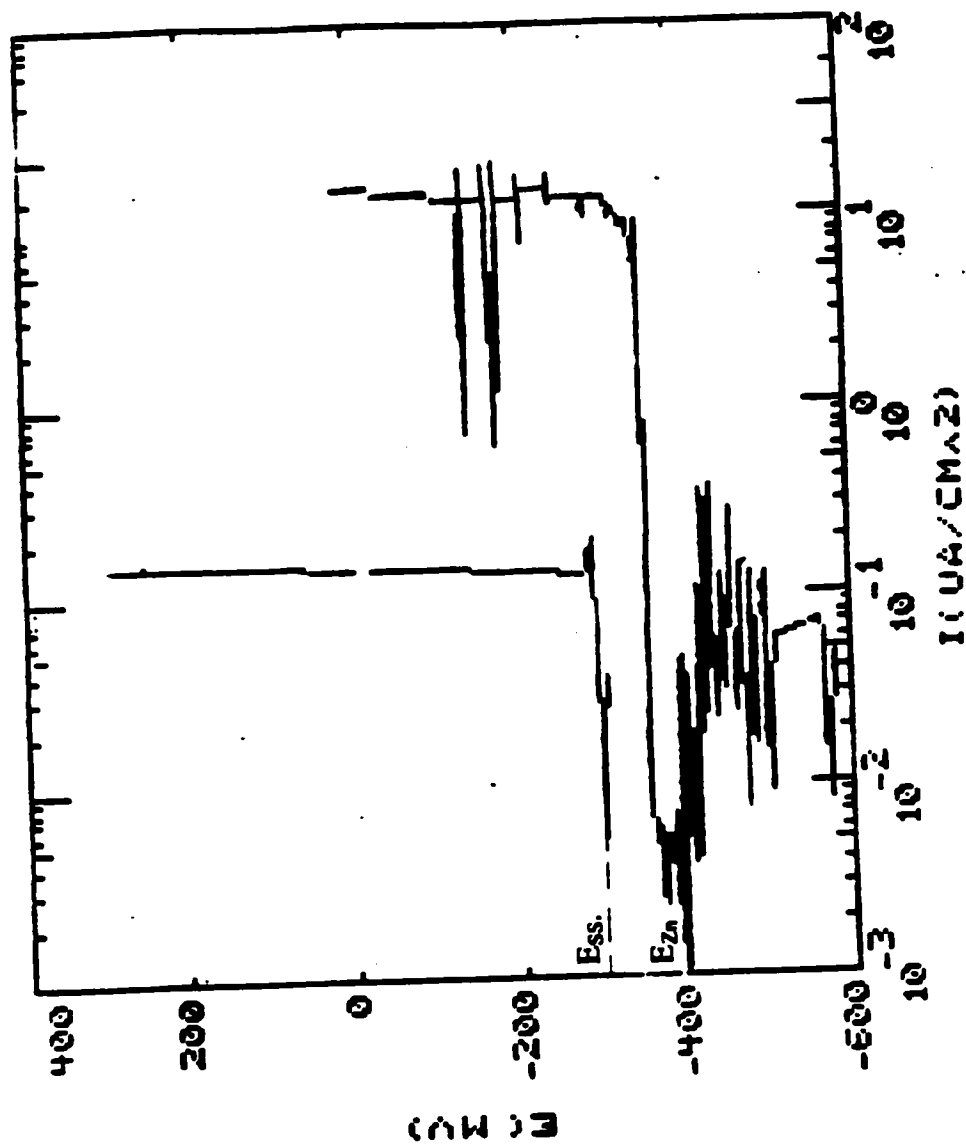
Figure 74. E_corr determination from SS-304 and Zn potentiodynamic Scan at 250°F and 50 ppb dissolve oxygen.

114

Figure 75. E_{corr} determination from SS-304 and Zn potentiodynamic Scan at 350°F and 50 ppb dissolve oxygen.

115
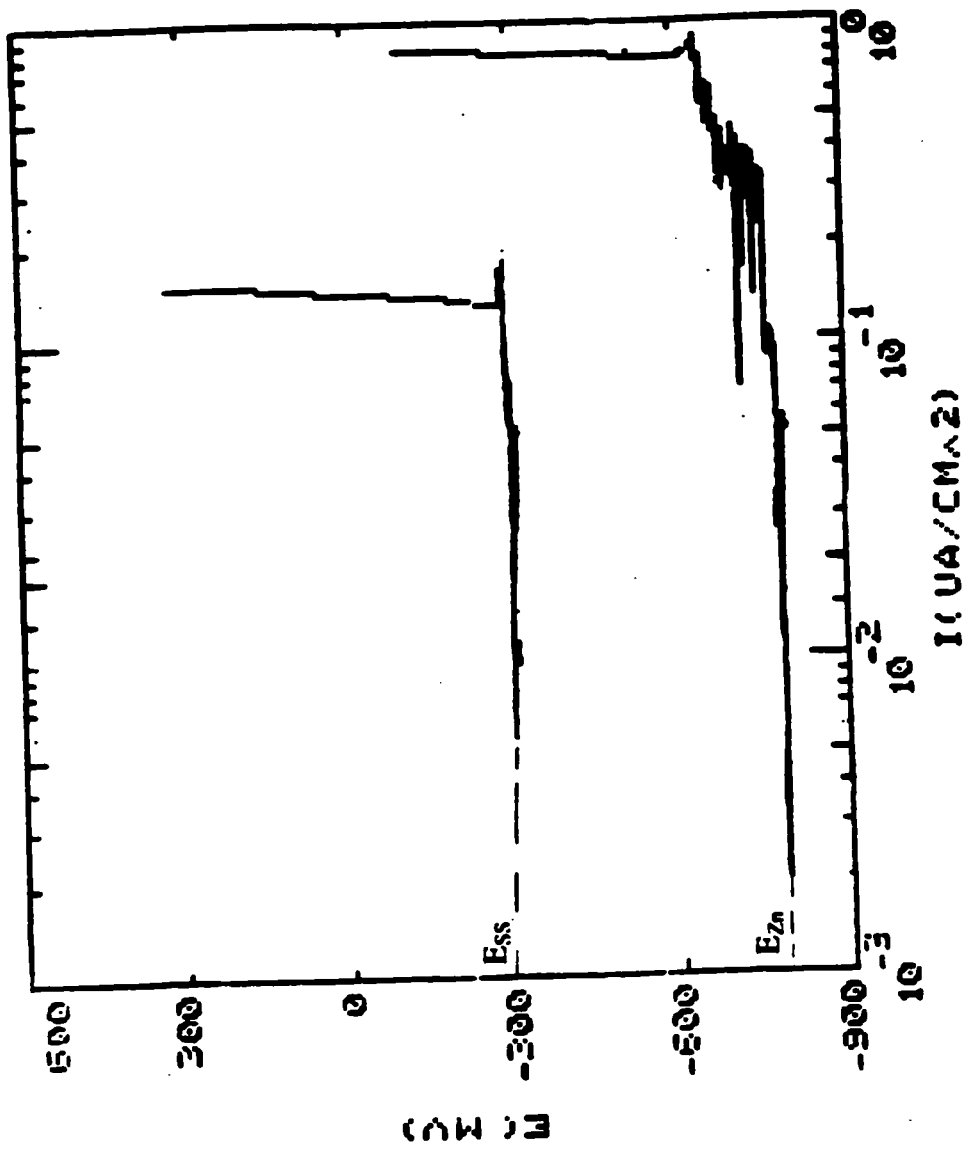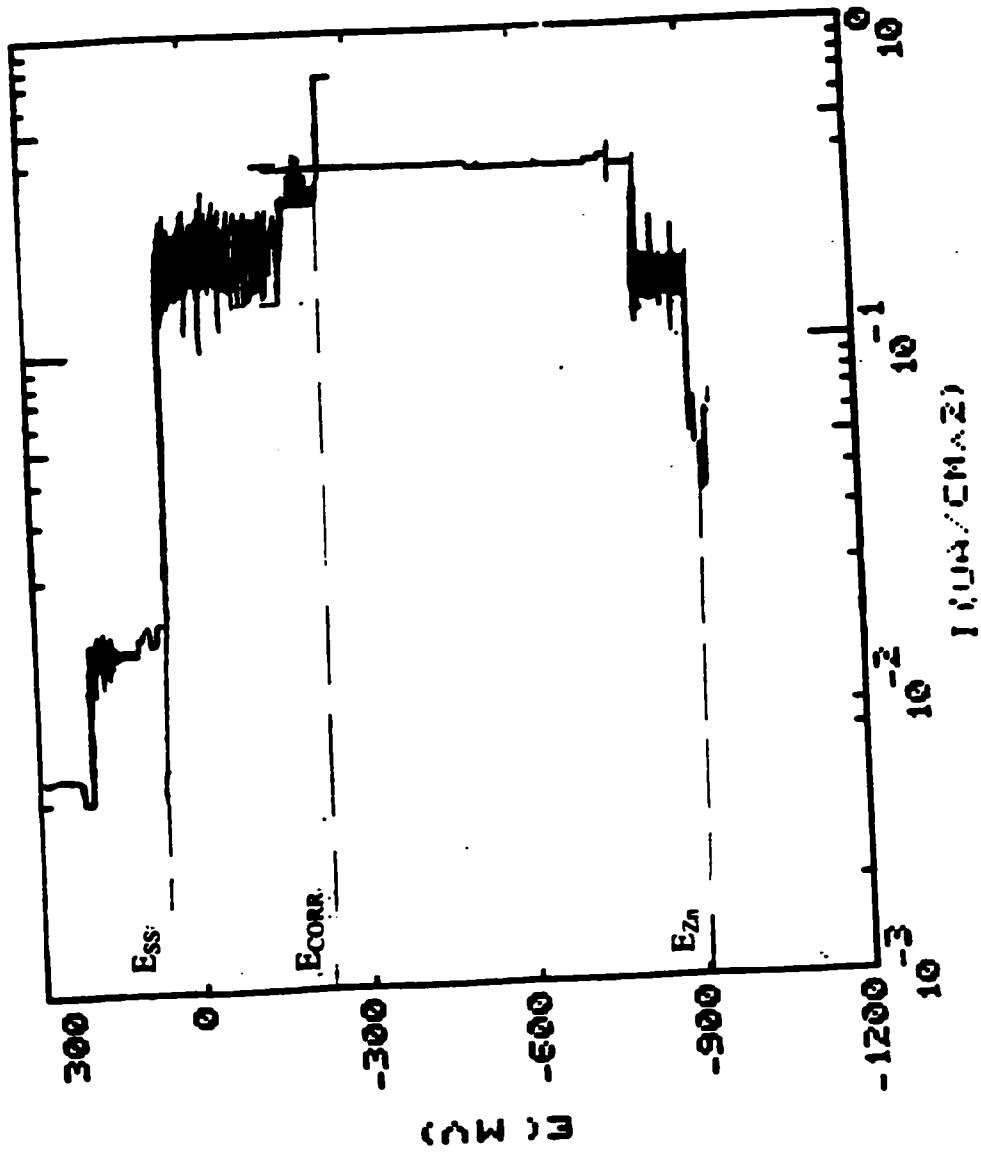
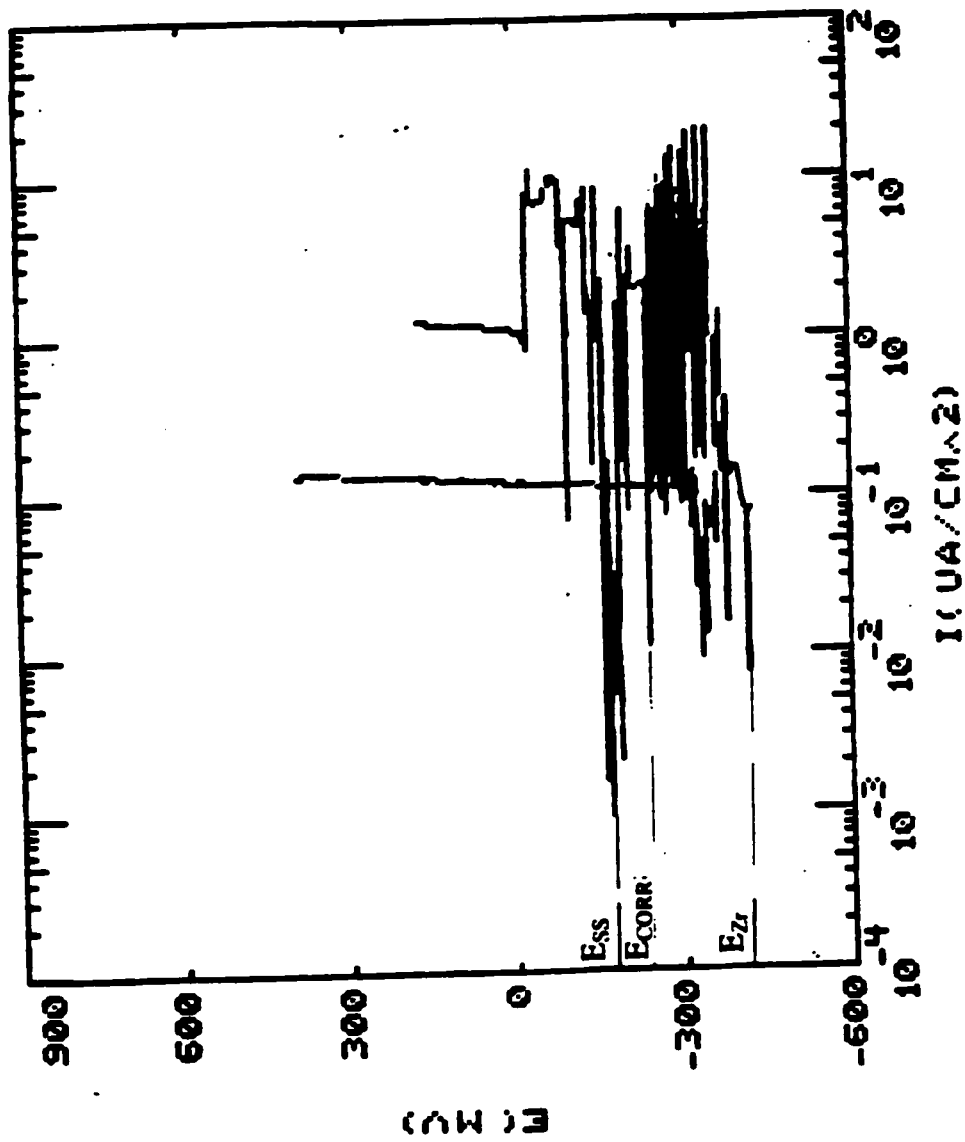Figure 76. E_{corr} determination from SS-304 and Zn potentiodynamic scan at 550°F and 50 ppb dissolve oxygen.
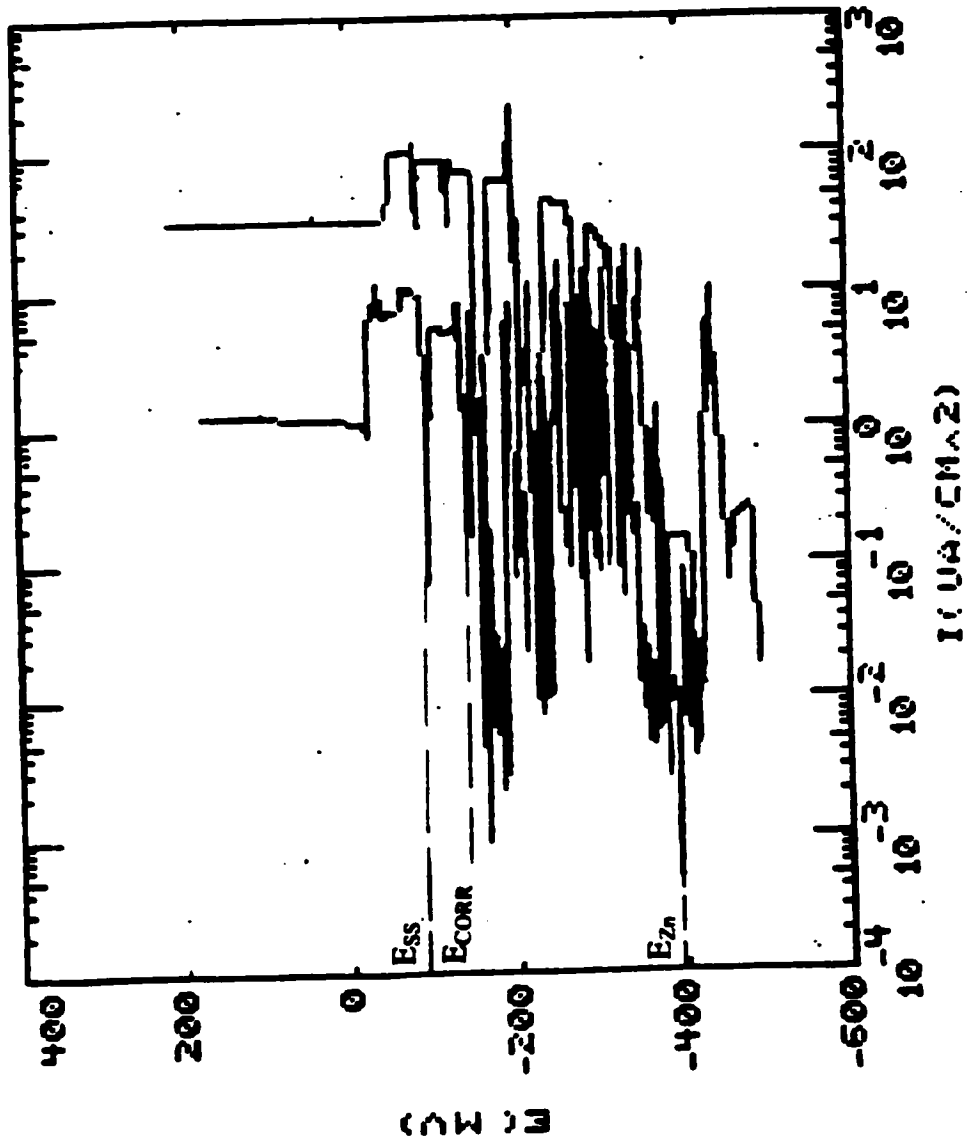
Figure 77. E_{corr} determination from SS-304 and Zn potentiodynamic scan at 250°F and 200 ppb dissolve oxygen.
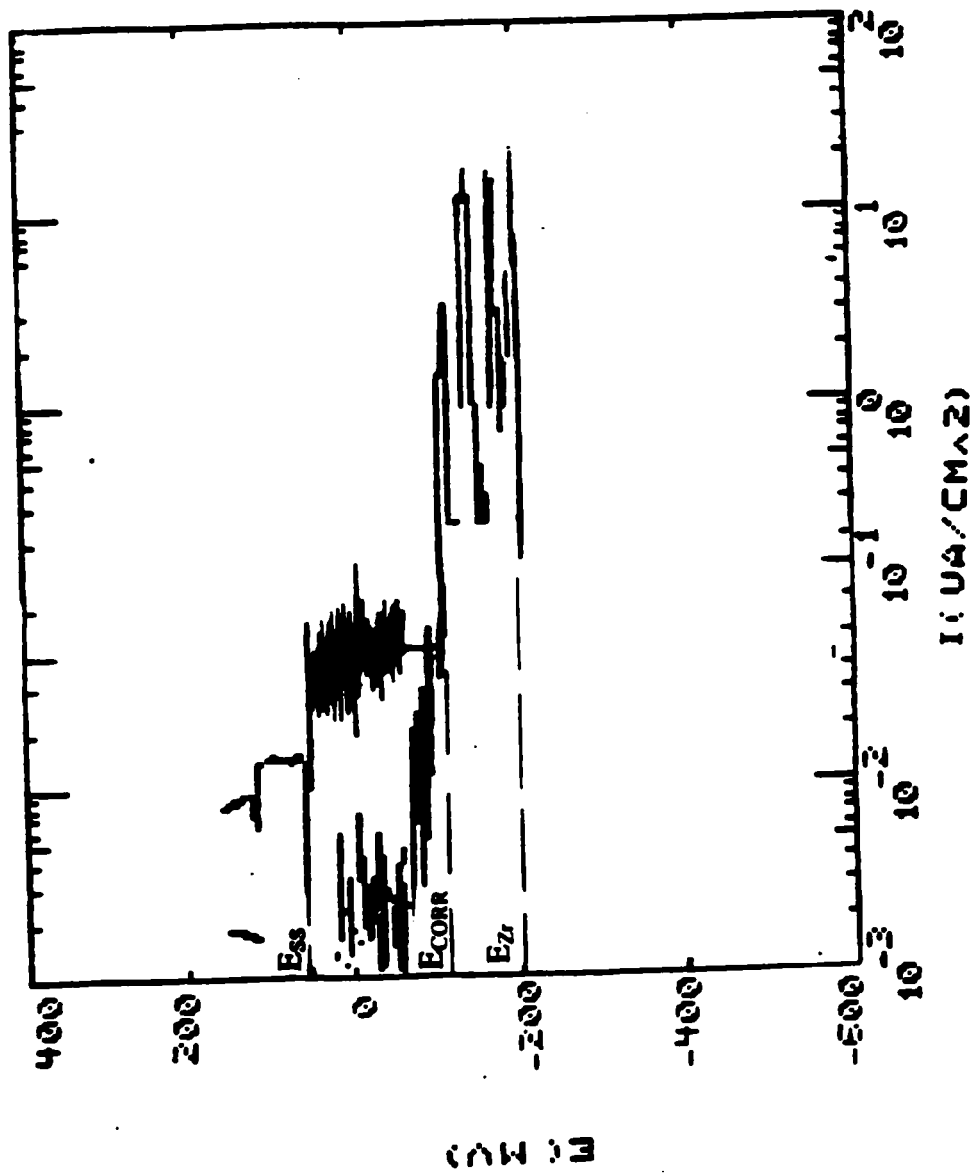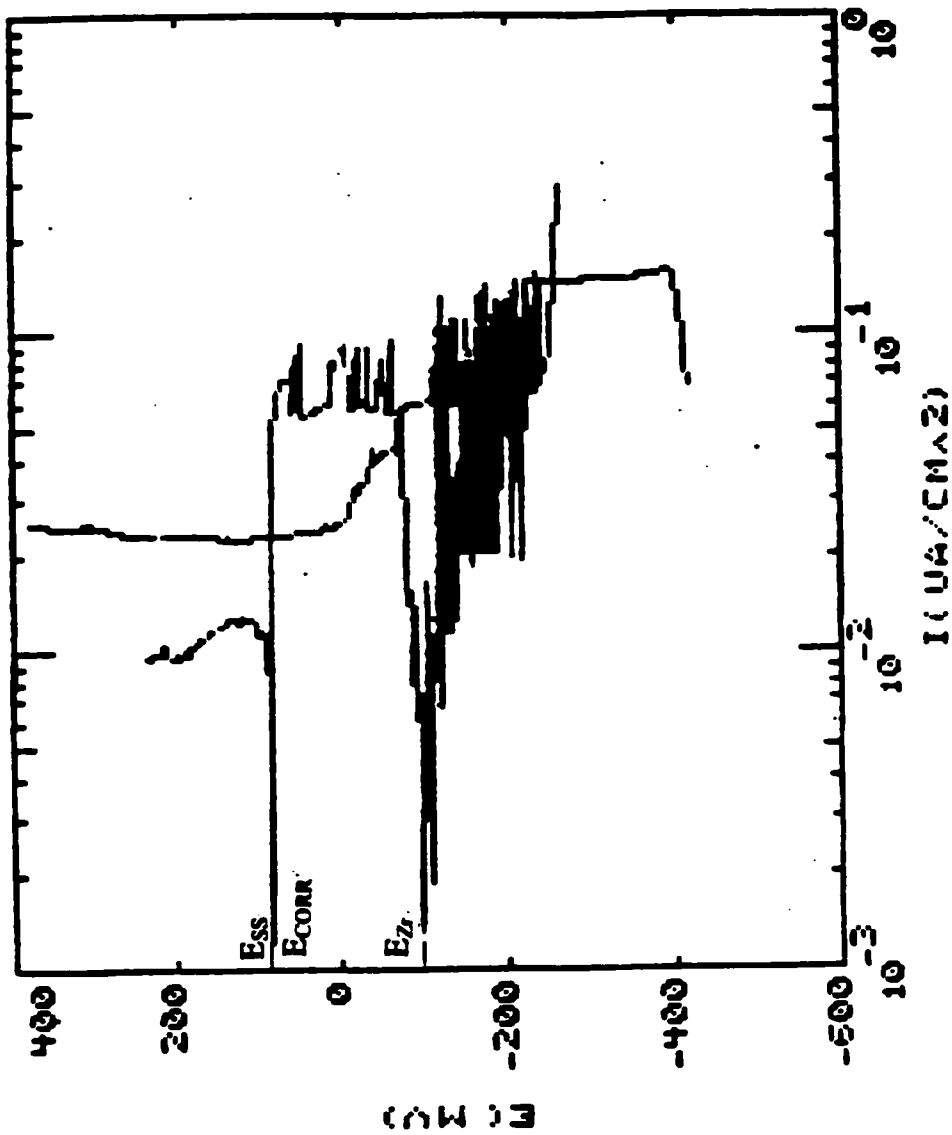
117

Figure 78. E_{corr} determination from SS-304 and Zn potentiodynamic scan at 350°F and 200 ppb dissolve oxygen.

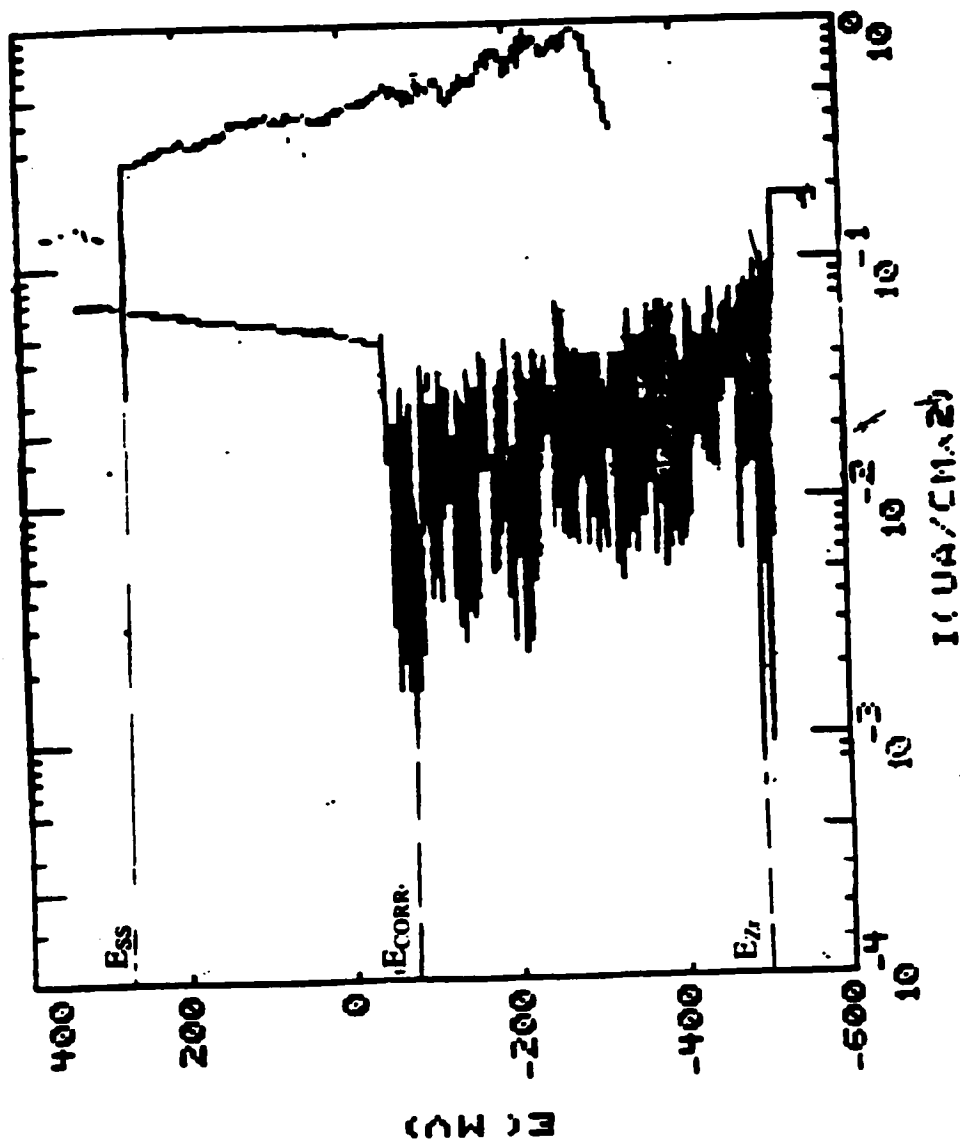Figure 79. E_{corr} determination from SS-304 and Zn potentiodynamic scan at 550°F and 200 ppb dissolve oxygen.

Figure 80. E_{corr} determination from SS-304 and Zn potentiodynamic scan at 250°F and 8000 ppb dissolve oxygen.

120

Figure 81. E_{corr} determination from SS-304 and Zn potentiodynamic scan at 350°F and 8000 ppb dissolve oxygen.

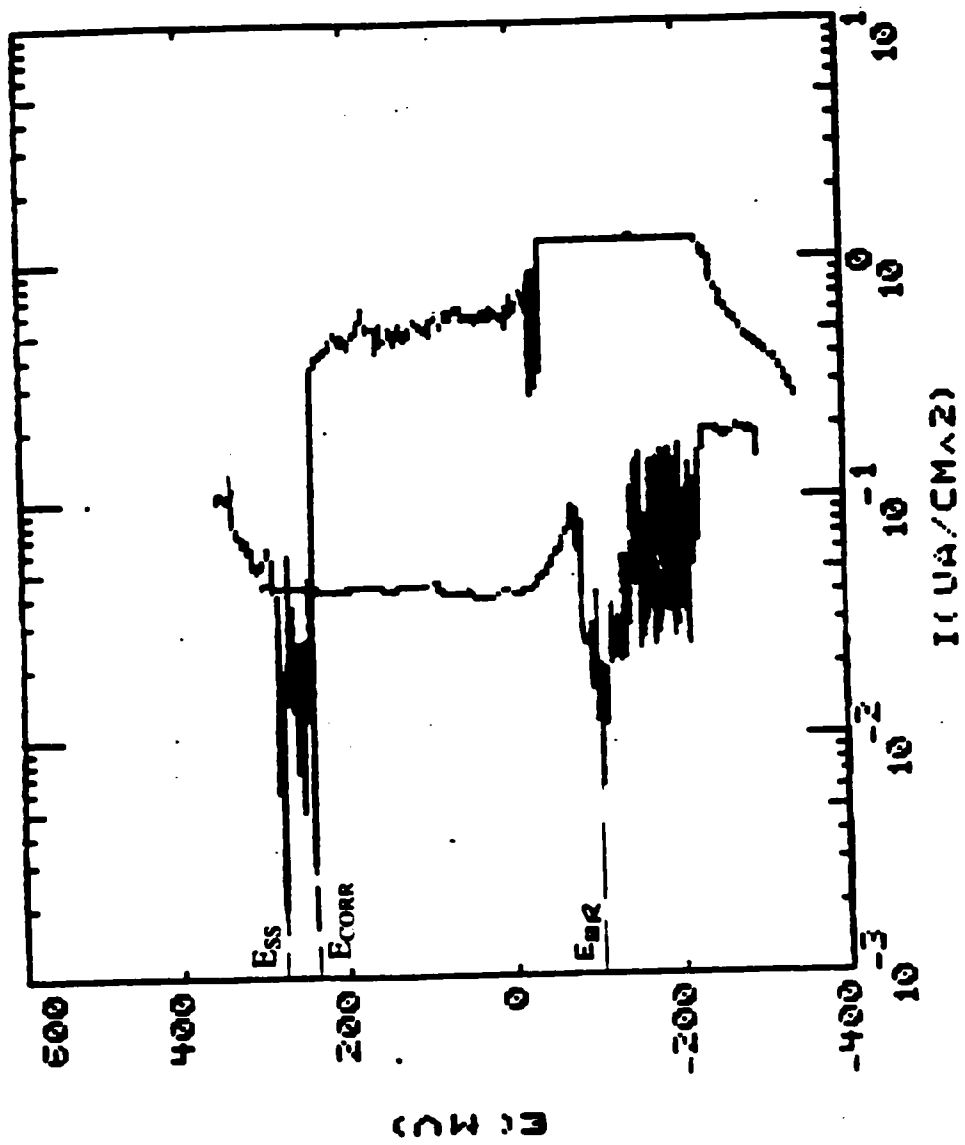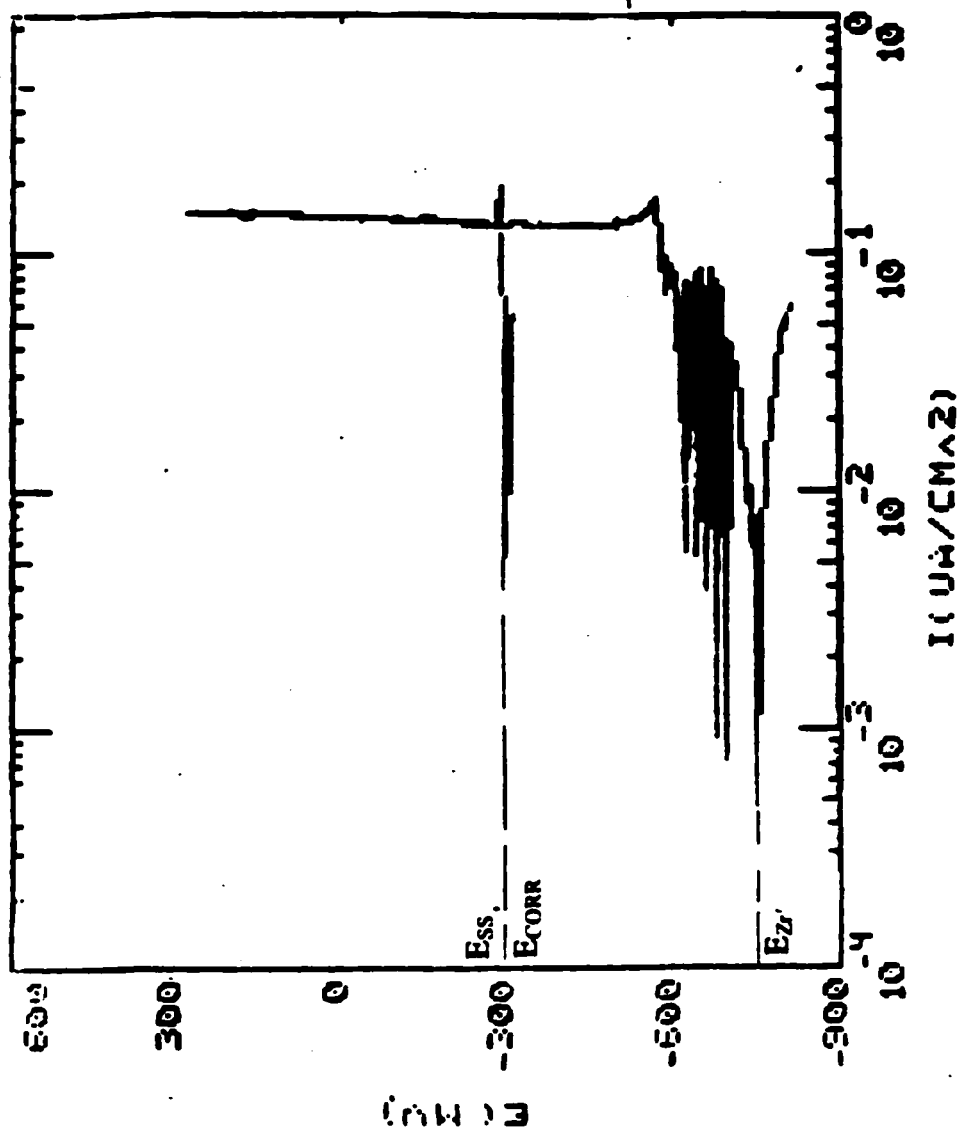Figure 82. E_{corr} determination from SS-304 and Zn potentiodynamic scan at 550°F and 8000 ppb dissolve oxygen.

122

Figure 83. E_{corr} determination from SS-304 and Zr potentiodynamic scan at 350°F and 50 ppb dissolve oxygen.

123

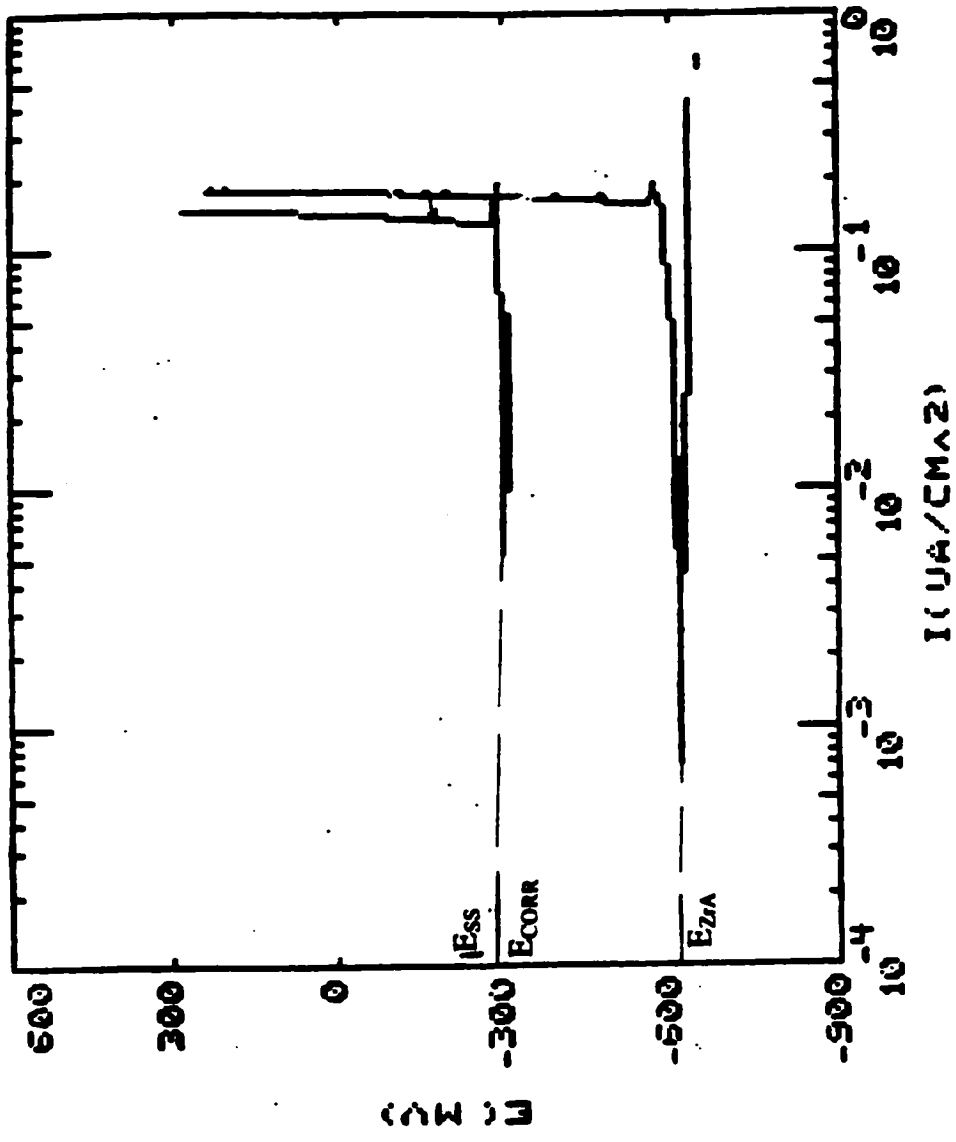Figure 84. E_corr determination from SS-304 and Zr potentiodynamic scan at 550°F and 50 ppb dissolve oxygen.

124

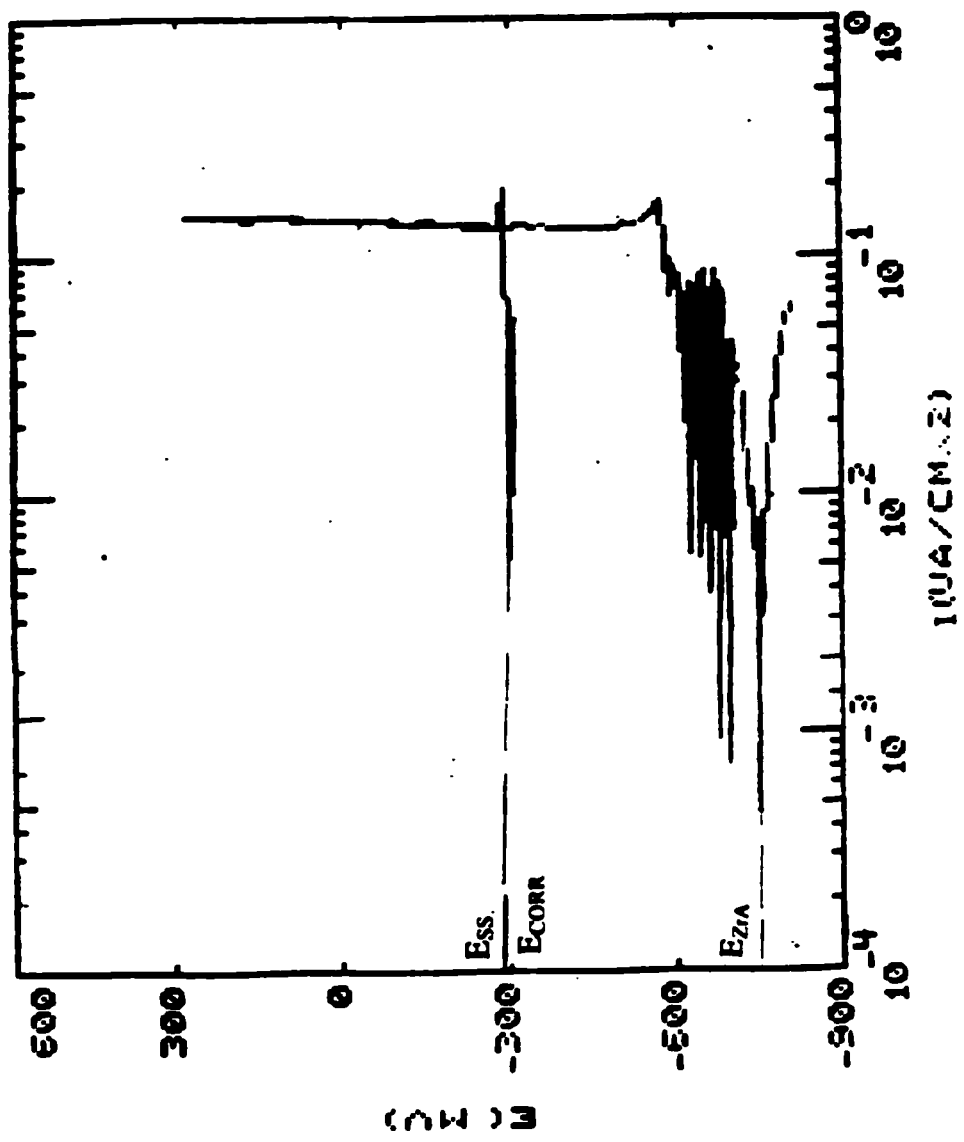Figure 85. E_{corr} determination from SS-304 and Zr potentiodynamic scan at 250°F and 200 ppb dissolve oxygen.

125

Figure 86. E_{corr} determination from SS-304 and Zr potentiodynamic scan at 350°F and 200 ppb dissolve oxygen.

126

Figure 87. E_{corr} determination from SS-304 and Zr potentiodynamic scan at 550°F and 200 ppb dissolve oxygen.

127

Figure 88. E_corr determination from SS-304 and Zr potentiodynamic scan at 250°F and 8000 ppb dissolve oxygen.

128

Figure 89. E_{corr} determination from SS-304 and Zr potentiodynamic scan at 350°F and 8000 ppb dissolve oxygen.

129

Figure 90. E_{corr} determination from SS-304 and Zr potentiodynamic scan at 550°F and 8000 ppb dissolve oxygen.
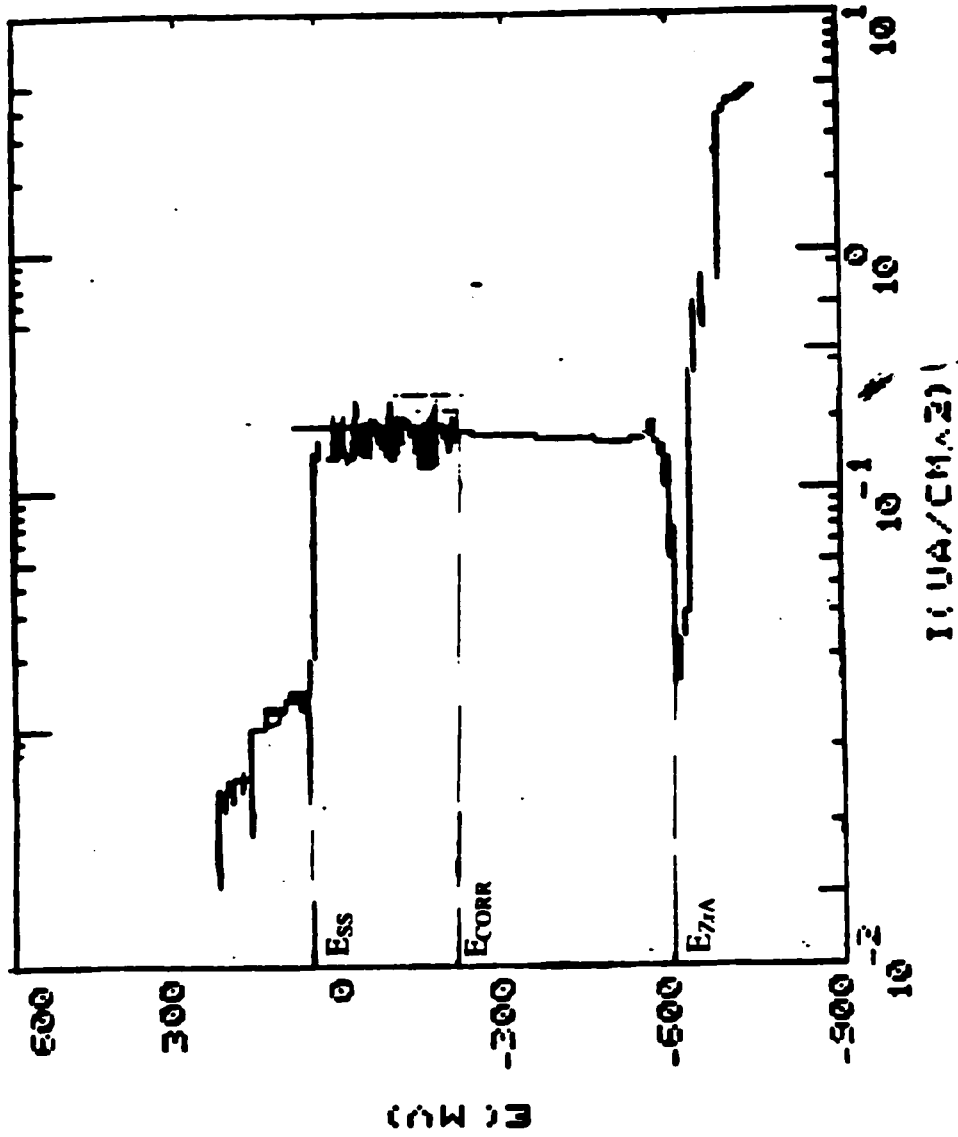
130

Figure 91. E_{corr} determination from SS-304 and Zr-alloy potentiodynamic scan at 250°F and 50 ppb dissolve oxygen.

Figure 92. E_{corr} determination from SS-304 and Zr-alloy potentiodynamic scan at 350°F and 50 ppb dissolve oxygen.
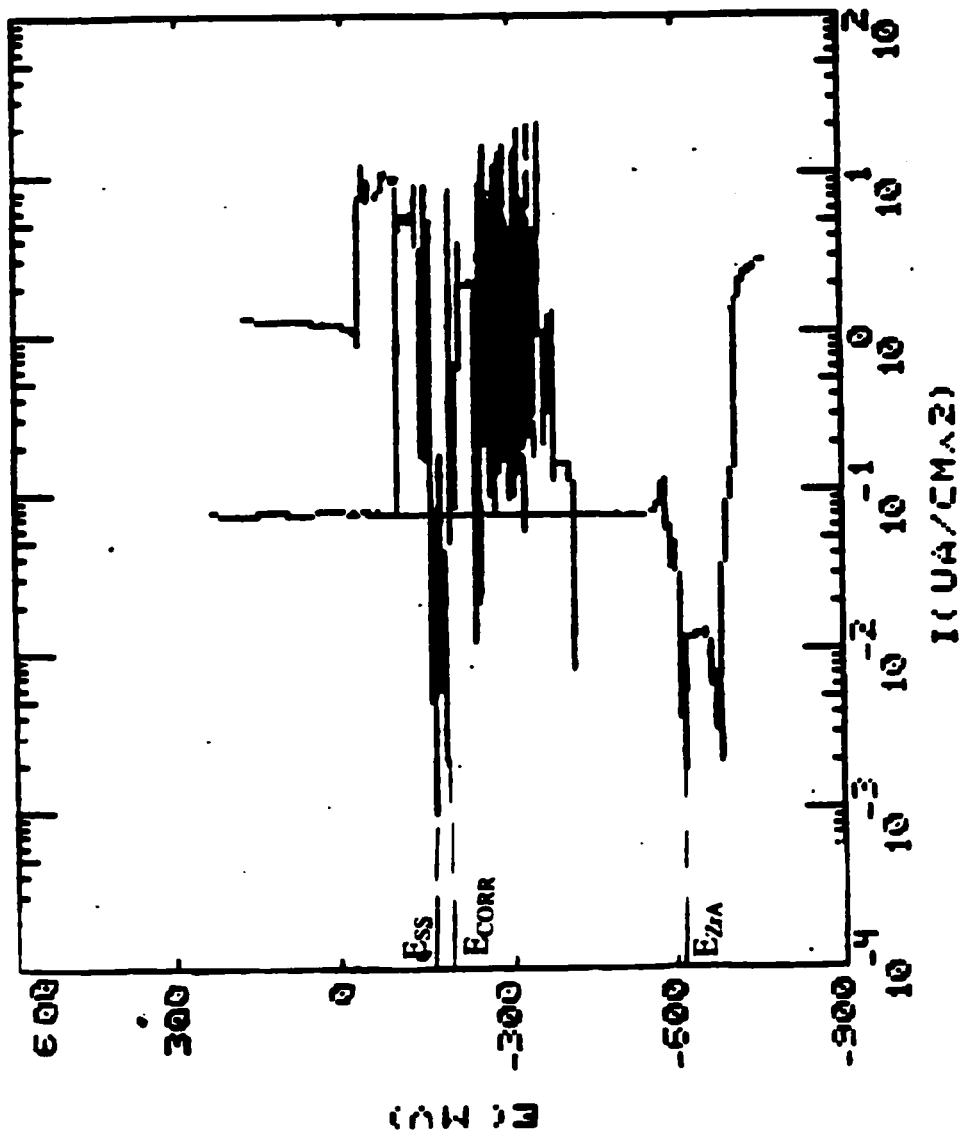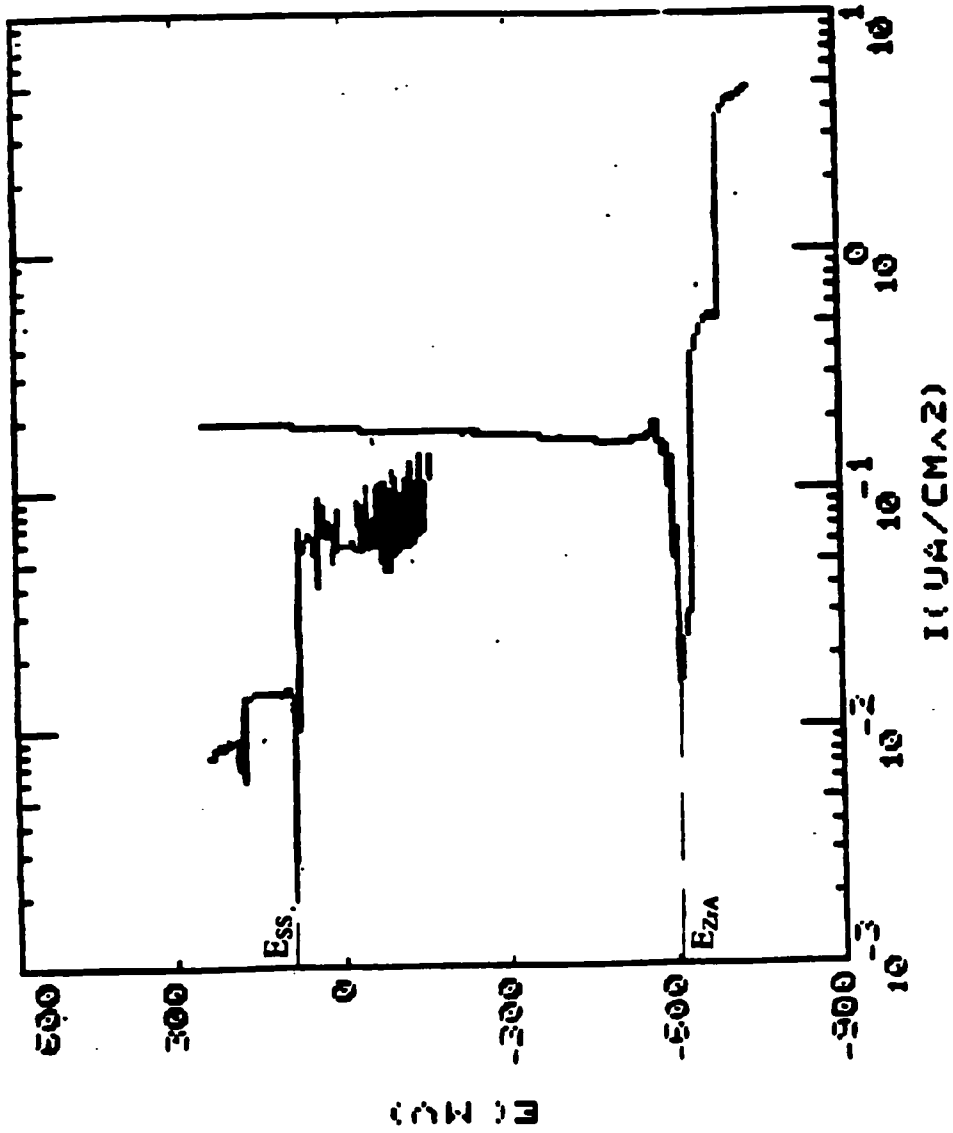
132

Figure 93. E_{corr} determination from SS-304 and Zr-alloy potentiodynamic scan at 550°F and 50 ppb dissolve oxygen.

133

Figure 94. E_{corr} determination from SS-304 and Zr-alloy potentiodynamic scan at 250°F and 200 ppb dissolve oxygen.

134

Figure 95. E_{corr} determination from SS-304 and Zr-alloy potentiodynamic scan at 350°F and 200 ppb dissolve oxygen.
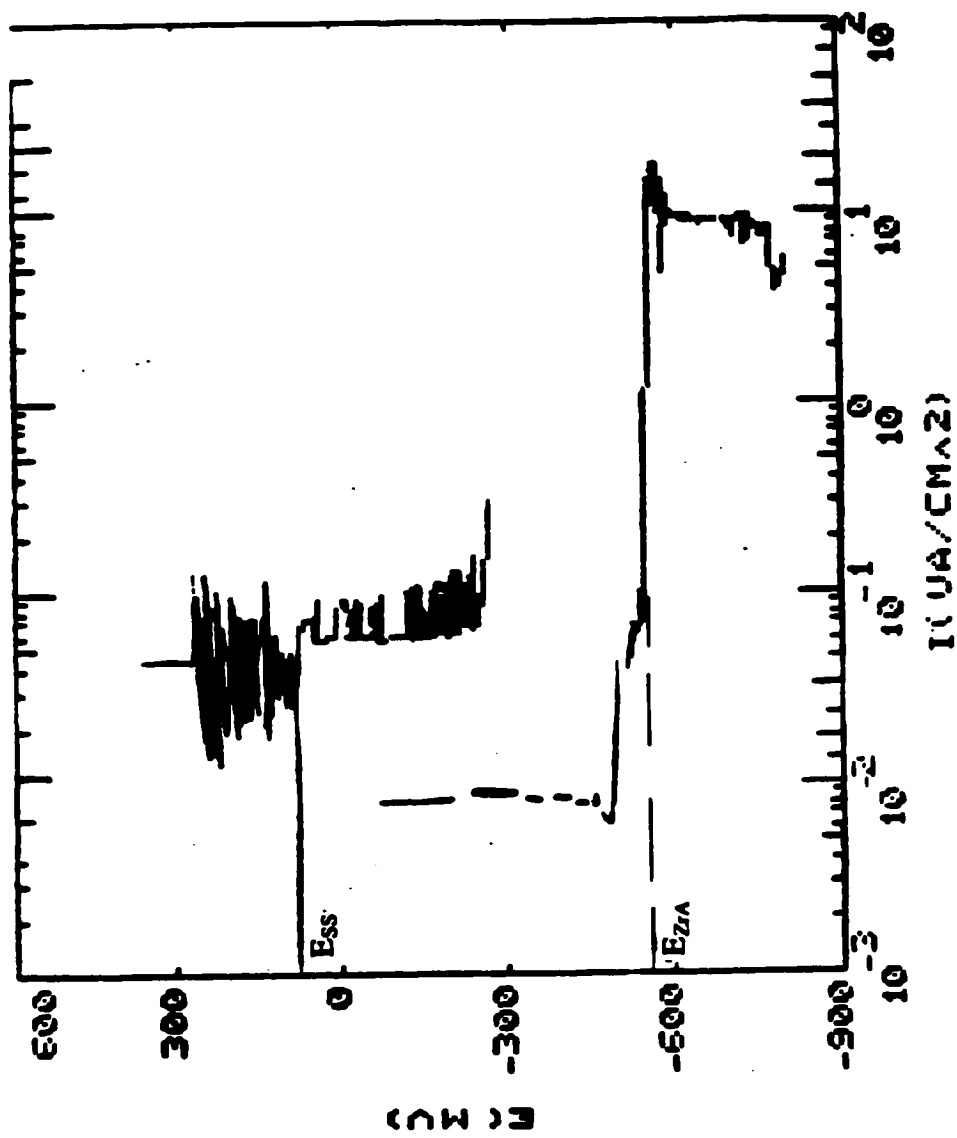
135

Figure 96. E$_{corr}$ determination from SS-304 and Zr-alloy potentiodynamic scan at 550°F and 200 ppb dissolve oxygen.
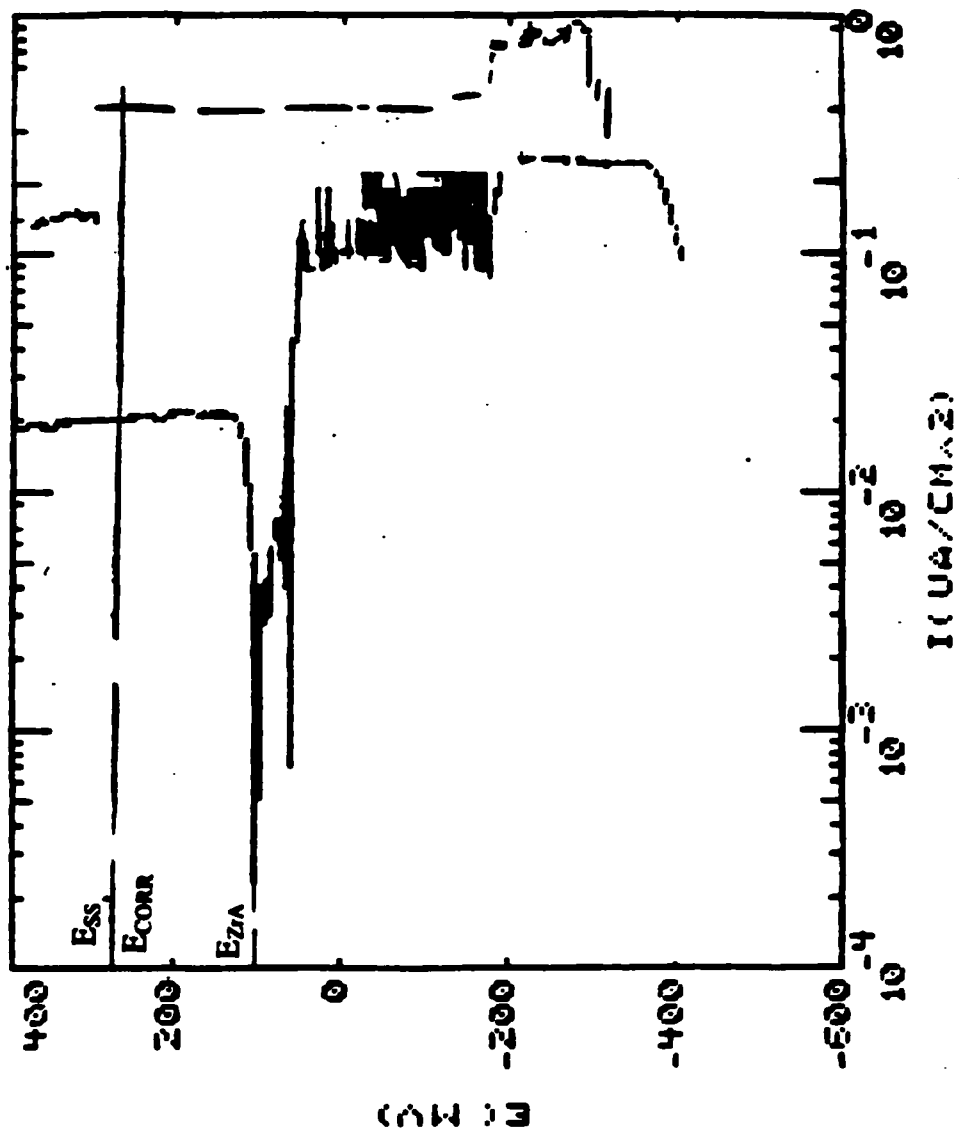
136

Figure 97. E_{corr} determination from SS-304 and Zr-alloy potentiodynamic scan at 250°F and 8000 ppb dissolve oxygen.
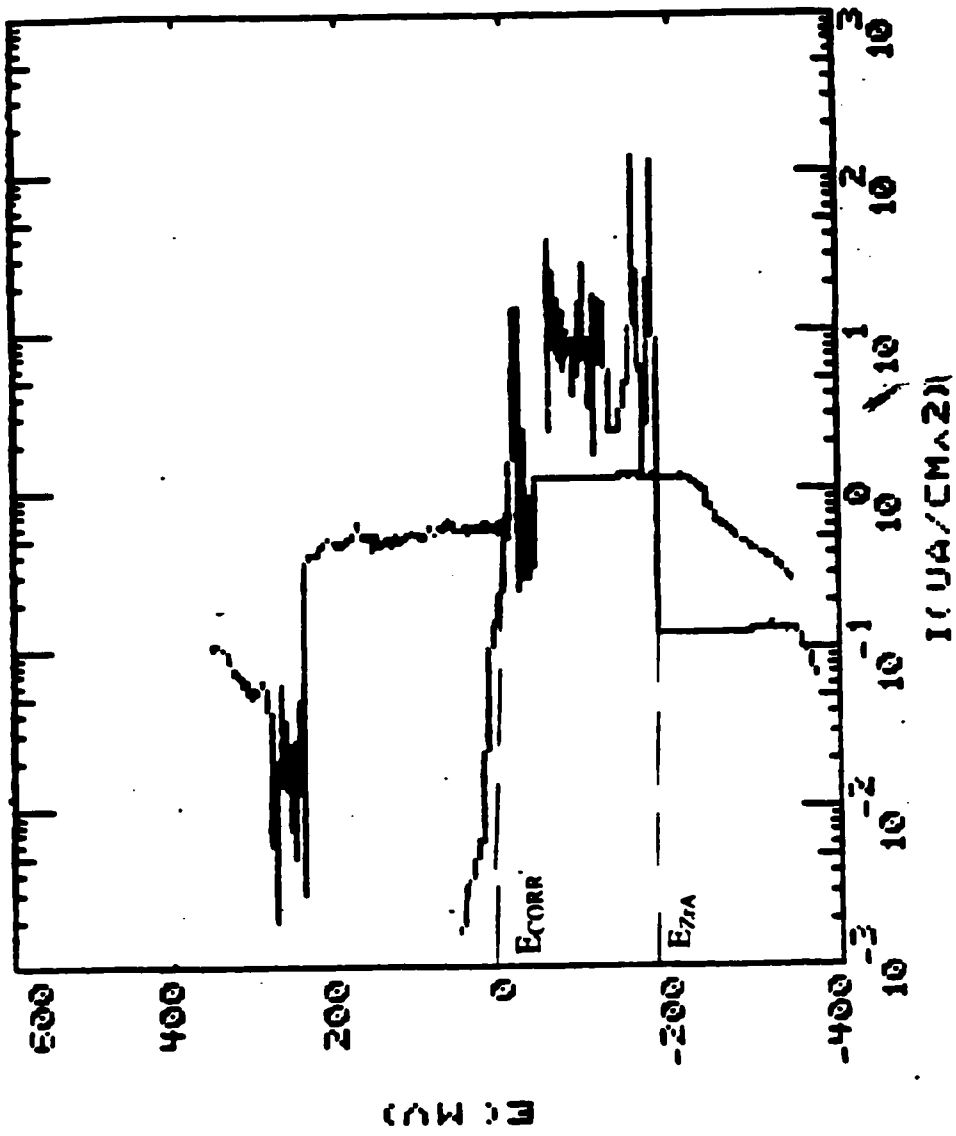
137

Figure 98. E_corr determination from SS-304 and Zr-alloy potentiodynamic scan at 350°F and 8000 ppb dissolve oxygen.